

İSTANBUL TECHNICAL UNIVERSITY ★ INSTITUTE OF SCIENCE AND TECHNOLOGY

**INVESTIGATION OF SURFACE PROPERTIES OF PLASMA NITRIDED
AND PVD COATED Ti-6Al-4V ALLOY FOR BIOMEDICAL
APPLICATIONS**

**M.Sc. Thesis by
Tuğçe AKYAZI**

Department: Metallurgical and Materials Engineering

Programme: Materials Engineering

SEPTEMBER 2011

**INVESTIGATION OF SURFACE PROPERTIES OF PLASMA NITRIDED AND
PVD COATED Ti-6Al-4V ALLOY FOR BIOMEDICAL APPLICATIONS**

**M.Sc. Thesis by
Tuğçe AKYAZI
(506081419)**

**Date of submission : 06 September 2011
Date of defence examination: 09 September 2011**

**Supervisor (Chairman) : Prof. Dr. Hüseyin ÇİMENOĞLU (ITU)
Second Supervisor) : Assoc. Prof. Dr. Turgut GÜLMEZ (ITU)
Members of the Examining Committee : Prof. Dr. Eyüp Sabri KAYALI (ITU)
Assoc. Prof. Dr. Murat BAYDOĞAN (ITU)
Prof. Dr. Mehmet KOZ (MU)**

SEPTEMBER 2011

İSTANBUL TEKNİK ÜNİVERSİTESİ ★ FEN BİLİMLERİ ENSTİTÜSÜ

**BİYOMEDİKAL UYGULAMALARDA KULLANILAN PLASMA
NİTRÜRLENMİŞ VE PVD KAPLANMIŞ Ti-6Al-4V ALAŞIMININ YÜZEY
ÖZELLİKLERİNİN İNCELENMESİ**

YÜKSEK LİSANS TEZİ

Tuğçe AKYAZI

(506081419)

Tezin Enstitüye Verildiği Tarih : 06 Eylül 2011

Tezin Savunulduğu Tarih : 09 Eylül 2011

Tez Danışmanları : Prof. Dr. Hüseyin ÇİMENÖĞLU (İTÜ)

Doç. Dr. Turgut GÜLMEZ (İTÜ)

Diğer Jüri Üyeleri : Prof. Dr. Eyüp Sabri KAYALI (İTÜ)

Doç. Dr. Murat BAYDOĞAN (İTÜ)

Prof. Dr. Mehmet KOZ (MÜ)

EYLÜL 2011

FOREWORD

This master thesis is supported by ITU Enstitute of Science and Technology and studied under the teaching supervision of Professor Hüseyin ÇİMENOĞLU, Department of Metallurgical and Materials Engineering and Associate Professor Turgut GÜLMEZ, Department of Mechanical Engineering.

I would like to express my deep appreciation and thanks to my advisor Professor Hüseyin ÇİMENOĞLU for his technical and spiritual guadience and Associate Professor Turgut GÜLMEZ for his great help during the development of my thesis.I owe a special thanks to Professor Mustafa ÜRGEN for his help.

I owe Ress. Asst. Özgür ÇELİK and Onur MEYDANOĞLU a great debt of gratitude for their support and endless help.

I would like to thank my parents Mehpare AKYAZI and Çetin AKYAZI for their standing back of me.

September 2011

Tuğçe Akyazı

(Metallurgical and Materials
Engineer)

TABLE OF CONTENTS

Page

| | |
|---|-------------|
| TABLE OF CONTENTS..... | vii |
| ABBREVIATIONS..... | ix |
| LIST OF TABLES..... | xi |
| LIST OF FIGURES..... | xiii |
| SUMMARY..... | xv |
| ÖZET..... | xix |
| 1. INTRODUCTION..... | 1 |
| 2. TITANIUM AND TITANIUM ALLOYS..... | 3 |
| 2.1 Physical, Chemical and Mechanical Properties..... | 6 |
| 2.1.1 Physical properties..... | 6 |
| 2.1.2 Corrosion resistance and chemical reactivity..... | 7 |
| 2.1.3 Mechanical properties..... | 8 |
| 2.2 Crystal Structure..... | 13 |
| 2.3 Alloy Types..... | 13 |
| 2.4 Applications..... | 21 |
| 2.4.1 Biomedical applications and comparison of titanium and titanium alloys..... | 21 |
| 3. NITRIDING OF TITANIUM AND TITANIUM ALLOYS..... | 27 |
| 3.1 Nitriding Process..... | 27 |
| 3.2 Types of Nitriding..... | 31 |
| 3.2.1 Plasma nitriding..... | 34 |
| 3.3 Nitriding of Titanium..... | 38 |
| 3.3.1 Plasma nitriding of titanium..... | 41 |
| 4. PVD COATING ON TITANIUM AND TITANIUM ALLOYS..... | 47 |
| 4.1 Physical Vapor Deposition (PVD) Process..... | 47 |
| 4.2 Physical Vapor Deposited (PVD) TiN Coating..... | 47 |
| 5. EXPERIMENTAL PROCEDURE..... | 49 |
| 5.1 Plasma Nitriding Process..... | 49 |
| 5.2 PVD Process..... | 49 |
| 5.3 Characterization Tests..... | 49 |
| 6.RESULTS AND DISCUSSION..... | 53 |
| 6.1 Cross Sectional Microstructure Analysis..... | 53 |
| 6.2 XRD Phase Identification..... | 56 |
| 6.3 GDOES Analysis..... | 59 |
| 6.4 Microhardness Profiles..... | 61 |
| 6.5 Wear Tests..... | 62 |
| 6.5.1 Results of Dry Sliding Tests..... | 66 |
| 6.5.2 Results of Sliding Tests in Simulated Body Fluid..... | 69 |
| 7. CONCLUSION..... | 65 |
| REFERENCES..... | 67 |

Page

APPENDICES.....87
CURRICULUM VITAE.....95

ABBREVIATIONS

| | |
|-----------------------------|---|
| Ti | : Titanium |
| Al | : Aluminum |
| V | : Vanadium |
| Cr | : Chromium |
| Zr | : Zirconium |
| Fe | : Iron |
| Sn | : Tin |
| Mo | : Molybdenum |
| Nb | : Niobium |
| Si | : Silicon |
| O | : Oxygen |
| C | : Carbon |
| H | : Hydrogen |
| N | : Nitrogen |
| C.P | : Commercially Pure |
| ELI | : Extra low interstitial |
| YS | : Yield Strength |
| UTS | : Ultimate Tensile Strength |
| EL | : Elongation |
| RA | : Reduction in area |
| K_{IC} | : Plane-strain Fracture Toughness |
| TNTZ | : Ti-29Nb-13Ta-4.6Zr |
| TNTZ_{STA} | : Ti-29Nb-13Ta-4.6Zr alloy subjected to ageing treatment after solution treatment |
| TNTZ_{598 K} | : Ti-29Nb-13Ta-4.6Zr alloy subjected to ageing treatments at 598 K |
| TNTZ_{673 K} | : Ti-29Nb-13Ta-4.6Zr alloy subjected to ageing treatments at 598 K |
| TNTZ_{723 K} | : Ti-29Nb-13Ta-4.6Zr alloy subjected to ageing treatments at 598 K |
| Ti64_{STA} | : Ti-6Al-4V alloy subjected to ageing treatment after solution treatment |
| DC | : Direct Current |
| SEM | : Scanning electron microscope |
| XRD | : X-Ray Diffraction |
| HV | : Vickers hardness number, unspecified applied load |
| HV_{0,5} | : Vickers hardness number, using an applied load of 0,5g |
| h | : Hour |
| s | : Second |
| ksi | : Kilo pounds per square inch |
| PVD | : Physical Vapor Deposition |
| scm | : Standard cubic meter |
| GDOES | : Glow Discharge Optic Emission Spectroscopy |

LIST OF TABLES

Page

| | |
|---|----|
| Table 2.1: Tensile properties of Ti-6Al-4V..... | 5 |
| Table 2.2: Typical room-temperature tensile properties of titanium alloy bars machined from castings..... | 9 |
| Table 2.3: Ranges and effects of some alloying elements used in titanium..... | 15 |
| Table 2.4: Three major types of titanium materials and influencing effects of major alloying elements..... | 15 |
| Table 2.5: Relative advantages of equiaxed and acicular morphologies in near-alpha and alpha-beta alloys..... | 19 |
| Table 2.6: Typical fracture-toughness values for high strength alpha-beta alloys... | 19 |
| Table 2.7: Typical applications of two phased α - β alloys..... | 20 |
| Table 3.1: Comparison of advantages and disadvantages of nitriding methods..... | 33 |
| Table 6.1: Wear depth profiles and wear track optic images of the untreated and plasma nitrided, and PVD coated Ti-6Al-4V samples after dry sliding tests | 63 |
| Table 6.2: Average wear track area values of the untreated and treated samples after dry sliding tests..... | 64 |
| Table 6.3: Relative wear resistance values of untreated and treated samples after dry sliding tests..... | 65 |
| Table 6.4: Wear depth profiles and wear track optic images of the untreated and plasma nitrided, and PVD coated Ti-6Al-4V samples after sliding tests in simulated body fluid..... | 67 |
| Table 6.5: Average wear track area values of untreated and treated samples after sliding tests in simulated body fluid..... | 68 |
| Table 6.6: Relative wear resistance values of untreated and treated samples after sliding tests in simulated body fluid..... | 68 |

LIST OF FIGURES

| | <u>Page</u> |
|--|-------------|
| Figure 2.1: Different microstructures that can be produced in Ti-6Al-4V; (a) acicular (lamellar), (b) equiaxed and (c) bomidal microstructure..... | 4 |
| Figure 2.2: Relationships between weight loss and load in Ringer’s solution of TNTZ _{ST} , TNTZ _{598K} , TNTZ _{673K} , TNTZ _{723K} and Ti64 _{STA} obtained from friction wear tests at various loads..... | 11 |
| Figure 2.3: Schematic drawings of relationships between weight loss and wear distance for TNTZ _{ST} , TNTZ _{STA} and Ti64 _{STA} under (a) low and (b) high loading conditions..... | 12 |
| Figure 2.4: Typical microstructures for α , $\alpha+\beta$ and β titanium alloys: (a) equiaxed α phase in unalloyed titanium; (b) acicular equiaxed $\alpha+\beta$; (c) acicular $\alpha+\beta$ in Ti-6Al-4V; (d) equiaxed β in Ti-13V-11Cr-3Al..... | 16 |
| Figure 2.5: Elongation at fracture as a function of the fatigue strength of metallic biomaterials..... | 24 |
| Figure 2.6: Fatigue strength and Young’s modulus of metallic biomaterials..... | 24 |
| Figure 2.7: Ti-550 McIntosh tibial plateau showing wear..... | 25 |
| Figure 3.1: A schematic ullustration of the corner fracturing due to the excessive nitride networks..... | 29 |
| Figure 3.2: Illustration of nitride networking..... | 29 |
| Figure 3.3: A typical nitrided structure..... | 30 |
| Figure 3.4: Principle of operations of a plasma nitriding furnace..... | 36 |
| Figure 3.5: Variable-pulse duty cycle for DC pulsed plasma nitriding..... | 36 |
| Figure 3.6: Photo of work pieces in a plasma nitriding process..... | 36 |
| Figure 3.7: Effect of interstitial alloying elements on strength and reduction in area of iodide titanium..... | 39 |
| Figure 3.8: Ti-N Phase Diagram..... | 40 |
| Figure 3.9: Hardness profile (Vickers, 0.3kg load) from plasma-nitrided Ti-6Al-4V..... | 41 |
| Figure 5.1: Plasma nitriding process..... | 49 |
| Figure 6.1: Cross-sectional images of Ti-6Al-4V alloy specimens nitrided at (a) 650°C, (b) 700°C,(c) 750°C, and (d)TiN coated by PVD taken by optic microscope at 500x..... | 53 |
| Figure 6.2: SEM images of the cross section of Ti-6Al-4V samples nitrided at (a) 650°C, (b) 700°C, (c) 750°C and (d) TiN deposited by PVD at 3000x..... | 56 |
| Figure 6.3: X-ray diffractions of Ti-6Al-4V alloy specimens plasma nitrided at (a) 650°C, (b) 700°C, (c) 750°C and (d) TiN deposited by PVD..... | 58 |
| Figure 6.4: GDOES results of Ti-6Al-4V alloy specimens plasma nitrided at (a) 650°C, (b) 700°C and (c) 750°C..... | 61 |
| Figure 6.5: Microhardness depth profiles foruntreated,plasma nitrided and PVD coated Ti-6Al-4V substrates..... | 63 |

| | |
|--|----|
| Figure 6.6: SEM images of the wear tracks of the (a) untreated sample, (b) sample plasma nitrated at 650°C, (c) sample plasma nitrated at 700°C, (d) sample plasma nitrated at 750°C and (e) PVD coated sample after dry sliding tests..... | 68 |
| Figure 6.7: SEM images of the wear tracks of the (a) untreated sample, (b) sample plasma nitrated at 650°C, (c) sample plasma nitrated at 700°C, (d) sample plasma nitrated at 750°C and (e) PVD coated sample after sliding tests in simulated body fluid..... | 75 |

INVESTIGATION OF SURFACE PROPERTIES OF PLASMA NITRIDED AND PVD COATED Ti-6Al-4V ALLOY FOR BIOMEDICAL APPLICATIONS

SUMMARY

Titanium and its alloys are widely used in many areas such as aerospace, military, biomedical engineering as surgical implants due to their excellent properties such as high strength, easy fabrication and corrosion resistance. Ti-6Al-4V is the most widely used titanium alloy. It has been firstly used for aerospace applications. Then, it has been discovered that this alloy also fits very well for biomedical applications. Recently, Ti-6Al-4V is the most commonly used biomaterial for surgical implants. It possesses high corrosion resistance due to protective passive oxide, good mechanical and excellent tissue compatibility properties, which make it well suited for especially for implant applications. Nevertheless, using a titanium alloy as an implant material may lead to problems due to its low wear resistance. In addition further studies have shown that the release of both V and Al ions from Ti-6Al-4V alloy are found to be associated with long-term health problems. In order to solve these problems, different surface modification techniques, such as the plasma assisted thermochemical treatment, ion implantation, and thin film deposition have been performed.

Nitriding of titanium alloys can lead to a great improvement in tribological properties because it favors formation of nitrides of titanium capable of resisting wear and corrosion much superior to substrate materials. Additionally, among the numerous deposition techniques that have been developed to achieve quality TiN films which has been extensively utilised to enhance wear and corrosion performance of Ti alloys, PVD coatings have been commonly used in recent years.

In present study, plasma nitriding and PVD processes are applied to improve hardness and sliding wear resistance of Ti-6Al-4V.

This study is developed in the aim of comparing plasma nitriding and PVD surface processes and optimizing the treatment temperature of plasma nitriding process in order to improve the surface properties of the Ti-6Al-4V alloy mainly used for biomedical applications.

Plasma nitriding treatment of Ti-6Al-4V has been performed in a DC glow discharge, in 25% H₂-75% N₂ gas mixture, for treatment time 4 h at the temperatures of 650 °C, 700 °C and 750 °C. TiN coating on the Ti-6Al-4V substrate was deposited by using cathodic arc PVD unit with a titanium cathode, with a bias voltage of 150V, at a temperature about about 600 °C for 30 minutes.

The influence of the surface processes on tribological properties of Ti-6Al-4V has been investigated using X-ray diffraction, optic microscopy, scanning electron microscopy, microhardness tester, reciprocating wear tester (both for dry sliding test and sliding test in simulated body fluid), and GDOES.

A thin, uniform and continuous layer attributed to nitrided layer can be observed by cross sectional microstructure analysis with SEM, for the samples nitrided at 700 and 750 °C. At 650°C, this layer is thinner, irregular and discontinuous. XRD analysis confirm the formation of cubic δ -TiN and tetragonal ϵ -Ti₂N phases which are known to have excellent wear resistance, in the surface modified layer. ϵ -Ti₂N is identified as the main phase. The proportion of both phases increases with the treatment temperature. Underneath the nitrided layer, a diffusion layer can be assigned for all the nitriding process temperatures. The thickness of this layer increases by the increasing treatment temperature likewise the nitrided layer. The PVD coated sample has significantly thicker, very uniform, dense and continuous TiN layer with a very distinct and flat interface with the substrate, with the lack of the diffusion layer. Single TiN phase can be observed to grow after the coating process as can be guessed.

It is confirmed that nitrogen has penetrated into a certain depth value for each plasma nitriding temperature. Nitrogen concentration decreases with increasing distance from the surface. Nitrogen penetration depth increases as the treatment temperature increases due to the accelerated rate of nitrogen diffusion at higher temperature, however there couldn't be seen any significant depth difference between the samples nitrided at 700 and 750°C.

Plasma nitriding treatment and PVD process significantly improve the surface hardness of the Ti-6Al-4V sample. TiN deposited sample has significantly higher hardness values than the plasma nitrided ones due to the high thickness of the nitrided layer. For the nitrided samples, the surface hardness values were found to increase as nitriding temperature increased, since the increase in surface hardness is caused by the formation of the hard surface layer (which is composed of titanium nitride phases as confirmed in XRD analysis) and the diffusion of the nitrogen into the sample which is highly effected by temperature, provides an optimal support to the hard surface layer. Also, a significant difference was not observed between the improvement of the hardness of the samples nitrided at 700°C and 750°C, as confirmed in GDOES results.

The plasma nitriding and PVD processes have a positive effect on the dry sliding behaviour of the Ti-6Al-4V alloy by improving the wear resistance. In case of the nitrided samples, wear resistance increases as temperature does, in consistence with the microhardness measurements. Thus, the sample plasma nitrided at 750°C has the highest wear resistance. The wear resistance of the PVD coated sample was found to be less than that of the samples nitrided at 700 °C and 750°C. However, the surface hardness of the PVD coated sample was found to be the higher than these samples. This result is attributed to the break down of the PVD coating due to the absence of the diffusion layer and distinct interface with substrate surface of the PVD coated sample.

The plasma nitriding and PVD coating processes have considerable effects on the sliding behaviour of the Ti-6Al-4V alloy in simulated body fluid. Additionally, simulated body fluid solution decreased the effect of wear on the samples. The wear resistance of both the sample plasma nitrided at 650°C and the PVD coated sample are less than the untreated sample, while nitriding processes at 700°C and at 750°C increase the wear resistance of the sample significantly. The result is not consistent with the microhardness profiles which have shown that the highest surface hardness results belong to the PVD coated sample. It is presumed that TiN coating is broken and TiN particles which have a hard nature, increase the wear rate and decrease the

wear resistance. This situation is attributed to the combined effect of the absence of the diffusion layer, the distinct interface with the substrate surface in the case of PVD coating and the corrosion caused by the simulated body fluid. Also, despite the hardness of the nitrided samples have shown considerable improvement at microhardness profiles, the sample plasma nitrided at 650°C has lower wear resistance than the untreated sample. This is assigned to the effect of broken, hard nitrided film particles which accelerate the wear rate due to the thinner nitrided layer and thinner diffusion layer. The corrosion effect by the simulated body fluid on the thin nitrided layer can be considered for this result.

As a result, the most ideal data for the improvement of the surface properties are obtained by the sample plasma nitrided at 750°.

BİYOMEDİKAL UYGULARMALARDA KULLANILAN PLASMA NİTRÜRLENMİŞ VE PVD KAPLANMIŞ Ti-6Al-4V ALAŞIMININ YÜZEY ÖZELLİKLERİNİN İNCELENMESİ

ÖZET

Titanyum ve titanyum alaşımları yüksek dayanım, yüksek korozyon direnci, kolay işlenebilirlik, düşük yoğunluk gibi özellikleri sayesinde, havacılık ve uzay sanayii, silah sanayii, biyomedikal mühendisliği gibi birçok alanda yaygınlıkla kullanılmaktadır.

Ti-6Al-4V, en sık kullanılan titanyum alaşımıdır. Bu alaşım uzun yıllar boyunca sadece havacılık ve uzay alanında kullanılmış olsa da, biyomedikal uygulama alanlarına uygun özellikleri sayesinde bu alanda kullanılmaya başlanmış ve biyomedikal uygulama alanında kullanılan en sık malzemelerden biri haline gelmiştir.

Ti-6Al-4V alaşımı, yüksek biyoyumluluk, mükemmel doku uyumluluğu, yüzeyinde oluşan koruyucu pasif oksit sayesinde sahip olduğu yüksek korozyon direnci ve mükemmel mekanik özellikleri sayesinde mükemmel bir implant malzemesi olarak gözüke de, düşük aşınma direnci ve düşük yüzey sertliğine bağlı olarak ciddi problemler ortaya çıkmaktadır. Bu tür problemlerin engellenmesi için çeşitli yüzey mühendislik uygulamalarına başvurulmaktadır.

Titanyum alaşımlarına uygulanan nitrürleme işlemi, yüzeyde yüksek korozyon ve aşınma direncine sahip titanyum nitrür fazlarının oluşmasına neden olarak, yüzey özelliklerinin büyük ölçüde iyileştirilmesini sağlamıştır. Ayrıca son yıllarda yaygın olarak kullanılan PVD kaplama yöntemi ile oluşturulan TiN filminin, titanyum ve titanyum alaşımlarının yüzey özelliklerinin geliştirilmesinde iyi sonuçlar verdiği bilinmektedir.

Bu çalışmada, Ti-6Al-4V alaşımının yüzey sertliğini ve aşınma direncini arttırmak amacıyla alaşıma farklı sıcaklıklarda plasma nitrürleme işlemi ve PVD kaplama prosesi uygulanmıştır. Çalışmanın amacı, biyomedikal alanında yaygın olarak kullanılan Ti-6Al-4V alaşımının yüzey özelliklerini geliştirmektir.

Plasma nitrürleme işlemi, Ti-6Al-4V numunelerine %25 H₂ ve %75N₂ oranındaki gaz ortamında, 650,700 ve 750°C sıcaklıklarında 4 saat işlem süresi boyunca uygulanmıştır. Diğer Ti-6Al-4V numuneler, yarım saatlik bir işlem süresi ve yaklaşık 600°C sıcaklıkta katodik ark PVD tekniği ile TiN kaplanmıştır.

Plasma nitrürleme ve PVD proseslerinin alaşım yüzey özellikleri üzerinde etkileri, X-ray difraktometre, optik mikroskop, SEM, microsertlik ölçme cihazı, aşınma cihazı (kuru ortamda ve yapay vücut sıvısı ortamında) ve GDOES kullanılarak incelenmiştir.

700 ve 750 °C' de nitrürlenmiş numunelerin SEM kesit mikroyapı görüntülerinde, nitrür tabakası olduğu kabul edilen ince ve sürekli bir tabakaya rastlanmıştır. 650 °C'de bu tabaka daha ince ve süreksiz bir haldedir. XRD analizleri oluşan nitrür

tabakasının yüksek aşınma direncine sahip olan kübik δ -TiN and tetragonal ϵ -Ti₂N fazlarından meydana geldiğini göstermektedir. Ana fazın ϵ -Ti₂N olduğu görülmüştür. Her iki faz miktarı da artan sıcaklıkla birlikte artmıştır. Nitrür tabakasının altında difüzyon tabakası olduğu öngörülen bir tabakaya rastlanmıştır. Difüzyon tabakası kalınlığının, nitrür tabakasında olduğu gibi sıcaklık arttıkça arttığı görülmüştür. PVD kaplanmış numunede nitrürlenmiş numunelerdeki nitrür tabakasından daha yüksek kalınlıkta olan, yoğun ve sürekli TiN filmi görülmüştür. Kaplama ile altlık arasında belirgin bir arayüzey görülmüş, difüzyon tabakasına rastlanmamıştır.

Azot penetrasyon derinliğinin artan proses sıcaklığı ile birlikte (difüzyonun hızının sıcaklığa bağlı olarak artması sonucu) arttığı gözlemlenmiştir. Fakat 700 °C and 750°C’de nitrürlenmiş numunelerin azot penetrasyon derinliği değerlerinde belirgin bir fark görülmemiştir.

Plasma nitrüleme ve PVD kaplama prosesleri, malzemenin yüzey sertlik özelliklerini büyük ölçüde etkilemiştir. Mikrosertlik değerleri, azot konsantrasyon profiline benzer bir profil göstererek, yüzeye olan mesafe arttıkça azalmaktadır. PVD kaplanmış numunenin yüzey sertliğinin, yüksek kaplama kalınlığı sebebiyle plasma nitrürlenmiş numunelerden daha fazla olduğu görülmüştür. Nitürlenmiş numunelerin yüzey sertliğinin (oluşan sert yüzey tabakasını destekleyen azot difüzyonu etkisiyle) proses sıcaklığı arttıkça arttığı görülmüştür. 700 °C and 750 °C’ de işlem görmüş numunelerin sertlik değerleri arasında azot penetrasyon derinliği sonuçları ile de uyumlu olarak belirgin bir fark görülmemiştir.

Plasma nitrüleme ve PVD prosesleri, Ti-6Al-4V alaşımının kuru ortamdaki aşınma davranışını büyük ölçüde geliştirmiştir. Nitrürlenmiş numunelerde aşınma direnci, mikrosertlik ölçüm değerleriyle uyumlu olarak proses sıcaklığı arttıkça artmıştır. PVD kaplanmış numune, 700 °C and 750°C’de nitrürlenmiş numunelerden daha yüksek yüzey sertliğine sahip olmasına rağmen, bu numunelerden daha düşük bir aşınma direncine sahiptir. Bu durum, PVD kaplanmış numunenin, kaplama-altlık arasındaki keskin arayüzeyine ve difüzyon tabakasına sahip olmamasına bağlanmıştır.

Plasma nitrüleme ve PVD kaplama prosesleri, malzemenin yapay vücut sıvısı ortamındaki aşınma davranışını da büyük ölçüde etkilemiştir. Yapay vücut sıvısı, numunelerdeki aşınma etkisini azaltmıştır. 650°C’de nitürlenmiş ve PVD kaplanmış numunelerin aşınma direncinin, işlemsiz numuneye göre daha düşük olduğu görülürken, 700°C ve 750°C’de nitrüleme işleminin aşınma direncini belirgin bir şekilde arttırdığı gözlemlenmiştir. Bu sonuç, en yüksek yüzey sertliğinin PVD kaplanmış numune olarak görüldüğü mikrosertlik ölçümleri ile uyumlu değildir. Bu durum, yapay vücut sıvısının neden olduğu korozyon, keskin kaplama-altlık arayüzeyi ve difüzyon tabakası eksikliğinin ortak etkisi ile TiN kaplamanın parçalanması, ve sert TiN partiküllerinin aşınma hızını arttırıp, aşınma direncini azaltması olarak tahmin edilmiştir. Ayrıca mikrosertlik profilinde, nitrürlenmiş numunelerin yüzey sertliklerinin, işlemsiz numuneden çok daha yüksek olmasına rağmen, 650°C’de nitrürlenmiş numunenin aşınma direncinin işlemsiz numuneden düşük olmasının nedeni, ince ve süreksiz nitrür tabakasının, korozyon etkisiyle daha hızlı parçalanması ve parçalanmış sert partiküllerin aşınmayı arttırıp, aşınma direncini azaltması olarak öngörülmüştür.

Tüm bu karakterizasyon testlerinin sonucunda, en ideal yüzey özellikleri 750°C’de plasma nitrürlenmiş numuneden elde edildiği söylenebilmektedir

1.INTRODUCTION

Titanium gained strategic importance and popularity just for the last decades due to the late invention of a process to obtain it from ores, eventhough it was discovered as an element in 1795 [1,2].

Use of titanium and its alloys has grown rapidly in many areas such as aerospace, military, gas turbine, biomedical engineering due to their lightweight, excellent corrosion resistance, high strength to weight ratio, good fatigue properties, easy fabrication, and low modulus of elasticity [1,3] Because of the requirements for high strength and high fatigue resistance for many applications, the Ti-6Al-4V alloy has to be used instead of CP titanium [4].

A more established application area of titanium is the biomedical field. Mainly CP titanium and Ti-6Al-4V have been used as implant materials. However, since toxicity of vanadium to the human body was suspected, vanadium free titanium alloys like Ti-6Al-7Nb and Ti-5Al-2.5Fe were developed [4]. Ti-6Al-4V is the most preferred material for biomedical applications due to its high strength-to-weight ratio, good high temperature properties, high corrosion resistance and excellent biocompatibility. However, the practical use of Ti-6Al-4V and other titanium alloys in a biomedical application (total hip, knee replacement, etc.) is limited in many cases by the need for the hard surface and high wear resistance. Since titanium based materials have poor tribological properties, wear debris produced by different wear mechanisms can lead to harmful biological reactions with the tissue inside the body and can even cause the removal of the prothesis.

Particularly in medical applications, minimal wear is essential. Surface engineering is expected to be the ideal solution for these problems. Due to this fact, the application of surface engineering techniques to improve the wear resistance of Ti-6Al-4V has consequently been widely researched [3,5].

In the present study, plasma nitriding process is used to improve hardness and sliding wear resistance of Ti-6Al-4V.

Nitriding of titanium alloys by low temperature surface treatments is one of the actual challenge in the metallurgy society. The issue is to obtain a thick nitride layer, with a high hardness and a good chemical stability, without aging the bulk material, which has a bad effect on the mechanical properties [6]. Plasma nitriding is a diffusional process, and produces a continuous hardness profile. During nitriding of titanium based materials, the formation of the hard layer including TiN and Ti₂N is known to improve wear resistance [7].

The aim of this study is to optimize plasma nitriding treatment temperature in order to achieve the desired surface properties of the Ti-6Al-4V alloy for biomedical applications. The surface layers grown at different nitriding temperatures on Ti-6Al-4V were characterized to reveal the dependence of the properties on temperature. The nitrided specimens were characterized by a number of techniques including optical microscopy, scanning electron microscopy, microhardness test, XRD, dry sliding test and GDOES.

2. TITANIUM AND TITANIUM ALLOYS

TITANIUM, occasionally mentioned as the “wonder metal”, was found by the German chemist Martin Heinrich Klaproth in 1795 and named with the Latin word for “Earth” (also name for the “Titans” of Greek Mythology) [1]. Although Titanium has been recognized as an element for 200 years, the metal received strategic importance only in the last 40 years or so [8], since the Kroll process made the extraction of this material from ores a commercial possibility in 1936 [2]. Commercial production of titanium and titanium alloys in the United States has increased from zero to more than 23 million kg/yr (50 million lb/yr) since then [8].

Alloy development had a fast progression. The beneficial effects of aluminum additions were realized early on and titanium aluminum alloys were soon commercially available. The Ti-6Al-4V alloy (or Ti-6/4), in fact, accounts for more than half of the current U.S. titanium market [8].

The rapid growth of the titanium materials (both unalloyed and alloyed) industry is due to their lightweight, high specific strength (which refers to a high strength-to-weight ratio), low modulus of elasticity, and superb corrosion resistance [1]. Pure titanium wrought products, which have minimum titanium contents ranging from about 98.635 to 99.5 wt% are used primarily because of their corrosion resistance. Titanium products are also useful in applications requiring high ductility for fabrication but relatively low strength in service [8].

Under the category of “unalloyed grades” of ASTM specification, there are five different materials; they include ASTM grade 1 (99.5%Ti), grade 2 (99.3%Ti), grade 3 (99.2%Ti), grade 4 (99.0%Ti), and grade 7 (99.4%Ti). Although each material contains slightly different levels of N, Fe, and O, C is specified <0.10 wt.% (wt.% or w/o) and H is also specified <0.015 wt.% [1].

ASTM CpTi grades 1–4 (unalloyed titanium) allow a hydrogen content up to 0.015 wt.% (i.e., 15 ppm). It was reported that if Cp (commercially pure) Ti contains over 250 ppm of hydrogen, the material would be susceptible to stress corrosion cracking

and hydrogen embrittlement [1]. The grade 2 is the most frequently used titanium grade in industrial service, having well-balanced properties of strength and ductility. The strength levels are similar to those of common stainless steel and its ductility allows good cold formability. Among many applications of CpTi materials in dental and medical fields, the dental CpTi implant is the most frequently and widely used [1].

Ti-6Al-4V is the most widely used titanium alloy [8], belonging to the $\alpha + \beta$ phase alloy group and is particularly popular because of its high corrosion resistance and low toxicity of ions released from the surface due to dense and protective passive oxide (which is mainly TiO_2) film formation. Ti-6Al-4V exhibits good mechanical and excellent tissue compatibility properties, which make it well suited for biomedical applications where a bone anchorage is needed, particularly for implant applications. Ti-6Al-4V ELI is also available and employed in the medical area [1].

Ti-6Al-4V is normally used in annealed condition [9]. It is processed to provide mill-annealed or β -annealed structures, and is also sometimes aged and solution treated. Ti-6Al-4V has useful creep resistance up to 300 °C, excellent fatigue strength and fair weldability [8].

Figure 2.1 illustrates the three distinct microstructures, acicular (lamellar), equiaxed and bimodal, that can be produced in Ti-6Al-4V by controlling the solution annealing temperature, cooling rate and final aging temperature [10].

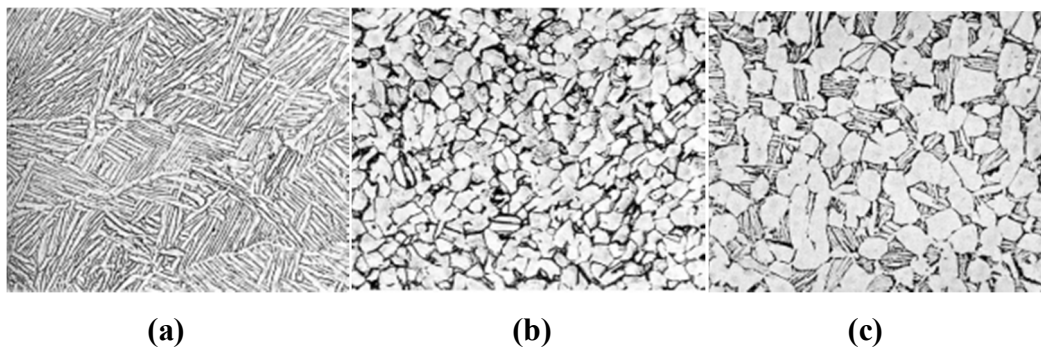


Figure 2.1: Different microstructures that can be produced in Ti-6Al-4V; (a) acicular (lamellar), (b) equiaxed and (c) bimodal [5].

The lamellar (acicular) structure shown in Figure 2.1 (a) is normally obtained following solution treatment above the β transus, followed by air cooling, and aging between 700 and 800 °C. The equiaxed structure, Figure 2.1(b), is obtained with solution annealing below the β transus, e.g., between 800°C and 925 °C. Finally, the bimodal structure, Figure 2.1(c), may be developed by solution treatment below the β transus, typically between 900°C and 950 °C followed by air cooling and aging below 700 °C [10].

Table 2.1 shows that equiaxed alpha microstructures provide high strength and ductility and relatively low fracture toughness, while lamellar (acicular) structure provides good fracture toughness but with worse strength and ductility. Finally, the high cycle fatigue response of Ti-6Al-4V can be modified by controlling its microstructure [10].

Table 2.1: Tensile properties of Ti-6Al-4V [5]

| Microstructure | YS (Mpa) | UTS (Mpa) | El. (%) | RA (%) | K _{1c} (Mpa/√m) |
|----------------|-------------|--------------|------------|-----------|-----------------------------|
| Equiaxed (Std) | 951 | 1020 | 15 | 35 | 61 |
| Lamellar (Std) | 884 | 949 | 13 | 23 | 78 |
| Equiaxed (ELI) | 830 | 903 | 17 | 44 | 91 |
| Equiaxed(CMG) | 1068 | 1096 | 15 | 40 | 54 |

Oxygen content : Std : 0.15-0.2% ; Eli : 0.13 Max ; Cmg : 0.18-0.2%.

YS: Yield Strength; UTS: Ultimate Tensile Strength; El.: Elongation; RA: Reduction in area; K_{1c}: Plane-strain Fracture Toughness

Extra low interstitial (ELI) grade Ti-6Al-4V is a version of Ti-6Al-4V with reduced interstitial impurities which improve ductility and toughness [8]. Cast Ti-6Al-4V ELI alloy exhibits excellent room-temperature impact strength [11]. Ti-6Al-4V-ELI has been used for cryogenic applications and fracture-critical aerospace applications such as critical cryogenic space shuttle service where fracture toughness is an important design criteria [8].

Although devices made of Ti-6Al-4V have been remarkably successful, primarily in orthopedic and dental applications, clinical reports have implicated as causes of

failure the biological response to released metal such as vanadium from the material and the formation of oxide [1].

As a result of searches for vanadium-free Ti-6Al-4V equivalent alloys, Ti-6Al-7Nb (or Ti-6/7) alloy was developed to enhance the wear resistance and castability. This custom-made alloy designed for implants shows the same alpha/beta structures as Ti-6Al-4V and exhibits equally good mechanical properties. The corrosion resistance of Ti-6Al-7Nb in sodium chloride solution was evaluated and found to be equal to that of pure titanium and Ti-6Al-4V, due to formation of a very dense and stable passive layer. Highly stressed anchorage stems of different medical prostheses (including hip, knee, and wrist joints) have been made from hot-forged Ti-6Al-7Nb [1].

Ti-3Al-2.5V alloy possesses an excellent ductility and cold formability, allowing it to be cold-worked by standard tube-making processes and bent for installation. It is easily welded, and may be heat-treated to obtain a wide range of strengths and ductilities [1].

Ti-5Al-3Mo-4Zr (or Ti-5/3/4) is a newly developed titanium alloy used for surgical implant application. It was reported that the new alloy is advantageous over Ti-6Al-4V ELI because it does not contain bio-hazardous alloying elements such as vanadium, has superior mechanical properties than stainless steel and its high corrosion abrasive wear resistance is also better. As a result, newly designed artificial hip joints are made with this alloy [1].

In the course of developing a vanadium-free titanium-based alloy, another new alloy Ti-5Al-2.5Fe (which is an $\alpha+\beta$ phase alloy) was developed. This new alloy contains no toxic vanadium either (which is an alloying element in the Ti-6Al-4V alloy and may increase to more than 15% in the β phase). Hip prostheses and hip prostheses' heads are fabricated from the Ti-5Al-2.5Fe alloy with a grain size of 20 μm or less [1].

2.1 Physical, Chemical and Mechanical Properties

2.1.1 Physical properties

The thermal, magnetic and electric properties are not the primary reason for the selection of titanium for an application, but the superconducting properties of titanium alloys have recently become an issue of interest [12]. Because titanium has

favorable film characteristics and lack of corrosion, it has a greater heat-transfer rate than most copper-base alloys even though its thermal conductivity is low compared to other metals [8].

2.1.2 Corrosion resistance and chemical reactivity

Although titanium is a highly reactive metal, it also has an extremely high affinity for oxygen due to which it forms a very stable and highly adherent protective oxide film on its surface. This oxide film, which forms spontaneously and instantly when fresh metal surfaces are exposed to air and/or moisture, makes titanium highly resistant to corrosion [8].

Another very advantageous property for biomedical applications is the spontaneous regeneration of the oxide layer in milliseconds even after damage in a poorly oxygenated environment [13].

However, anhydrous conditions in the absence of a source of oxygen may result in titanium corrosion, because the protective film may not regenerate if damaged. This is particularly true of crevice corrosion. Titanium and titanium alloys may be corroded in tight crevices exposed to hot (>70 °C) chloride, bromide, iodide, fluoride, or sulfate-containing solutions [8].

For α - β alloys like Ti-6Al-4V or Ti-6Al-7Nb, information on the composition of the oxide layer is contradictory. Some authors affirm that the passive layers on Ti-alloys is the same as the one on pure Ti while others say that, depending on the phase, the oxide layers on Ti-alloys also contain oxides of the alloying elements [13].

Even though titanium and its alloys form a very stable oxide layer in physiological environments making them exceptionally biocompatible compared to other metal implant materials, surface reactions with the natural environment do sometimes happen. These reactions, such as ion exchange or absorption of proteins, lead to changes in the layer's composition and thickness and determine the quality and stability of the bone-implant-interface. Therefore mechanical activation of the surface plays an important role [13].

An important factor determining the corrosion resistance of Ti alloys is the microstructure (phase composition and shape). Microstructures with a more even distribution of the alloying elements have an improved corrosion resistance than two

phase microstructures which have pronounced differences in the content of the alloying elements [13].

2.1.3 Mechanical properties

The mechanical properties of titanium alloys are very sensitive to the characteristics of the microstructure. The phase, grain size and shape, morphology, and distribution of the fine microstructure ($\alpha+\beta$ phases) determine the properties and thus the application of every titanium alloy [1]. Titanium alloys mechanical properties depend on forming conditions [13]. These alloys can be strengthened and their mechanical properties can be varied by controlling their composition and applying thermomechanical processing techniques [11]. The mechanical properties of ($\alpha+\beta$)-Ti alloys may be specifically influenced by the right combination of thermomechanical treatments and surface hardening [13].

A significant improvement in the mechanical properties of high-strength titanium alloys can be obtained by using a special heat treatment based on rapid heating into the beta region. This treatment allows the production of a high-temperature beta-phase with a fine-grained microstructure and optimal chemical inhomogeneity, which strongly determines the mechanism and kinetics of phase transformations on cooling and further annealing or aging. A wide range of final microstructures with an enhanced combination of mechanical properties can be obtained [1].

Table 2.2 is a summary of room-temperature tensile properties for different alloys. These properties, which are typical, vary depending on microstructure as influenced by foundry parameters such as solidification rate, any postcast HIP and heat treatments [8].

Table 2.2: Typical room-temperature tensile properties of titanium alloy bars machined from castings (Specification minimums are less than these typical properties) [3].

| Alloy ^{(a)(b)} | Yield Strength | | Ultimate Strength | | Elongation (%) | Reduction of area,% |
|--|----------------|-----|-------------------|-----|----------------|---------------------|
| | Mpa | ksi | Mpa | ksi | | |
| Commercially pure (grade 2) | 448 | 65 | 552 | 80 | 18 | 32 |
| Ti-6Al-4V, annealed | 885 | 124 | 930 | 135 | 12 | 20 |
| Ti-6Al-4V-ELI | 758 | 110 | 827 | 120 | 13 | 22 |
| Ti-1100, Beta-STA ^{received} | 848 | 123 | 938 | 136 | 11 | 20 |
| Ti-6Al-2Sn-4Zr-2Mo, annealed | 910 | 132 | 1006 | 146 | 10 | 21 |
| IMI-834, Beta-STA ^{received} | 952 | 138 | 1069 | 155 | 5 | 8 |
| Ti-6Al-2Sn-4Zr-6Mo, Beta-STA ^(c) | 1269 | 184 | 1345 | 195 | 1 | 1 |
| Ti-3Al-8V-6Cr-4Zr-4Mo, Beta-STA ^(c) | 1241 | 180 | 1330 | 193 | 7 | 12 |
| Ti-15V-3Al-3Cr-3Sn, Beta-STA ^(c) | 1200 | 174 | 1275 | 185 | 6 | 12 |

(a) Solution-treated and aged (STA) heat treatments may be varied to produce alternate properties.

(b) ELI, extra low interstitial.

(c) Received Beta-STA, solution treatment with β -phase field followed by aging.

Normally, the fatigue life for a certain stress amplitude is determined by the resistance against crack formation and/or crack growth [13]. Therefore, in order to avoid the failure of titanium based biomaterials, it is necessary to understand their fatigue crack initiation and fatigue crack propagation characteristics [14]. It has been found that machining operations like wire drawing, pressing and cutting, and surface hardening methods like cold rolling or shot peening induce compressive surface residual stresses which mainly increase the endurance limit and decrease the crack

growth velocity [13]. These residual strains are normally fixed by an annealing process. If these residual strains are not removed, the grains become distorted. Distorted microstructures decrease the plastic formability under repeated stressing, causing a cracks early[1].However, in the case of relaxation of residual stresses, for example due to plastic deformation during cyclic loading, the influence of the surface roughness predominates and the endurance limit and the crack growth velocity are influenced in a negative way [13].

By combining thermal treatments and mechanical working the stability of the resulting tailored surface is improved. The stability of the surface is especially important for resistance to fatigue crack nucleation and growth [1].

The rotating bending fatigue strength is relatively higher in $\alpha + \beta$ titanium alloys [14]. Ti-6Al-4V alpha-beta alloy ,which is the most common titanium alloy used for surgical implants has a high fatigue resistance even in the annealed condition. For Ti-6Al-4V, significant improvements in fatigue resistance can be achieved by heat treating below the beta transus at 900°C and water quenching which causes changes in the microstructure (resulting in a microstructure with 50% alpha-titanium and 50% alpha-prime-titanium + beta titanium). This way the fatigue life of this material is significantly improved over most of the other forms of the material [11].

Corrosion fatigue may occur under the bending condition as the passive film formed on the surface of titanium alloys is considered to fracture more easily under this condition [14].

Titanium alloys are more susceptible to fretting degradation than other metal alloys. This may be because titanium alloys transfer more material when they slide over other materials or themselves. The harmful nature of fretting is more evident when it often leads to other degradation mechanisms such as pitting corrosion or crevice corrosion [15]. The fretting fatigue strengths of biomedical titanium alloys are affected by various factors, including contact pressure, frequency, contact conditions, material quality, stress amplitude, relative slip distance, friction coefficient, mean stress and circumstance [16].

The wear mechanisms for titanium alloys can be separated in two groups: abrasive wear and adhesion wear. Since the wear loss of biomedical titanium alloys is smaller in a simulated body fluid than in air, adhesive wear is considered to be the

predominant wear mechanism within a living body. The wear resistance of biomedical titanium alloys depends on the kind of alloy and its microstructures. However, the wear resistance is altered according to the testing conditions such as the load, as shown in Figure 2.2 [16].

Based on friction wear tests at various loads, Figure 2.2 shows the relationships between weight loss and load in a Ringer's solution of asolutionized Ti-29Nb-13Ta-4.6Zr (or TNTZ(TNTZ_{ST}))and TNTZ subjected to ageing treatments at 598 °K, at 673 °K and 723 °K (shown as (TNTZ_{598 K}), (TNTZ_{673 K}), and (TNTZ_{723 K}) respectively) and aged Ti-6Al-4V (or Ti64_{STA}) alloy after solution treatment. At a certain load, the order of the wear resistance of each material is changed. The reason for this can be schematically explained as in Figure 2.3 [11].

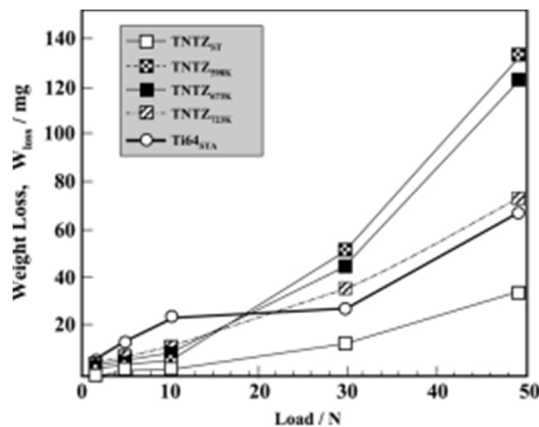


Figure 2.2: Relationships between weight loss and load in Ringer's solution of TNTZ_{ST} , TNTZ_{598K}, TNTZ_{673K} and TNTZ_{723K}, and Ti64_{STA} obtained from friction wear tests at various loads [16].

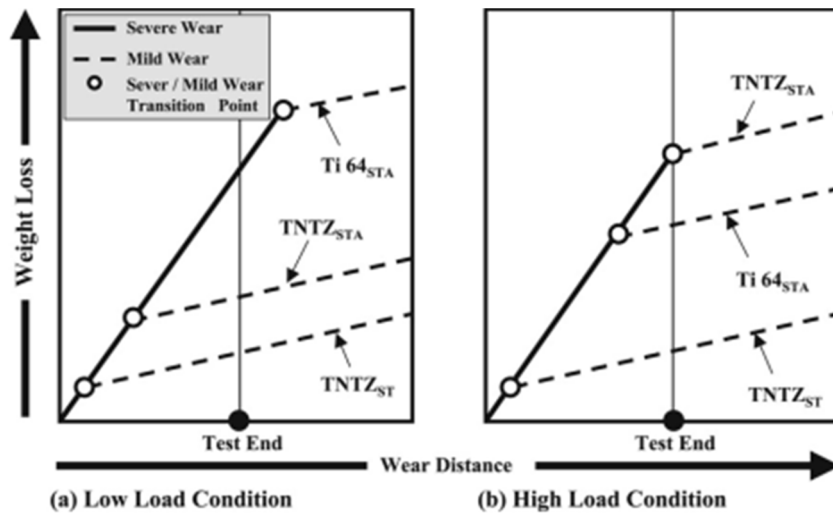


Figure 2.3: Schematic drawings of relationships between weight loss and wear distance for TNTZ_{ST}, TNTZ_{STA}, and Ti64_{STA} under (a) low and (b) high loading conditions [16].

In Figure 2.3 (a), for the low load condition, the wear of the Ti64_{STA} is in the stage of severe wear, but the wear of the TNTZ_{STA} (Ti-29Nb-13Ta-4.6Zr alloy subjected to ageing treatment after solution treatment) as well as the TNTZ_{ST} is in the stage of mild wear. On the other hand, in the Figure 2.3 (b), for the highload condition, the transfer from severe wear to mild wear is more delayed in the case of TNTZ_{STA} than in the cases of TNTZ_{ST} and Ti64_{STA}[16].

Unlike dental implants, most orthopedic implants will be exposed to biotribological actions. Metal ions released from the implant surface are suspected of contributing in the loosening of hip and knee prostheses, which are substantially subjected to biotribological environments. Also, the solid powder particles resultant from wear/friction produce allergic reactions on the living tissue [1]. For these reasons, although titanium and titanium alloys are very suitable for the biomedical applications, the wear resistance of the titanium alloys used in these applications should be improved [11]. Various methods have been investigated for hardening the surfaces of titanium alloy components, including gas nitriding, ion-implantation, and chemical or physical vapor deposition [12].

2.2 Crystal Structure

The microstructure of unalloyed titanium at room temperature is typically a 100% alpha-crystal structure, which transforms to a beta (body-centered cubic) structure at a temperature of about 885 °C. This transformation temperature can be increased or reduced depending on the type and quantity of the impurities or alloying additions. As amounts of impurity elements increase (primarily iron), small but increasing amounts of beta can be observed metallographically, normally at alpha grain boundaries [8].

While having an hcp (alpha) structure, Ti exhibits surprisingly high room-temperature ductility and can be cold-rolled with over 90% reduction in thickness without crack formation. This occurs because of the relative ease of activating slip systems and the availability of twinning planes in the crystal lattice [17].

Annealed unalloyed titanium may have an equiaxed or an acicular alpha microstructure. Acicular alpha occurs during beta-to-alpha transformation on cooling through the transformation temperature range. Platelet width decreases with cooling rate. Equiaxed alpha can only be produced by recrystallization of material that has been extensively worked in the alpha phase. The presence of acicular alpha, therefore, is an indication that the material has been heated to a temperature above the beta transus. A beta structure cannot be retained at low temperatures in unalloyed titanium, unless it is in small quantities and in materials containing beta stabilizing contaminants like iron [8].

2.3 Alloy Types

Titanium exists in two crystallographic forms. At room temperature, unalloyed (commercially pure) titanium has a hexagonal close-packed (hcp) crystal structure referred to as alpha (α) phase. At 885 °C, this transforms to a body-centered cubic (bcc) structure known as beta (β) phase. Between these temperatures, both alpha and beta are present [3].

By increasing the α phase portion, it is generally recognized that:

- 1- β -transus temperature increases.
- 2- Creep strength as well as high temperature strengths enhance.
- 3- Flow stress increases.

4- Weldability improves.

By increasing the β -phase portion, it is known that:

- 1- Room temperature strength increases.
- 2- Heat treatment and forming capabilities enhance.
- 3- Strain-rate sensitivity increases, so that superplastic forming is more favorably applicable [1].

The manipulation of these crystallographic variations by alloying additions and thermomechanical processing is the basis for the development of a wide range of alloys with different properties [8]. The α to β transformation temperature of pure titanium either increases or decreases based on the nature of the alloying elements. The alloying elements such as Al, O, N, etc. that tend to stabilize the α phase are called alpha stabilizers and the addition of these elements increase the beta transus temperature. Elements like V, Mo, Nb, Fe, Cr, etc. that stabilize β phase are known as beta stabilizers and adding these elements decreases the β transus temperature [9]. Ranges and effects of some alloying elements used in titanium are shown in Table 2.3.

Based on the phases present, titanium alloys can be classified as either α alloys, β alloys, or $\alpha + \beta$ alloys [8]. Three major types of titanium materials and influencing effects of major alloying elements are shown in Table 2.4 [1]. Additionally, Figure 2.4 shows typical equiaxed and transformed microstructures which can be found in α , α - β and β titanium alloy semi-finished mill products [2].

Table 2.3: Ranges and effects of some alloying elements used in titanium [13]

| Alloying element | Range (approx.) (wt.%) | Effect on structure |
|--------------------------|------------------------|------------------------------------|
| Carbon, oxygen, nitrogen | - | α stabilizer |
| Aluminum | 2-7 | α stabilizer |
| Tin | 2-6 | α stabilizer |
| Vanadium | 2-20 | β stabilizer |
| Molybdenum | 2-20 | β stabilizer |
| Chromium | 2-12 | β stabilizer |
| Copper | 2-6 | β stabilizer |
| Zirconium | 2-8 | α and β strengtheners |
| Silicon | 0.05-1 | Improves creep resistance |

Table 2.4: Three major types of titanium materials and influencing effects of major alloying elements [1].

| Type/material property | α and near α | $\alpha + \beta$ | β and near β |
|--------------------------------|---|--|---|
| α -Stabilizing elements | Al, Sn, Ga, Zr, C, O, N | | |
| β -Stabilizing elements | | | V, Mo, Nb, Ta, Cr |
| Typical materials | Commercially pure Ti Ti-5Al-2.5Sn Ti-5Al-6Sn-2Zr-1Mo Ti-6Al-2Sn-4Zr-2Mo Ti-8Al-1Mo-1V | Ti-5Al-2.5Fe Ti-5Al-2Mo-2Fe Ti-5Al-3Mo-4Zr Ti-5Al-2.5Fe Ti-6Al-7Nb Ti-6Al-4V Ti-6Al-6V-2Sn Ti-6Al-2Sn-4Zr-6Mo | Ti-3Al-8V-6Cr-4Mo-4Zr Ti-4.5Al-3V-2Mo-2Fe Ti-5Al-2Sn-2Zr-4Mo-4Cr Ti-6Al-6Fe-3Al Ti-10V-2Fe-3Al Ti-13V-11Cr-3Al Ti-15V-3Cr-3Al-3Sn Ti-35V-15Cr Ti-8Mo-8V-2Fe-3Sn Ti-11.5Mo-6Zr-4.5Sn Ti-30Mo, Ti-40Mo Ti-13Nb-13Zr Ti-25Pd-5Cr Ti-20Cr-0.2Sn Ti-30Ta |
| β -Transus temperature | Higher | ←-----→ | Lower |
| Specific density | Lower | -----→ | Higher |
| Room temperature strength | -----→ | -----→ | -----→ |
| Room temperature toughness | -----→ | -----→ | -----→ |
| Modulus of elasticity | ←----- | ←----- | ←----- |
| Machinability | ←----- | ←----- | ←----- |
| Age hardenability | -----→ | -----→ | -----→ |
| Heat resistance | ←----- | ←----- | ←----- |
| Weldability | ←----- | ←----- | ←----- |
| High-temperature strength | ←----- | ←----- | ←----- |
| Heat-treatability | -----→ | -----→ | -----→ |
| Plastic formability | -----→ | -----→ | -----→ |
| Strain-rate sensitivity | -----→ | -----→ | -----→ |
| Superplastic formability | -----→ | -----→ | -----→ |
| Creep resistance | ←----- | ←----- | ←----- |

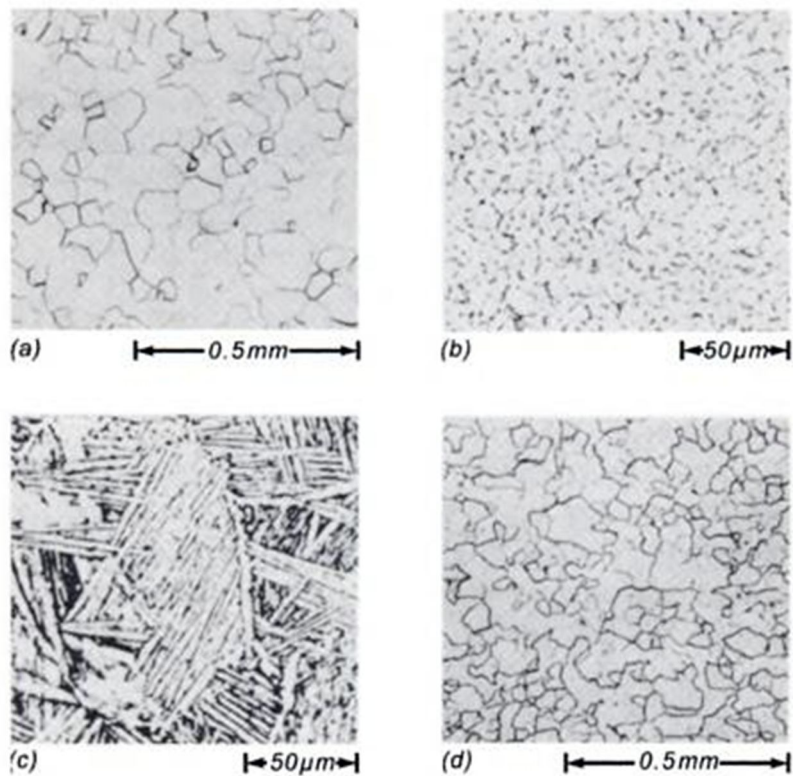


Figure 2.4: Typical microstructures for α , α - β and β titanium alloys: (a) equiaxed α phase in unalloyed titanium (after 1h/1,290 °F); (b) acicular equiaxed α + β ; (c) acicular α + β in Ti-6Al-4V; (d) equiaxed β in Ti-13V-11Cr-3Al [2].

Alpha alloys are obtained by stabilizing low temperature hexagonal α -phase with O, N, and C impurities as well as with Al and Sn [18]. These α -stabilizing elements work by either avoiding change in the phase transformation temperature or by increasing it [8].

Commercially pure grades of titanium (purity range 99.0–99.5%) can actually be considered α -phase alloys since they contain levels of O, N, C, and Fe, obtained from the manufacturing process [18].

Alpha phase Ti alloys generally have a greater creep resistance than β alloys, and are preferred for high-temperature applications. This kind of alloys are characterized by their notable strength, toughness, and weldability, but their forgeability is poorer than that of β alloys. This latter characteristic results in a greater tendency for forging defects. Smaller reductions and frequent reheating can minimize these defects [8]. Alpha alloys have a high solid solubility at room temperature and are weldable [18].

The absence of a ductile-to-brittle transition (a feature of β alloys) makes α alloys suitable for cryogenic applications [8].

The alpha structure is a stable phase, therefore, alpha alloys are most often used in annealed or recrystallized condition to eliminate residual stresses caused by working because unlike β alloys, they cannot be strengthened by heat treatment [8].

Beta alloys contain transition elements like vanadium, niobium, and molybdenum, which tend to decrease the temperature of the α to β phase transition promoting the development of the bcc β phase [8] and expanding the β -phase stability region [18].

They have excellent forgeability over a wider range of forging temperatures than α alloys, and β alloy sheet is cold formable in the solution treated condition [8].

Beta alloys have excellent hardenability, and respond very well to heat treatment. A common thermal treatment which results in the formation of finely dispersed α particles in the retained, involves solution treatment followed by aging at temperatures of 450 to 650 °C.

Beta alloys (including beta, metastable beta, and beta-rich alpha/beta compositions) are one of the most promising groups of titanium alloys in terms of processing, properties, and potential applications because they possess the highest range of strength, fatigue resistance, and environmental resistance among all titanium materials [1].

Although they offer the highest strength levels of the Ti alloys and the ability of cold working, the usage of β -phase alloys is rather limited compared with pure α or $\alpha+\beta$ -alloys [18].

Alpha + beta alloys have compositions that support a mixture of α and β phases and may contain between 10 and 50% β phase at room temperature [8].

The most common $\alpha + \beta$ alloy is Ti-6Al-4V [8]. The most widely used group (about 60%) of Ti alloys are two-phase $\alpha+\beta$ -alloys, being Ti-6Al-4V the most used of all [18]. $\alpha + \beta$ alloys generally have good formability but the Ti-6Al-4V alloy is quite difficult to form even in the annealed condition[8].

The properties of these alloys can be controlled through heat treatment, which is used to adjust the amounts and types of β phase present. Solution treatment followed by ageing at 480 to 650 °C precipitates α , resulting in a fine mixture of α and β in a

matrix of retained or transformed β phase [8]. Therefore, these alloys are heat treatable and allow large variations of the microstructure by altering the cooling and heat-treatment conditions [18].

In $\alpha + \beta$ titanium alloys the rotating bending fatigue strength is relatively higher, Young's modulus is relatively low [14] and their treated structures have higher strength, higher ductility and higher low cycle fatigue while the β treated structures have higher fracture toughness [9].

Within the alpha-beta class, an alloy that contains much more alpha than beta is often called a near-alpha alloy [8]. Like the near-alpha alloys, the microstructure of alpha-beta alloys can have different forms. It can be equiaxed, acicular or some combination of both. Equiaxed structures are obtained working an alloy in the alpha-beta range and annealing at lower temperatures. Acicular structures are obtained by working or heat treating above the beta transus and rapidly cooling. Equiaxed primary (prior) alpha and acicular alpha from the transformation of beta structures can be obtained by rapidly cooling from temperatures high in the alpha-beta range. Each type of structure presents different property advantages and disadvantages. Table 2.5 compares, relatively, the advantages of each structure [8]. Table 2.6 illustrates how material behaviour changes according to the various morphologies of the phase present in some α - β alloys [2]. Also, Some typical applications of α + β alloys and the conditions of their usage are given in Table 2.7 [18].

Table 2.5: Relative advantages of equiaxed and acicular morphologies in near-alpha and alpha-beta alloys [8].

| Equiaxed | Acicular |
|---|--|
| Higher ductility and formability | Superior creep properties |
| Higher threshold stress for hot-salt stress corrosion | Higher fracture-toughness values and lower crack-propagation rates |
| Higher strength (for equivalent heat treatment) | Slight drop in strength (for equivalent heat treatment) |
| Better low-cycle fatigue (initiation) properties | Superior stress-corrosion resistance |

Table 2.6: Typical fracture-toughness values for high strength alpha-beta alloys [2].

| Alloy | Alpha morphology | Yield strength | | Fracture toughness, | |
|--------------------|------------------|----------------|-------|---------------------|---------|
| | | [ksi.] | [Mpa] | [ksi.×in] | [Mpa×m] |
| Ti-6Al-4V | Equiaxed | 130 | 910 | 40-60 | 44-66 |
| | Transformed | 125 | 875 | 80-100 | 88-110 |
| Ti-6Al-4V-2Sn | Equiaxed | 155 | 1085 | 30-50 | 33-55 |
| | Transformed | 140 | 980 | 50-70 | 55-77 |
| Ti-6Al-2Sn-4Zr-6Mo | Equiaxed | 165 | 1155 | 20-30 | 22-33 |
| | Transformed | 160 | 1120 | 30-50 | 33-55 |

Table 2.7: Typical applications of two phase α - β alloys [18].

| Alloy composition | Condition | Typical applications |
|---------------------------------------|---------------------------|---|
| 6% Al, 4%V | Annealed; solution+age | Rocket motor cases; blades and disks for aircraft turbines and compressors; structural forgings and fasteners; pressure vessels; gas and chemical pumps; cryogenic parts: ordenance equipment; marine components; steam-turbine blades. |
| 6% Al, 4%V, low O ₂ , Sn | Annealed | High pressure cryogenic vessels operating down to -196°C |
| 6%Al, 6%V, 2%Sn | Annealed; solution+age | Rocket motor cases; ordenance components; structural aircraft parts and landing gears; responds well to heat treatments; good hardenability. |
| 7% Al, 4% Mo | Solution+age | Airframes and jet engine parts for operation at up to 427°C; missile forgings; ordenance equipment |
| 6%Al, 2%Sn, 2%Zr, 2%Mo, 2%Cr, 0.25%Si | Solution+age | Strength, fracture toughness in heavy sections; landing-gear wheels |
| 6%Al, 2%Sn, 4%Zr, 6%Mo | Solution+age | Components for advanced jet engines |
| 10%V, 2%Fe, 3%Al | Solution+age | Heavy airframe structural components requiring toughness at high strengths. |
| 8% Mo | Annealed | Aircraft sheet components, structural sections and skins; good formability, moderate strength |
| 3%Al, 2.5%V | Annealed | Aircraft hydraulic tubing, foil, combines strength, weldability and formability |

2.4 Applications

Many of the processes which involve the use of titanium materials, such as research and development in materials design, manufacturing technologies, characterization or evaluation methods, are some of the best examples of interdisciplinary work, including disciplines like physics, chemistry, metallurgy, mechanics, surface and interface sciences, biological science, engineering or technology [1].

Different industrial sectors have been looking for different types of development in new titanium alloys. They include Ti-5.8Al-4Sn-3.5Zr-0.7Nb-0.5Mo-0.35Si-0.06C, Ti-6Al-2Sn-4Zr-6Mo, and Ti-4Al-4Mo-2Sn-0.5Si for gas turbine engine materials, Ti-10V-2Fe-3Al, Ti-15V-3Cr-3Sn-3Al, and Ti-15Mo-2.8Al-3Nb-0.2Si for airframe materials, Ti-6Al-1.8Fe-0.2Si for ballistic armor, Ti-6.8Mo-4.5Fe-1.5Al for geothermal and offshore tubular materials, Ti-15V-3Cr-3Sn-3Al (having higher-strength and lower modulus) for sporting goods, V-free Ti-6Al-4V equivalent alloys for medical and dental applications, and NiTi-Cu alloys for medical orthopedic devices [1].

Being about 55% as dense as steel, titanium alloys have been commonly used for highly loaded aerospace components [8] and titanium materials have been of great importance for the aerospace industry since the early 1950s [1]. Although this area will continue to be a significant percentage of total consumption of titanium materials during the next years [1], over the last decade, the focus of titanium alloy development has shifted from aerospace to many other industrial applications [1].

Since titanium has a high corrosion resistance which is based on the formation of a stable, passive, protective oxide layer, the metal is useful in applications ranging from chemical processing equipment to surgical implants and prosthetic devices [8]. Therefore, in the last years titanium has received equal attention and interest from both the engineering and medical/dental fields [1].

2.4.1 Biomedical applications and consideration of titanium and titanium alloys

Metallic devices have been used to repair and replace parts of the human body since the 16th century. Before the introduction of antiseptic surgical techniques about 100 years ago, however, their success was very limited due to complications with postsurgical infections. As methods to avoid infections were learnt, the relationships between material properties and the success of implant surgeries became more clear.

Tissue compatibility, corrosion resistance, and strength were the critical characteristics found to be necessary [11]. Although many attempts have been made to replace missing roots with all sorts of metallic implants, the satisfactory use of a screwed in implant was found only in the mid-1980s [1].

When titanium became commercially developed in the late 1940s, it was very soon viewed as a surgical implant material due to its good combination of mechanical and corrosion resistance and an excellent tissue compatibility [11].

The mechanical behavior of commercial pure titanium is generally considered to lie below that desired for total joint replacement. This led to the early introduction of annealed Ti-6Al-4V, which is still today the most used titanium alloy for biomedical device manufacturing [10]. Titanium and its alloy Ti-6Al-4V have been used as implant biomaterials since the 1950s and their alloy compositions and surface properties have been modified in numerous occasions to improve the function and duration of implants made from them in the human body [9]. Since then, other new titanium alloys for biomedical applications have been included in ASTM standardizations [1].

Titanium and its alloys cover a huge range of applications in the medical area. Some of them are: dental implants and parts for orthodontic surgery, joint replacement parts for hip, knee, shoulder, spine, elbow and wrist, bone fixation materials (nails, screws, nuts and plates), housing devices for pacemakers and artificial heart valves, surgical instruments and components in high-speed blood centrifuges [9]. Titanium implants with specially prepared porous surfaces aid the ingrowth of bone, which results in stronger and longer-lasting bonds between bone and implant [8].

A metal's ability to be formed, machined and polished is very important in metallic implant materials, as these metals must be capable of being utilized with state-of-the-art metallurgical techniques [11]. In addition, the orthopedic and dental implants are subjected to a complex interaction of mechanical and chemical-biological components: High mechanical loads such as friction and wear together with multiaxial, multistep fatigue in the body electrolytes (proteins, enzymes, salts) that are very corrosive [13]. Thus, the implant device must remain functional during its expected performance life; it must not be degraded with time in the body through fatigue, fretting, corrosion, or impact loading. Titanium and its alloys meet all of these requirements [11].

In the body, where it is critical that an implant possesses as similar as possible properties as the part it replaces, the compatibility of the elastic modulus between the implant and the bone is of great importance to its long-term performance. Surgical implants must be stronger than the bone and their elastic modulus must be close to that of the bone. A low Young's modulus equivalent to that of cortical bone is simultaneously required in order to avoid bone absorption [16] which titanium possesses, as its modulus of elasticity is comparatively lower than that of other metals used for implants [11].

The yield strengths of titanium and its alloys vary between 207 and 1379 Mpa, while bone has a maximum strength of 83 to 117 Mpa. The Ti-6Al-4V extra-low-interstitial (ELI) alloy, with a minimum yield strength of 827 Mpa, provides a great performance in critical applications such as hip prostheses [11].

The density of titanium, 4.51 g/cm^3 , is half that of other implant metals. The low weight of titanium implants is especially important for older people or those with weaker builds (e.g. children). The implants' light weight provides greater comfort and improves the ability to function of the recipients [11].

The value of titanium in biomedical applications lies in its inertness in the human body (resistance to corrosion by body fluids) [8]. Titanium is resistant to general corrosion, pitting attack, and crevice corrosion, which occur in several other alloys as a result of contact with aggressive organic fluids. Implants made of other alloys require to be replaced every seven to ten years due to degradation but titanium implants are expected to last over 20 years. It is of course of great importance to the patient to avoid as much as surgery as possible, therefore, a properly designed titanium implant must be functional (easily sterilized, positioned, and attached) in order to shorten the length of surgery [6].

Figures 2.5 and 2.6 show the relationship between the rotating bending fatigue limit and the elongation up to fracture and that between the fatigue strength and Young's modulus respectively for various metallic biomaterials. The rotating bending fatigue strength increases with the elongation up to fracture. The rotating bending fatigue strength is relatively higher and Young's modulus is relatively low in $\alpha + \beta$ titanium alloys [14].

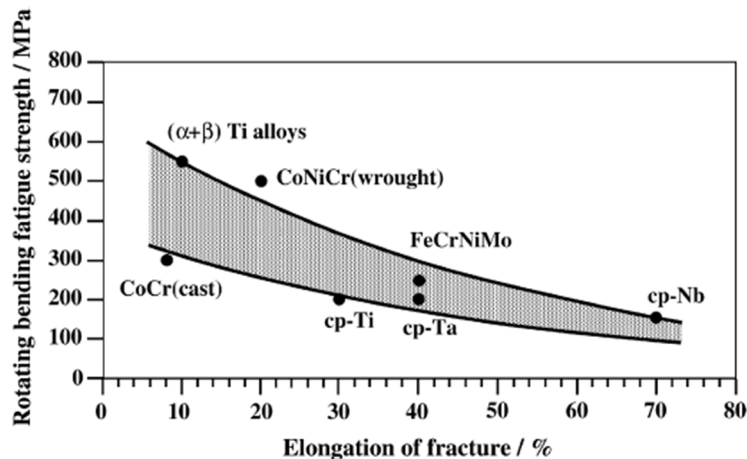


Figure 2.5: Elongation at fracture as a function of the fatigue strength of metallic biomaterials [14].

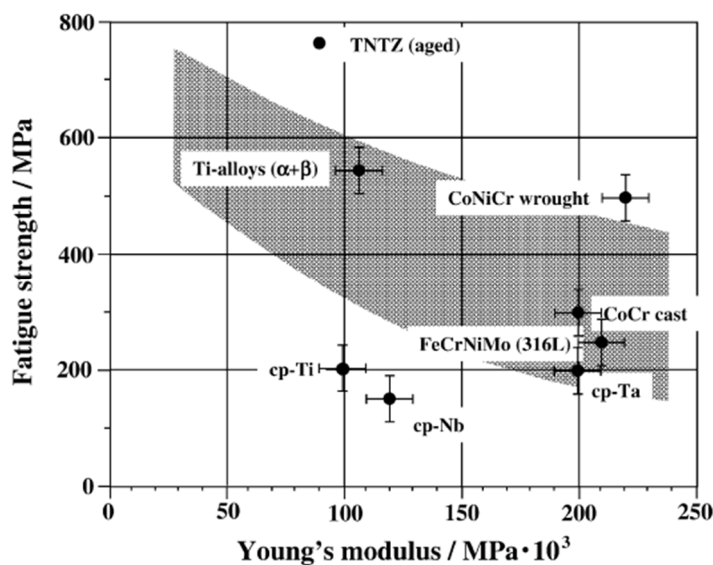


Figure 2.6: Fatigue strength and Young's modulus of each metallic biomaterial TNTZ means low modulus β type titanium alloy, Ti-29Nb-13Ta-4.6Zr [14].

Although titanium and its alloys (mainly Ti-6Al-4V) have an excellent reputation for corrosion resistance and biocompatibility, there are some long-term performance concerns due to release of aluminium and vanadium which can be found in the Ti-6Al-4V alloy [9]. Further studies have shown the release of both V and Al ions from Ti-6Al-4V alloy might cause long-term health problems, such as peripheral neuropathy, and Alzheimer diseases [9]. In addition, to its elemental state, vanadium oxide V_2O_5 (which is present at the surface) is also toxic. This has caused the biocompatibility of this alloy to be questioned which has led to further studies [9].

New alloys were created in response to concerns of potential cytotoxicity and adverse tissue reactions caused by V. This alloys showed similar properties to Ti-6Al-4V [1].

Fretting fatigue may occur at the contact area of two bodies, for example, between bone plate and screw [16]. It is important to consider this for biological applications and titanium has proved to have poor shear strength, making it less desirable for bone screws, plates and similar applications [9]. Titanium also tends to suffer severe wear when it is rubbed with itself or with other metals. Titanium-based alloys that have a high coefficient of friction can lead to formation of wear debris (dust residues) that can cause an allergic reaction on the living tissue and result in inflammatory reactions causing pain and the loosening of implants due to osteolysis [9]. Besides, it is generally believed that the biological effects of wear debris should be considered separately from the biocompatibility of the implants. To avoid such wear debris toxicity, the wear resistance should be improved [1].

Figure 2.7 shows a Ti-550 McIntosh tibial plateau removed from the left knee of a 67-year-old patient suffering from rheumatoid arthritis after two years because of pain. The figure shows that the component has worn as a result of contact with the femoral condyle [19].

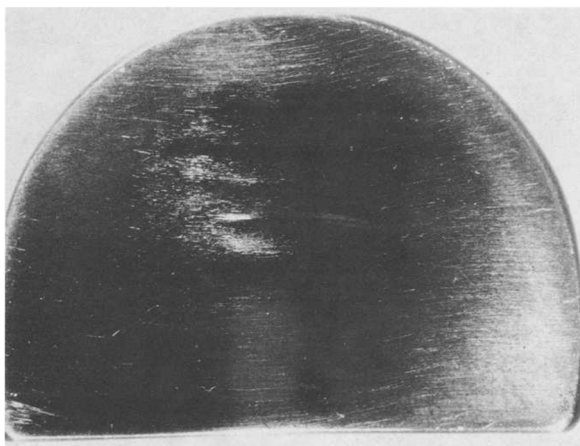


Figure 2.7: Ti-550 McIntosh tibial plateau showing wear [14].

The wear is an important problem for titanium alloys used in biomedical applications that should be improved. Surface modification techniques are commonly applied on them. Surface hardening is one of the most effective ways of improving the wear

resistance of titanium alloys. Several techniques such as oxidizing, nitriding, electroplating, PVD/CVD coating, thermal spray, etc. have been investigated to accomplish this goal [16].

3. NITRIDING OF TITANIUM AND TITANIUM ALLOYS

In spite of their high strength, low density, and good corrosion resistance, the usefulness of Ti alloys in general engineering components is often limited by their poor wear resistance. If the alloy undergoes sliding or fretting, adhesive wear can make it fail unless appropriate surface engineering is carried out [1].

Also, long-term performance of surgical implants is often conditioned by surface properties. The poor tribological properties of titanium and its alloys, such as low wear resistance leads to a reduced service life of the implants. This problem can be solved again through surface engineering. The performance of orthopedic devices made of titanium can be prolonged several times beyond their natural capability.

Various surface treatments have been explored for improving the tribological properties of titanium and its alloys [8].

Surface modification techniques where the surface structure is changed through physical deposition methods (ion implantation, laser and electron beam treatment, plasma spray coating) and thermochemical surface treatments (where both the surface composition and structure are changed by diffusion) such as nitriding, carburization and boriding have been used to improve the surface hardness and the wear resistance of titanium alloys [8].

The nitriding process will be discussed and especially the plasma nitriding process which has been very successful and has received a great deal of interest during the last 10 years. Then nitriding process on titanium and titanium alloys which are used mainly for biomedical application will be mentioned briefly.

3.1 Nitriding Process Properties

The process of nitriding and its derivative processes are seen today as a future surface enhancement technique for many ferrous and nonferrous metals [18]. Interest in the subject of nitriding has grown even more as a recognized and proven surface engineering process. Adding to this (and particularly during the past 10 years) it has

been recognized as a very simple process without serious problems such as the problem of distortion. The process of nitriding, while not distortion free, is a process that can cause only minimal distortion compared to that seen on other surface treatment process techniques such as carburizing and carbonitriding, which involve higher process temperatures as well as a quench from a high austenitizing temperature [20].

The main reasons for nitriding are:

- To obtain high surface hardness.
- To increase wear resistance and antigalling properties.
- To improve fatigue life.
- To improve corrosion resistance.
- To obtain a surface that is resistant to the softening effect of heat at temperatures up to the nitriding temperature [21].

There have been developments in the applications area of the nitriding process. The automotive industry has shown serious interest in the use surface enhanced high-strength low-alloy to reduce material costs as well as giving a good performance. Still, the majority of the work on all of the process methods and process metallurgy is still dedicated to ferrous materials and only a small amount of research work into nonferrous materials such as aluminum and titanium. One of the areas of investigation with nonferrous materials is conducted on the nitriding surface treatment of titanium to form a nonbrittle surface layer of titanium nitride [20].

Nitrogen is in the periodic table of nonmetals in Group IVA, along with four other nonmetals. It will readily form gases with both hydrogen and oxygen. In addition, it is diffusible into metals especially at low temperature and it will not only diffuse, but also react with metals with which it can form nitrides. Nitrogen is colorless, odorless, and tasteless. I should not be breathed although it is not considered to be a poisonous gas, it is actually considered to be an almost inert gas. This is not quite true because it will react with oxygen, hydrogen, and certain other metals to form nitrides.

Nitrogen is generally obtained for gas nitriding by the decomposition of ammonia in the following reaction sequence during the gas nitriding procedure using heat as the method of decomposition and the material as the catalyst: $2\text{NH}_3 \rightleftharpoons \text{N}_2 + 3\text{H}_2$ [20].

The nitriding process requires perhaps the lowest temperature range of all the thermochemical diffusion techniques: 315 °C to 540°C. However, the higher the nitriding process temperature, the greater the potential for nitride networking to occur (Figure 3.1) [20].

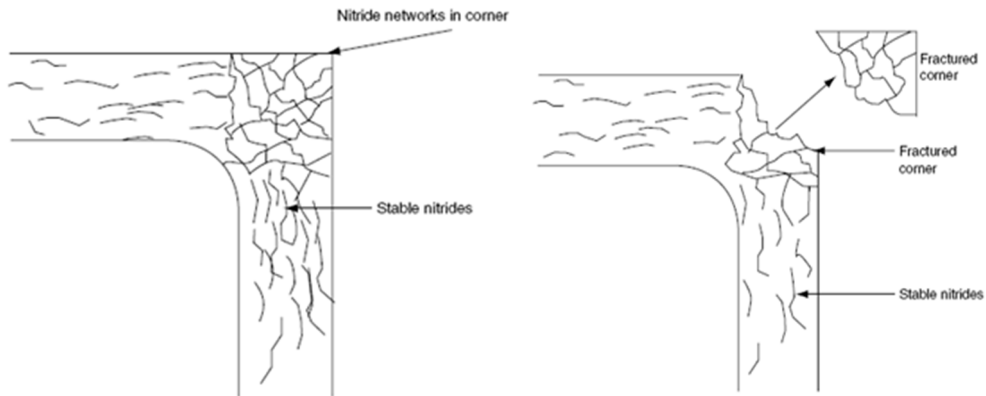


Figure 3.1: A schematic illustration of the corner fracturing due to the excessive nitride networks [20].

If the nitride network is allowed to form, then the nitriding case will be extremely brittle and might easily chip as shown in Figure 3.1. particularly at sharp corners. This means that both temperature control and gas flow control are of great importance to the success of both the surface metallurgy (compound zone) and the diffusion zone (the area beneath the formed surface compound zone in which the stable nitrides of the nitride- forming elements are formed) (Figure 3.2).

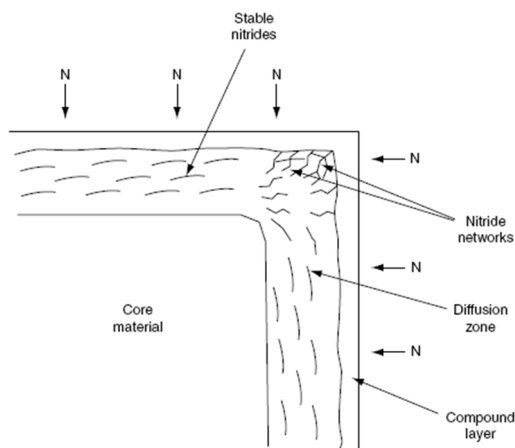


Figure 3.2: Illustration of nitride networking [20].

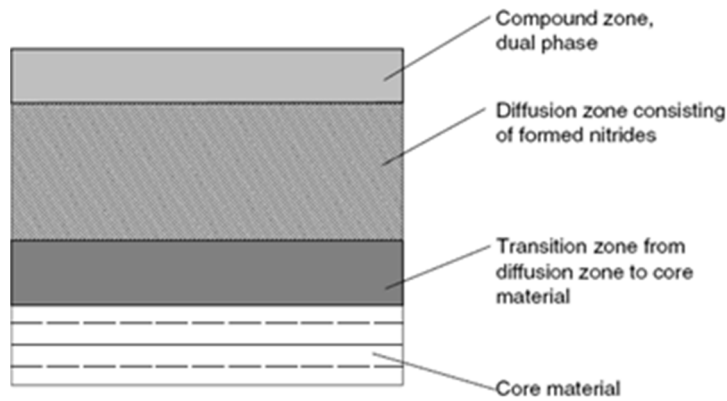


Figure 3.3: A typical nitrided structure [20].

The control of the compound layer thickness will depend on the following process parameters:

- Process time.
- Process temperature selection.
- Process gas composition.
- Gas dissociation (if gas nitriding).
- Steel composition.

Strict control of these areas will determine the thickness and quality of the compound layer. The dilution method of nitriding and FNC gives a very precise control over the process parameters. In order to accomplish this and control the process, precisely the use of a combination of a PC and a programmable logic controller is necessary [20].

Some of the problems commonly encountered in nitriding are:

- Low case hardness or shallow case.
- Discoloration of workpieces.
- Excessive dimensional changes.
- Cracking and spalling of nitrided surfaces.
- Variations in percentage of ammonia dissociation.
- White layer deeper than permitted.
- Plugging of exhaust lines and pipette lines.

Knowing the causes of these problems should help to avoid, prevent, or correct them [21].

3.2 Types of Nitriding

There are three basic nitriding processes which greatly interest engineers and metallurgical process engineers:

- Gas Nitriding (Dissociated ammonia).
- Salt Bath (Liquid) Nitriding.
- Plasma Nitriding [22].

Advantages and disadvantages of nitriding methods are compared in Table 3.1.

Gas Nitriding, being the earliest method applied in industry [23], is a case-hardening process through which nitrogen is introduced into the surface of a solid alloy by holding the metal at a suitable temperature in contact with a nitrogenous gas, usually ammonia. However, quenching is not needed for the production of a hard case [21].

Atomic nitrogen [N] is obtained through the partial catalytic cracking of ammonia, according to the following reaction: $2\text{NH}_3 \rightleftharpoons \text{N}_2 + 3\text{H}_2$ [23].

Traditionally, control of the gas nitriding process was done by monitoring the ammonia dissociation rate, which, depends on temperature and on atmosphere flow [23].

The modern, gas nitriding process employs pure ammonia or ammonia with one or two additive gases and is controlled by the nitriding potential instead of the dissociation rate. The nitriding potential determines the equilibrium concentration of nitrogen in the material surface, which cannot be exceeded. Gas Nitriding can be done in either one or two stages. The main purpose of the two-stage process (known also as the Floe process) is to reduce the thickness of a formed compound zone, and to produce deeper total case depths than the ones obtained from a single-stage process [23]. It is used for applications that require a more precise control of the surface compound layer [20].

Liquid nitriding which has become a generic term for a number of different fused-salt processes, is a subcritical (below the critical transformation temperature) case-hardening process which operates at the same temperature range as gas nitriding. Therefore, processing of finished parts is possible because dimensional stability can be maintained. Operating at these subcritical temperatures, the treatments are based on chemical diffusion and influence metallurgical structures mainly through

absorption and reaction of nitrogen. The case-hardening medium is a molten, nitrogen-bearing, fused-salt bath containing either cyanides or cyanates [21]. Process control variables of the salt bath nitriding process are time, temperature and salt chemistry [20].

Liquid nitriding processes are not suitable for many applications that require deep cases and hardened cores. For these applications, the gas nitriding process may be preferred. Anyhow, these processes have successfully replaced other types of heat treatment on a performance or economic basis. In general, the uses of liquid nitriding and gas nitriding are similar, and at sometimes even identical. Both processes provide the same advantages: improved wear resistance and antigalling properties, increased fatigue resistance and less distortion than other case-hardening processes which employ heating at higher temperatures [21].

Table 3.1: Comparison of advantages and disadvantages of nitriding methods [21].

| Method | Advantages | Disadvantages |
|---|---|--|
| Salt-bath nitriding | <ul style="list-style-type: none"> ·Rapid Heating and processing ·Ease of obtaining good quality layers on low-carbon and low-alloy steels(if bath composition well -controlled) ·Possibility of quenching parts immediately after process | <ul style="list-style-type: none"> ·No in-process control ·Limited to those applications that can be heated to higher temperatures without losing core hardness ·Short processes ·Only requires thorough washing to remove salt residues ·Health hazard and expensive waste-disposal problems ·No possibility of masking |
| Traditional Gas Nitriding | <ul style="list-style-type: none"> ·Low temperature in comparison with carburizing ·Simple control techniques | <ul style="list-style-type: none"> ·Controlling parameter (ammonia dissociation rate) inadequate for precise process control ·Problems with meeting zero white layer (where required) |
| Gas Nitriding controlled by nitriding potential | <ul style="list-style-type: none"> ·Precise control of white layer thickness and phase composition ·Full automation ·Total integrated control of all process variables and functions ·Predictability and repeatability of nitriding results ·Meeting zero white layer (where required) possible ·Ease and simplicity of operation ·No finishing, grinding required low temperature nitriding possible | <ul style="list-style-type: none"> ·Masking requires plating or application of protective pastes ·Stainless steels require special activation techniques |
| Plasma Nitriding | <ul style="list-style-type: none"> ·Simple mechanical masking of surfaces to be protected from nitriding ·Ease of surface activation of stainless steels by cathodic sputtering ·Low-temperature nitriding possible | <ul style="list-style-type: none"> ·Difficult temperature control and measurement ·Poor temperature uniformity ·Process requires frequent human monitoring ·Results critically sensitive to part geometry and arrangement in furnace |

3.2.1 Plasma nitriding

Plasma based technology can be used for many process applications, which include the treatments of a metal, plastic, or other surface treatment methods.

Plasma nitriding, is a method of surface hardening that uses glow discharge technology to introduce nascent (elemental) nitrogen to the surface of a material which then diffuses [22].

Since the mid-1960s, nitriding equipment using glow-discharge technology has been commercially available [21]. The use of plasma nitriding as a process system has been very successful during the past 10 years and its acceptance by engineers and metallurgists has experienced a great growth. It is now seen not so much as a new process, but as an accepted process that has a great deal to offer in terms of repeatable and consistent metallurgy [20]. The process was originally named glow-discharge nitriding but is now generally referred to as ion, or plasma nitriding. The term plasma nitriding is the most widely used nowadays [21].

Among general applications requiring metallurgical properties obtainable by ion nitriding are:

- Structural elements subject to cyclic loading.
- Workpieces requiring precision dimensions.
- Components subject to sliding wear.
- Parts exposed to mild corrosion.

Metallurgical properties required by these applications are used frequently in combination for such products as: plastics processing machinery (screws and cylinders for plastic extrusion), automotive engine (engine components), transmission (synchronizer components for transmissions), chassis and accessory components, marine steam turbines (reduction gears), cold-forming tools (deep-drawing punches) and hotforming tools (hot-forging dies) [21].

Plasma nitriding uses voltage applied between two electrodes in a sealed chamber to ionize gas under low pressure. Positive ions are accelerated toward the workpieces which act as a cathode. There, the potential drop emits visible radiation (popularly called “glow”). The process gas contains nitrogen and its positive ions hit the treated surface when a potential of several hundred volts is applied [23]. In this way, the plasma completely covers the cathode, exposing the surface of the whole work piece

to a flux of ions [24]. This ion bombardment process heats the workpiece and cleans the surface providing active nitrogen, which under the influence of the glow discharge, forms the nitrated case [22]. The addition of diffusive atoms improves the hardness of work pieces [24]. The inner wall of the chamber is the anode. A gas mixture containing nitrogen (usually nitrogen and hydrogen) is introduced into the chamber. During the process a pump continuously evacuates the gas to maintain a soft vacuum of between 0.1 and 10 mbar [23]. The pressure during the plasma process is measured by a pressure transducer [24]. The temperature of the work pieces is monitored by thermocouples used in combination with an insulation amplifier to separate the plasma voltage from their own temperature signal [24]. The treatment can be performed at temperatures as low as 350°C due to plasma activation (which does not exist in gas nitriding) [22]. The plasma generator generates the voltage for the plasma process. This voltage is typically between 400 and 800 V [24]. The principle of operation of the plasma nitriding furnace is shown in Figure 3.4.

During these last years, the pulsed plasma generation technique has been preferred for the plasma nitriding process. This technique is based on the ability to interrupt the continuous DC power at specific and variable time intervals. Through this pulse system used in combination with additional heating, a high temperature uniformity is obtained over all the work pieces in the furnace [24]. The pulse time of both power on and power off can be varied to suit the part geometry as shown in the Figure 3.5 [20].

The presence of plasma is easy to recognize because of the “glow”, as the flow of electrical current makes the gas glow. Figure 3.6 shows this glow effect in a plasma nitriding process [24].

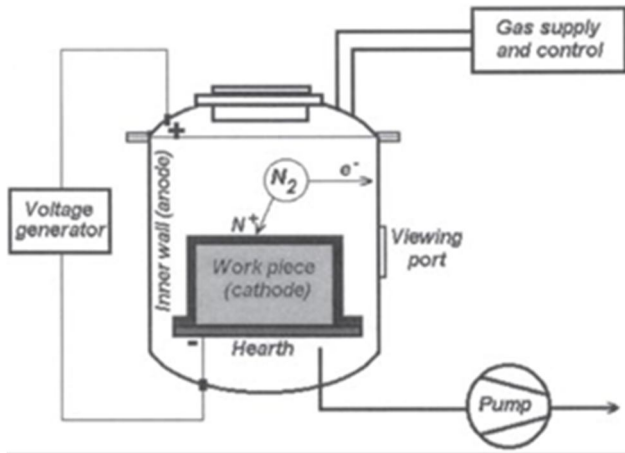


Figure 3.4: Principle of operation of a plasma nitriding furnace [23].

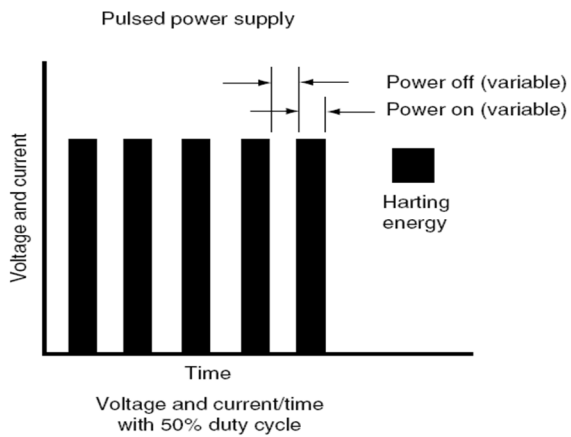


Figure 3.5: Variable-pulse duty cycle for DC pulsed plasma nitriding [20].

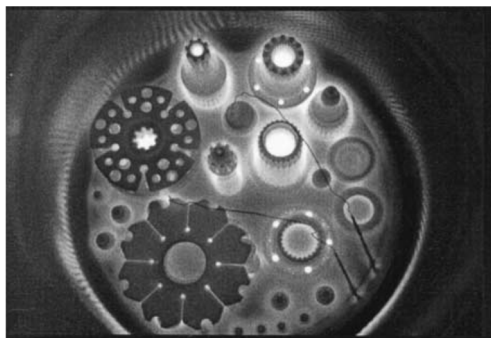


Figure 3.6: Photo of work pieces in a plasma nitriding process (wires are thermocouples)[24].

The surface metallurgy of a material can be manipulated through plasma nitriding, combining nitrogen and hydrogen and varying the ratios of the two gases [20].

Most of the thickness of the nitride case is the diffusion zone where fine metal/alloy nitride precipitates produce increased hardness and strength. Compressive stresses are also developed, as in other nitriding processes. The hardness resulting from ion nitriding is similar to ammonia-gas nitriding, but due to a lower processing temperature, the near-surface is usually harder. The hardness of the nitride case is determined by the concentration and size of the alloy nitride precipitates formed and the hardness of the parent material [21]. The thickness of the nitrided case and the compound layer are determined by process gas ratios, process time and temperature and material composition [20].

To make obtain a uniform surface metallurgy with consistent and repeatable results, all the following process parameters must be carefully and precisely controlled during the plasma nitriding process [20].

- Time
- Temperature of the workpiece
- Temperature of the process chamber
- Process gas flow (nitrogen, hydrogen, methane, and argon)
- Work surface area
- Support fixturing surface area
- Process power voltage
- Current density
- Power time on
- Power time off
- Process amperage
- Rate of temperature rise
- Process pressure (vacuum level) [20]

Nowadays, a computer and programmable logic controller are used to control all of the above-mentioned process parameters [20]. Excellent results may be obtained through plasma nitriding but a highly skilled, knowledgeable, and experienced operator is always required [23].

Plasma nitriding typically offers to the engineers and the metallurgists a number of advantages including: total absence of pollution, very good process control and reproducibility [24], total process automation [21], precise phase control of the nitrided surface layers and improved control of case thickness, possibility of selective nitriding by simple masking techniques, reduced nitriding time [21], lower surface treatment temperatures [24], lower distortion [21], process span that encompasses all subcritical nitriding, wide range of process gas composition possibilities [15], relatively low energy, gas consumption [21] and operating costs [20] and cleaning and activation of surfaces by initial sputtering [24].

The limitations or disadvantages of plasma nitriding include high capital cost (expensive furnace technology), need for precision fixturing with electrical connections, long processing times compared to other short-cycle nitrocarburizing processes, lack of feasibility of liquid quenching for carbon steels, the need to fixture parts to avoid localized overheating [21] and not being able to treat loose material [24]. Temperature uniformity and measurement can be problematic because the process is carried out in partial vacuum where the only viable means of heat transfer is radiation and temperature readings by a thermocouple in spaces between parts are not representative. Thermocouples may not touch electrically charged nitrided surfaces, unless measures are taken to isolate the thermocouple circuit from the load. Temperatures can be read using an optical pyrometer but correction factors must be applied, and these depend on the time of process because of changing emissivity with progressing surface coverage by nitrides. Results critically depend on part geometry and arrangement in the chamber. Certain minimum distances between parts must be maintained to prevent overheating [23].

3.3 Nitriding of Titanium

Nitriding of titanium and titanium alloys has been investigated for many years and is used effectively on a small scale for protection against wear. Through a very favorable phase equilibrium relationship between the elements this resistance can be obtained [25]. The nitriding of titanium and its alloys is nowadays a widely applied industrial practice [23].

Titanium causes less problems when compared with other elements like aluminum that can also benefit from surface hardening through nitriding. The thermal

expansion and electrical resistivity of titanium and of the TiN are practically identical. The oxidation limit, at 2.3×10^{-33} bar, although still very low, is much easier to handle in industrial conditions [23].

Nitrogen has a high solid solubility in α -Ti, and interstitial nitrogen provides a great increase in strength, as shown in Figure 3.7 [25].

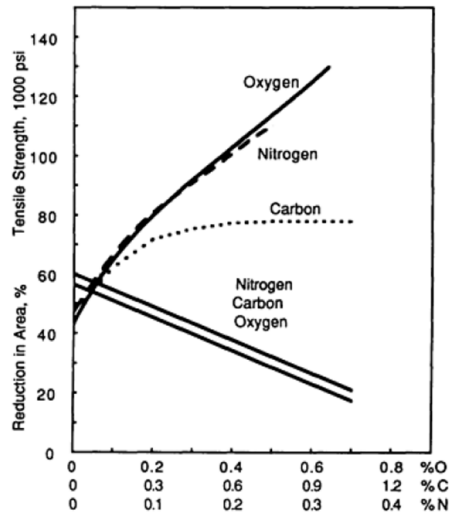


Figure 3.7: Effect of interstitial alloying elements on strength and reduction in area of iodide titanium [25].

Pure Ti exists at lower temperatures in a hexagonal α structure, which can be stabilized by nitrogen. The structures of nitrated layers depend on the type of the alloy and the process temperature. Depending on the composition, alloys can exhibit the hexagonal α structure, a body-centered cubic β structure or an $\alpha + \beta$ mixture. High-strength Ti alloys are typically of the $\alpha + \beta$ group [23].

Reference to a titanium-nitrogen equilibrium phase diagram illustrated in Figure 3.8, shows that above 12.7 wt% N, the compound Ti_2N is formed (tetragonal crystal structure and a hardness of ~ 1500 HV) at temperatures below $1100^\circ C$. At higher nitrogen contents, over a wide range of compositions, TiN is formed (NaCl-type crystal structure and a hardness of ~ 3000 HV). Nitriding produces a thin compound layer of TiN at the surface, above a thicker compound layer of Ti_2N , which is above a diffusion zone of nitrogen-strengthened titanium. At the surface opposed to what is obtained through oxidizing, a useful, hard compound layer is created [25]

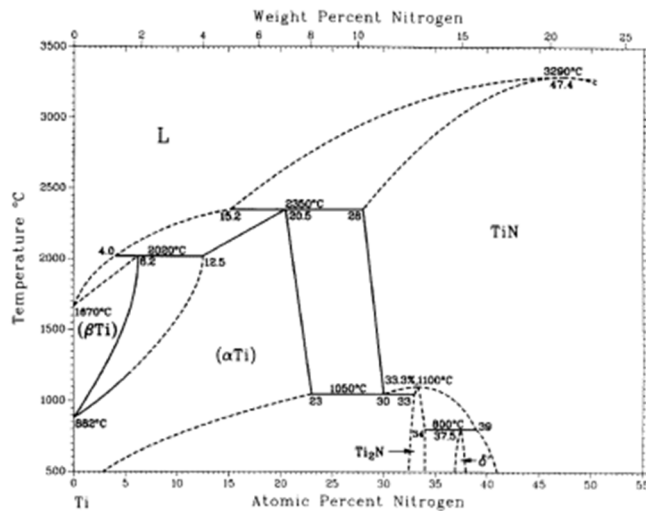


Fig 3.8: Ti-N Phase Diagram [23].

Hydrogen, has a great affinity with titanium, which causes an excess of this element in the surface layers of alloys treated in H₂-containing atmospheres, which is detrimental to ductility. However, hydrogen can be removed through heating in vacuum or an inert-gas atmosphere, after nitriding.

Nitrogen's diffusion coefficient on titanium is relatively low, so nitriding is carried out at relatively high temperatures (800° to 950°C), which can considerably reduce core strength, unless a more complex process is adopted. (E.g. A combination of nitriding and solution treatment, with a quench from the nitriding temperature, followed by a low-temperature aging anneal) [23].

In the Ti-6Al-4V alloy, contact of the surface with atomic nitrogen (both in a gas or plasma process) leads to the formation of a compound layer, composed of δ-TiN (1-x) and ε-Ti₂N nitrides. Because they do not dissolve aluminum, the latter is displaced toward the diffusion zone, which contains an increased proportion of the alpha phase. When temperature decreases, dispersed nitrides may precipitate in this zone increasing hardness. The growth of the diffusion layer depends mainly on the temperature and duration of the process, regardless of whether this is gas or plasma nitriding. However, the composition of the process atmosphere can affect the growth of the compound layer. An increase of the H₂ content in the plasma process and of NH₃ in the gas process makes the nitride zone grow faster [21].

3.3.1 Plasma nitriding of titanium

An alternative way to introduce and diffuse nitrogen into the surface of titanium and its alloys is to use plasma. Nitrogen, nitrogen-hydrogen, nitrogen-argon, or cracked ammonia may be used as the treatment gas. Nitriding may be achieved at temperatures down to 300 °C, but normally, the process is carried out at hotter temperatures, in the range of 700 to 900 °C because the value of processing at low temperatures is doubtful due to the very thin (1 μm) hardened region obtained. The plasma process uses and exhausts smaller volumes of gas than any gaseous treatment. However, an experience technician is needed to monitor and control the temperature throughout the process. Because all the heat input comes from the plasma, sections of component with significantly different surface area-to-volume ratios may differ in temperature. The thicknesses of compound layers found adjacent to corners also differ from layers on continuous surfaces of workpieces. This effect is attributed to variations in the sputtering rates at these different points. Some well known successfully plasma-nitrided components include racing car steering racks, gears, and ball valves. Plasma nitrided components are ready for use directly after treatment and have the characteristic gold color of TiN [25].

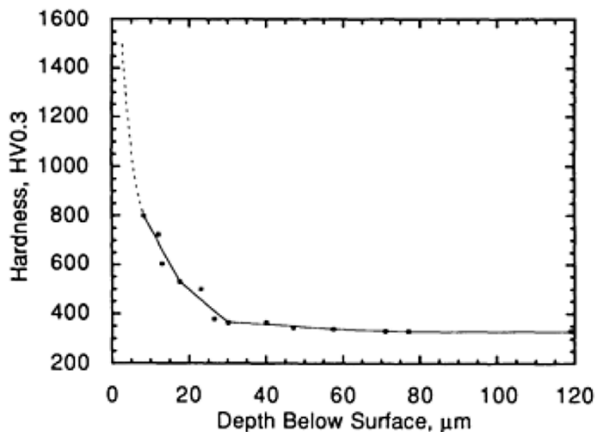


Figure 3.9: Hardness profile (Vickers, 0.3 kg load) from plasma-nitrided Ti-6Al-4V [25].

Nitriding titanium-base materials improves wear resistance significantly, being two the sources of these benefits; the hard surface compound layers of TiN and Ti₂N and the support given by the nitrogen-strengthened diffusion zone beneath them. A

typical hardness profile from plasma nitrided Ti-Al-4V is shown in Figure 3.9, in which the dashed line represents the hardnesses of the thin TiN and Ti₂N compound layers. The processing conditions used were 850 °C for 20 h in ammonia. A loss of about 10% of fatigue strength is associated with nitriding, but this can be mitigated designing the component appropriately [26].

In the study of Molinari et al. [27], the properties of DC Plasma nitrided Ti-6Al-4V alloy have been investigated. Plasma nitriding was carried out in a laboratory furnace at a tension range (V) of 400-430 with a gas composition (%) of 80N₂-20H₂ and under a current density (mA×mm⁻²) range of 0.12-0.15 and 8 mbar pressure, at temperatures of 700, 800 and 900 °C respectively for 24 hours.

The thickness of the nitrided layer which consists of both TiN and Ti₂N was observed about 1-2 μm for the sample nitrided at 700 °C, 3-4 μm for the sample nitrided at 800 °C and 5-7 μm for the sample nitrided at 900 °C. The thickness of the diffusion layer had a value of about 25 μm for sample nitrided at 700 °C, 40-50 μm for the one nitrided at 800 °C, and 75-90 μm for the one nitrided at 900 °C. The increase in the nitriding temperature is reported to increase the thickness of both the compound and the diffusion layer.

Microhardness profiles have shown that microhardness is increased by increasing nitriding temperature and decreased by depth. It has been clarified that the effect of the nitriding and the nitriding temperature depends on the wear mechanism which takes place during the test. At low loads and low sliding speeds (wear is determined by the resistance of the compound layer) in order to maximize the resistance of this layer, the nitriding treatment has to be carried out at 800 °C.

The compound layer has optimal properties with respect to resistance to adhesion and microfragmentation. At high loads and high sliding speeds-when the alloy is exposed to delamination, the properties of the diffusion layer tend to be as important as or more important than the compound layer since the compound layer is destroyed rapidly, the nitriding temperature should be as high as possible (900 °C in this investigation) in order to enhance the hardening and strength of diffusion layer.

In the study of Yıldız et al. [7], DC plasma nitriding treatment of Ti-6Al-4V has been performed in a gas mixture of 25%Ar-75%N₂, at the temperature range of 650-750 °C, for process times of 1-4 h under a pressure of 5×10² Pa. After the nitriding, a

compound layer was obtained on the material surface, which consists of ϵ -Ti₂N and δ -TiN phases by depending on the nitriding temperature and time. The densest phase is TiN and as both the treatment temperature and time increases, the intensity of the δ -TiN phase increases. For the specimen nitrided at 650 °C, the low intensity of TiN phase shows that the treatment temperature limits the formation of TiN phase. ϵ -Ti₂N phase which has a low intensity, forms at the lower temperatures than 700 °C and disappeared with increasing nitriding time and temperature. The thickness of compound layer formed at temperatures lower than 700°C, is too thin (about 1-2 μ m) to observe. Thickness of compound layer is about 2-3 μ m for the samples nitrided at 700°C for 4 hours and about 3-5 μ m for the samples nitrided at 750°C for 4 hours.

Compound layer thickness increased with increasing nitriding time and temperature. During the wear tests, the contact wear area decreases between pin and surface with increasing surface hardness due to hard TiN layer formed on the surface. As treatment time and temperature increase, the surface hardness is increased, as a result, the wear rate decreases and wear resistance is increased.

Yılbaş et al. [28] also have studied the properties of DC plasma nitrided Ti-6Al-4V alloy samples. The process is performed in an N₂-H₂ (8:1) plasma within the DC bias voltage range of 400-700V, under the pressure range of 0.46-0.51 kPa during a process time varying between 54-72 ks. The temperature of the samples during nitriding was varied in the range 450-520°C. δ -TiN and ϵ -Ti₂N phases are detected in the structure of the nitrided samples. The concentration of δ -TiN phase decreases with increasing depth while α -Ti concentration increases. The microhardness decreases with the increasing distance from surface and increases as the process temperature increases due to solid solution formed by nitrogen, which results in hardening at dislocation-pinning effects. High temperature nitriding results in improved wear resistance than low temperature nitriding and untreated, due to increased N₂ diffusion process and hardness.

In the investigation of Chen and Jaung [29], DC plasma nitriding of Ti-6Al-4V samples was carried out by using a DC power supply, at a nitriding temperature, varied from 500 to 900°C, at a working pressure of 2.66×10^2 Pa for each nitriding duration of 20h with a gas composition (%) of 75N₂-25H₂. As observed from XRD patterns, the threshold nitriding temperature is 600°C for the ϵ -Ti₂N and is 700°C for δ -TiN to form on Ti-6Al-4V. From the optical graph showing the cross-

section of the specimens nitrided, the surface layers of both specimens nitrided at a lower temperature of 600°C are unable to be observed. Surface layers grown on the nitrided specimens at higher temperature consists of two sublayers: namely δ -TiN on the top and ϵ -Ti₂N below, as also detected from XRD.

As nitriding process temperature increased, thickness of nitrided and diffusion layer is increased also. Hardness tests again have shown that as nitriding temperature increases, surface hardness increases.

Raman et al. [30] have investigated the properties of DC plasma nitrided Ti-6Al-4V samples. The nitriding process was performed at 520°C in two environments (pure nitrogen and a mixture of nitrogen and hydrogen with a gas composition (%) of 75N₂-25H₂) for two different time periods (4 and 18h). In nitrided samples two new phases ϵ -Ti₂N and δ -TiN are detected. In samples nitrided in pure nitrogen gas environment, absence of ϵ -Ti₂N phase peaks which were present in the samples nitrided in nitrogen–hydrogen mixture environment are realized and more TiN peaks are observed, compared to the samples nitrided at nitrogen-hydrogen gas mixture.

The samples nitrided for 18 h exhibited relatively thicker nitrided layer compared to the samples nitrided for 4 h. Increase in nitriding time resulted in increase in the thickness of the nitrided layer.

As the nitriding was done at a relatively lower temperature of 520°C, compound layer and diffusion layer could not be distinguished in this study. The samples nitrided in gas mixture environment exhibited higher hardness compared to the samples nitrided in pure nitrogen gas environment. The dependence of the hardness on the nitriding gas composition has been attributed to the increased rate of nitriding when nitrogen–hydrogen gas mixture was employed.

In the study of Zhecheva et al. [31], plasma nitriding process on Ti-6Al-4V alloy was carried out at 700 °C for 6h, at 900 °C for 6h and 900 °C for 14h. XRD patterns and SEM micrographs of samples nitrided at 900 °C and 700 °C for 6 hours show the presence of TiN (on the top) and Ti₂N phases on the surface of plasma-nitrided Ti-6Al-4V. A clear boundary between the compound and the diffusion layer can be seen. Underneath the compound layer is the diffusion zone that consists of an interstitial solution of nitrogen in the hcp α -titanium phase. As the plasma nitriding time and temperature increases, the diffusion layer thickness of Ti-6Al-4V increases.

The thickness of the nitrided layers depends also on the voltage and the gas pressure when plasma nitriding is performed. An increased rate of nitriding, increased surface hardness and increased thickness of compound layer (μm) is observed when nitrogen–hydrogen gas mixture of (%) $80\text{N}_2\text{-}20\text{H}_2$ was employed compared to pure N_2 gas environment for the plasma nitriding for 14h at 900°C .

Batista et al. [32] investigated Ti-6Al-4V alloy samples that were plasma nitrided by DC triode plasma nitriding method at 600°C , 650°C , 700°C and 750°C for 120 min and at 800°C for 100 min. For plasma nitriding at 700°C , two bias voltages were used: -500 V and -2000 V . No thin, continuous titanium nitride layer on the surface could be identified on samples treated at 600°C , 650°C and at 700°C for both bias voltages. The formation of titanium nitride (Ti_2N only) was detected by XRD analyses at nitriding temperatures of 700°C , 750°C and 800°C ; as the nitriding temperature is increased, the amount of titanium nitride formed also increases. For the Ti-6Al-4V alloy, hardening seems to be mainly accomplished by incorporation of nitrogen in the $\alpha\text{-Ti}$ phase at temperatures up to 700°C as the formation of a titanium nitride layer on the surface could not be detected by SEM. For these conditions, the maximum surface hardness ($560\text{--}600\text{ HV}_{0.05}$) and nitrided layer depth ($30\text{--}40\ \mu\text{m}$) were achieved at 700°C . At 800°C , a titanium nitride layer (Ti_2N) was formed on the surface.

In the investigation of Nolan et al. [33], plasma nitriding of Ti-6Al-4V was performed at 850°C for 8 h using a 100% N_2 atmosphere at a pressure of $300\text{--}400\text{ kPa}$. The major XRD pattern for the plasma nitrided sample is that of the Ti_2N phase, with only minor pattern of TiN phase. (not clear due to the overlap with Ti_2N peaks). The microhardness depth profiles show that the substrate immediately beneath the nitride layer has significantly high hardness ($>800\text{ HV}_{0.02}$) in the plasma nitrided sample. This confirms the expectation that a nitrogen diffusion layer in the plasma nitrided sample provides increased strength of the $\alpha\text{-Ti}$ phase, presumably as a result of solid solution and/or precipitation hardening. According to the wear tests on the Ti-6Al-4V, the plasma nitrided surface has not been penetrated at a lowest normal load of 10 N . At a normal load of 20 N , the plasma nitrided coating is only starting to breakdown locally. The wear track for plasma nitrided sample after testing at 40 N load is 0.6 mm wide. Another point of interest is the observation that the TiN phase appears to form only very localized and small deposits at the very surface of the

compound layer in the plasma nitrated sample. As a result, the contribution of TiN to wear resistance of the plasma nitrated sample is likely to be negligible.

4. PHYSICAL VAPOR DEPOSITED (PVD) COATING ON TITANIUM AND TITANIUM ALLOYS

In recent years, PVD coatings have been used in many tribological situations, due to their several advantages by improving surface properties, diminishing friction force in the contact and diminishing the project costs, among others.

4.1 Physical Vapor Deposition (PVD) Process Properties

Physical Vapor Deposition (PVD) processes are atomistic deposition processes in which material is vaporized from a solid or liquid source in the form of atoms or molecules, transported in the form of a vapor through a vacuum or low pressure gaseous (or plasma) environment to the substrate where it condenses [34].

These processes are typically used to deposit films with thicknesses in the range of a few nanometers to thousands of nanometers; however they can also be used to form multilayer coatings, graded composition deposits, very thick deposits and freestanding structures. The substrates can range in size from very small to very large. Typical PVD deposition rates are 10–100Å (1–10 nanometers) per second.

PVD processes can be used to deposit films of elements and alloys as well as compounds using reactive deposition processes. In reactive deposition processes, compounds are formed by the reaction of depositing material with the ambient gas environment such as nitrogen (e.g. titanium nitride, TiN) or with a co-depositing material (e.g. titanium carbide, TiC) [35].

Arc vapor deposition is a PVD technique which uses a high current, low-voltage arc to vaporize an electrode and deposit the vaporized material on a substrate. The vaporized material is highly ionized and usually the substrate is biased in order to accelerate the ions (“film ions”) to the substrate surface.

If the vaporization primarily occurs from the cathode surface by arc erosion the system is called a continuous cathodic arc source. The cathode can be molten or solid with a water cooled solid cathode (“cold cathode”). The cold cathode source is the most common cathodic arc source for film deposition. In order for a stable arc to

form there must be a minimum current passing through the arc. Minimum arc currents vary from about 50–10A for low melting point materials such as copper and titanium to 300–400A for refractory materials such as tungsten. Most of the arc voltage drop will occur near the cathode surface. The arc voltage can be from about 15 volts to 100 volts depending on the ease of electron motion from the cathode to the anode [36].

4.2 Physical Vapor Deposited TiN Coating

TiN is known to possess high hardness, good tribological properties, excellent chemical stability and biocompatibility. Numerous deposition techniques have been developed to achieve quality TiN films which has been extensively utilised to enhance wear and corrosion performance of Ti alloys .

Physically vapor deposited (PVD) TiN coatings became commonly available in the early 1980s from various sources [37].

Among the various processes in order to improve the surface properties of Ti-6Al-4V alloy, PVD can produce coating layers at lower process temperature and, therefore, it has the advantage of less detrimental effects on substrate mechanical properties. However, low-temperature processes tend to produce only very thin compound and shallow nitrogen diffusion layers. The limitation of the common use of this hard and thin coating especially in the case of machine elements is the load carrying capacity of the coating-substrate system and adhesion problems. The substrate must have sufficient hardness and flow strength to support the coating without plastic deformation when subjected to a high-intensity loading [36].

5. EXPERIMENTAL PROCEDURE

This study covers the investigation and characterization of surface properties that belongs to DC plasma nitrided and PVD coated Ti-6Al-4V alloy samples. Ti-6Al-4V disc samples of 2 cm in diameter by 0.60 cm thickness were grinded with 320, 500, 800, 1000, 1200, 2400 grit silicon carbide abrasive papers respectively and polished by MD-Nap cloth and silica solution before undergoing the surface processes.

5.1 Plasma Nitriding Process

DC Pulsed Plasma Nitriding of the Ti-6Al-4V alloy samples was carried out in a gas mixture of 75% N₂, 25% H₂, under the chamber pressure of 10 torr, with an applied DC voltage of 500V, at the cathode temperatures of 650 °C, 700 °C, and 750 °C, for the process time of 4 h. The close up view of the plasma nitriding process taking place is shown in Fig.5.1.

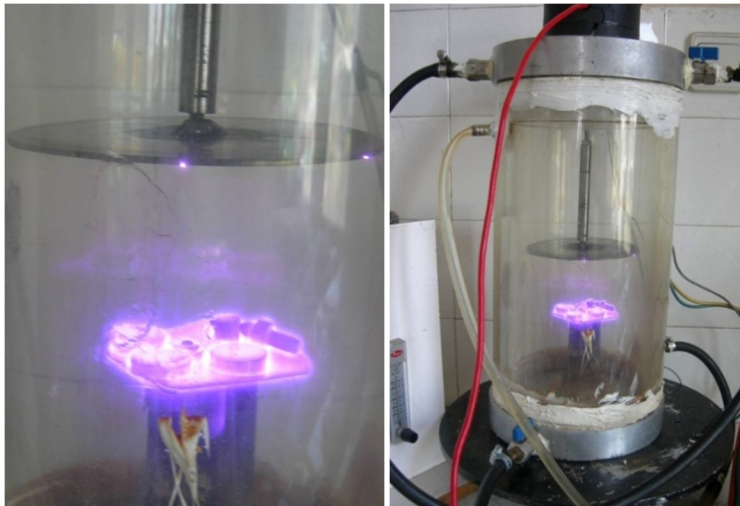


Figure 5.1: Plasma nitriding process.

5.2 PVD Process

TiN coating on the Ti-6Al-4V substrate was deposited by using cathodic arc PVD unit with a titanium cathode, with a bias voltage of 150V, at a temperature about 600°C, under the chamber pressure of $7,5 \times 10^{-3}$ torr, for 30 minutes. The arc current was set at 100 A and reactive gas (N_2) was bled in a volumetric flow of 30 scm.

5.3 Characterization Tests

The nitrided and PVD coated specimens were characterized in order to compare their surface properties after the processes. Additionally nitrided samples were investigated in order to describe the microstructural features as function of the treatment temperature.

Cross-sectional microstructure analysis is carried out by Leica DM600M optical microscope and TM-1000 Hitachi Scanning electron microscope (SEM). Before the microstructural analysis, a cut was performed to obtain the cross section of the samples. Then the samples which were mounted, were grinded with 800, 1000, 1200, 2400 grit silicon carbide abrasive papers respectively and polished with MD-Nap cloth and silica solution. After, etching was carried out to identify the microstructure by keeping the samples in a solution of 5%HF and 10% HNO_3 for 30 seconds.

Thin film XRD analysis of the specimens was carried out at a glancing angle of 2° in order to minimize the contribution of the structural constituents on the XRD pattern. XRD was conducted on each sample using a Philips PW 3710 diffractometer operating with $CuK\alpha$ source, in the 2θ range from 20° to 60° .

Penetration depth and intensity change of the nitrogen and other elements were examined by Glow Discharge Optic Emission Spectroscopy (GDOES) analysis with an average burning rate of $3 \mu\text{m}/\text{min}$.

Microhardness-depth profiles of the untreated, nitrided and PVD coated samples were obtained by CSM depth sensing microhardness tester at 50mN- 1000mN increasement load conditions on continuous multi cycle test mode.

Dry sliding tests of the untreated, plasma nitrided and PVD coated samples were carried out with a reciprocating wear tester using a 10mm alumina ball in contact with the surface. These wear tests were performed under a load of 2N for 10^4 cycles

with a stroke distance of 10mm at 23 ± 1 °C and with a relative humidity of 31 ± 3 %. Sliding tests in the simulated body fluid were carried out on the same conditions. Simulated body fluid is a solution that consists of pure water, NaCl, NaHCO₃, KCl, K₂HPO₄.3H₂O, MgCl₂.6H₂O, CaCl₂, Na₂SO₄, H₂NC(CH₂OH)₃, and HCl, with a pH of 7.4. Appearance of the worn surfaces and wear track areas were examined to understand the wear behaviour of Ti-6Al-4V depending on the nitriding temperature and to compare the wear behaviour of plasma nitriding and PVD processes. Thus, after testing, wear tracks were observed by Leica DM600M optical microscope and TM-1000 Hitachi scanning electron microscope. Wear track profiles were recorded by Dektak 6M Stylus profilometer. Relative wear resistance of the plasma nitrided and coated samples were calculated by the wear track areas obtained from the profiles.

6.RESULTS AND DISCUSSION

6.1 Cross Sectional Microstructure Analysis

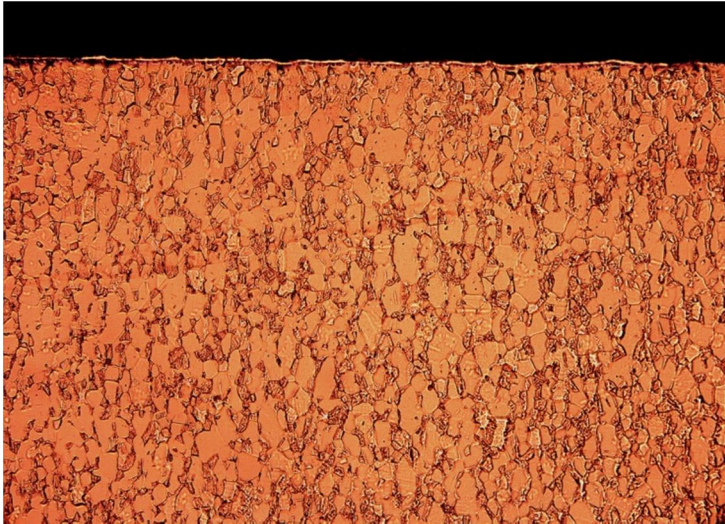
After the PVD process, the surface of the sample appeared smooth, bright and gold in colour, consistent with the typical appearance of TiN coatings. The plasma nitrided coatings were also golden in colour, but less bright and uniform than the PVD coatings.

The cross-section images of thenitrided (at 650 °C, 700 °C and 750°C) and PVD coated Ti-6Al-4V samples by optic microscope at 500x magnification are shown in Figure 6.1. On the samples nitrided at 700°C and 750°C, a very thin nitrided layer is detected whereas there can not be seen any nitrided layer on the sample nitrided at 650 °C. On PVD coated sample, TiN coating thickness is relatively high and TiN layer can be clearly distinguished.

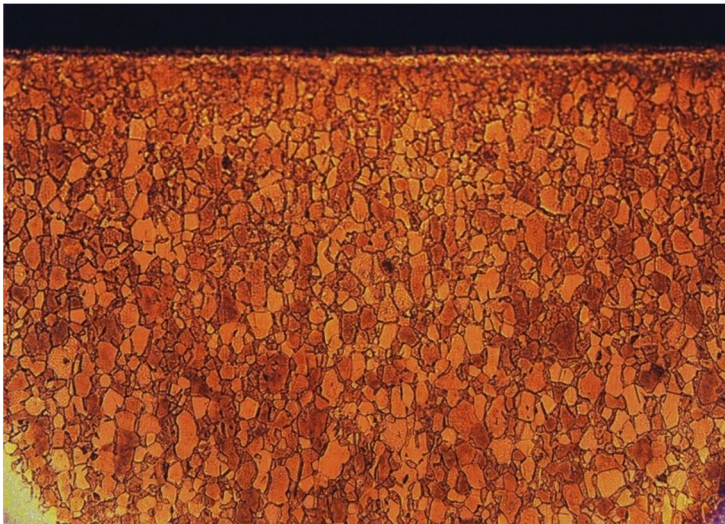


(a) Plasma nitrided at 650 °C, 500x.

Figure 6.1: Cross-sectional images of Ti-6Al-4V alloy specimens plasma nitrided at (a) 650 °C, (b) 700 °C, (c) 750°C, and (d) TiN coated by PVD taken by optic microscope at 500x.

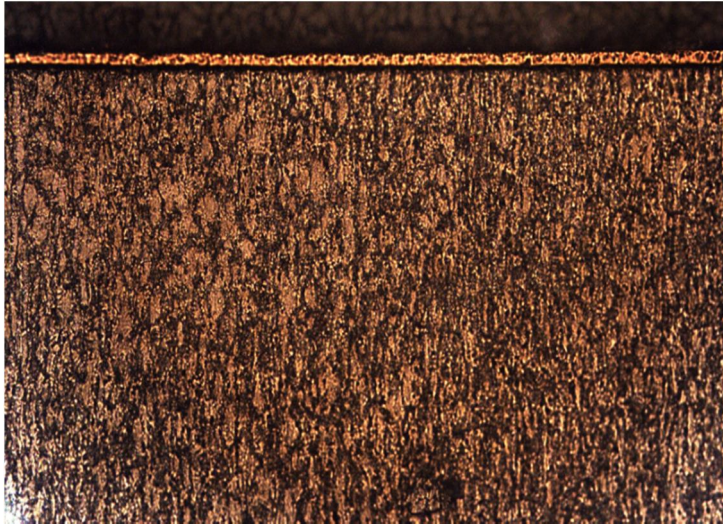


(b) Plasma nitrided at 700 °C, 500x.



(c) Plasma nitrided at 750°C, 500x.

Figure 6.1: (continued) Cross-sectional images of Ti-6Al-4V alloy specimens plasma nitrided at (a) 650 °C, (b) 700 °C, **(c)** 750°C, and (d) TiN coated by PVD taken by optic microscope at 500x.



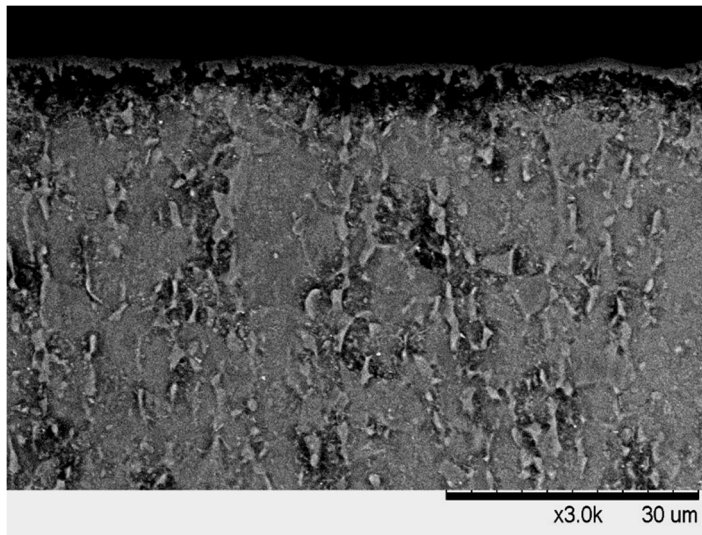
(d) TiN coated by PVD, 500x.

Figure 6.1: (continued) Cross-sectional images of Ti-6Al-4V alloy specimens plasma nitrided at (a) 650 °C, (b) 700 °C, (c) 750 °C, and (d) TiN coated by PVD taken by optic microscope at 500x.

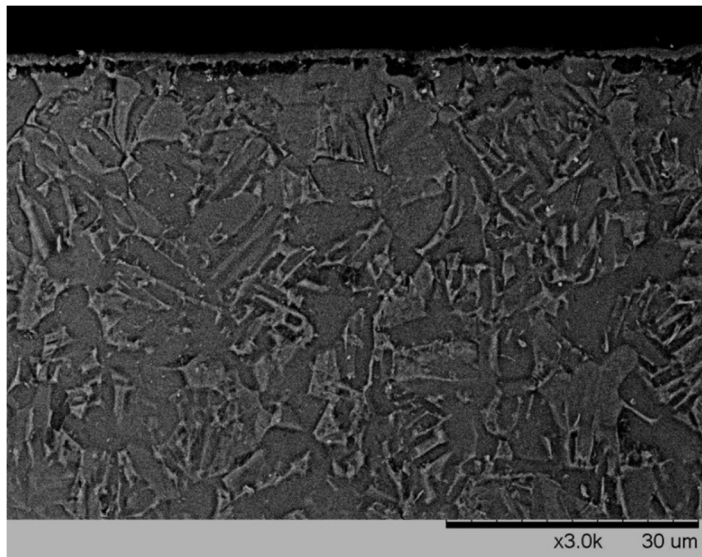
More accurate results are obtained by SEM images. Cross-sectional images taken by SEM at 3000x magnification of the nitrided and PVD coated Ti-6Al-4V samples are shown in Figure 6.2. Regardless of the process and the nitriding temperature, a typical $\alpha+\beta$ microstructure can be seen, characterised by elongated α grain in an $\alpha+\beta$ matrix. A uniform, continuous thin layer, devoid of structure can be clearly observed in the SEM micrograph of the samples nitrided at 700 °C and 750 °C with a thickness about 1,5 μm and is presumed to be a nitrided layer. There can not be seen an obvious difference in the nitrided layer thickness of two samples on the micrograph. In the SEM micrograph of the sample nitrided at 650 °C, a less pronounced, discontinuous and irregular nitrided layer with a thickness varying between 1-1,5 μm is detected on the surface. As can be seen from the SEM micrograph, PVD coated Ti-6Al-4V sample has a very uniform, dense, and continuous TiN layer which has a very smooth surface, with a thickness of about 6 μm . PVD coating has a very distinct and flat interface with the substrate, while plasma nitrided samples are characterized by a less uniform surface profile and more variable interface with the substrate.

In case of plasma nitrided samples, at 750 °C, it is significant that parent $\alpha+\beta$ structure undergoes grain growth. At 650 °C, 700 °C and 750 °C, below the nitrided layer, we can observe a region a little more different from internal substrate features,

which can be attributed to change in surface chemistry. In these conditions, we can presume that in the case of nitrated samples, there is a diffusion layer in addition to the resulting nitrated layer. At 650 °C, this layer is not as clear as it is at 700°C and 750 °C. As the nitrating treatment temperature increases, diffusion layer thickness is observed to increase. On PVD coated sample, there is no diffusion layer observed.

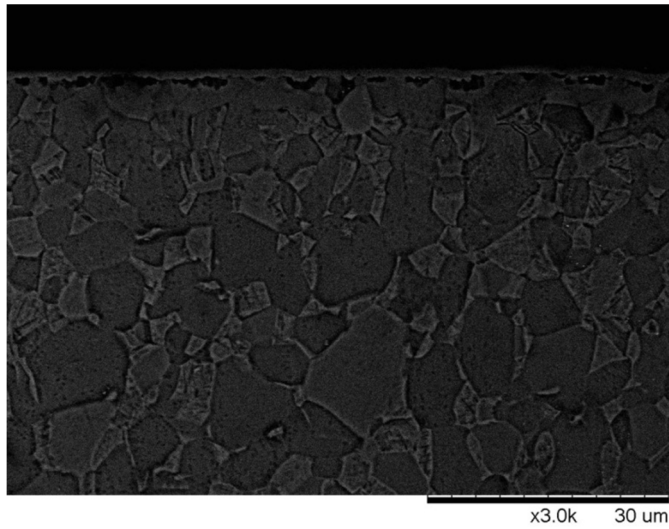


(a) Plasma nitrated at 650 °C, 3000x

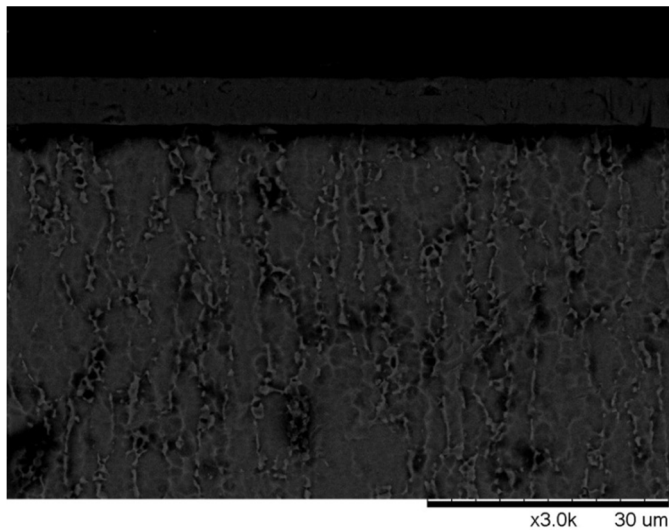


(b) Plasma nitrated at 700 °C, 3000x.,

Figure 6.2: SEM Images of cross section of Ti-6Al-4V samples plasma nitrated at (a) 650 °C, (b) 700 °C, (c) 750°C and (d) TiN deposited by PVD.



(c) Plasma nitrided at 750°C, 3000x.

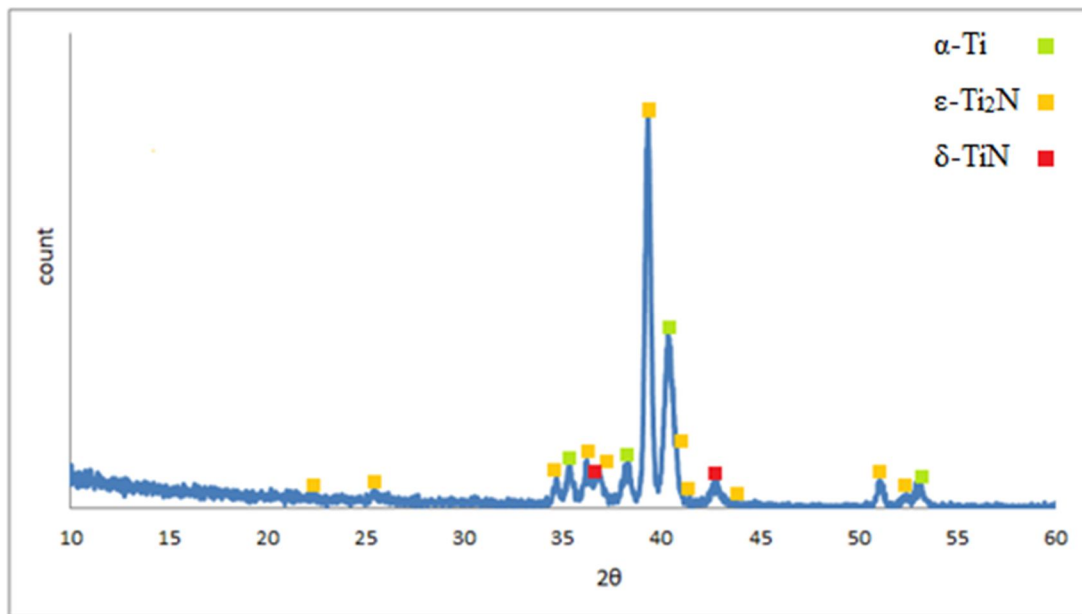


(d) TiN deposited by PVD, 3000x.

Figure 6.2: (continued) SEM Images of cross section of Ti-6Al-4V samples plasma nitrided at (a) 650 °C, (b) 700 °C, (c) 750°C and (d) TiN deposited by PVD.

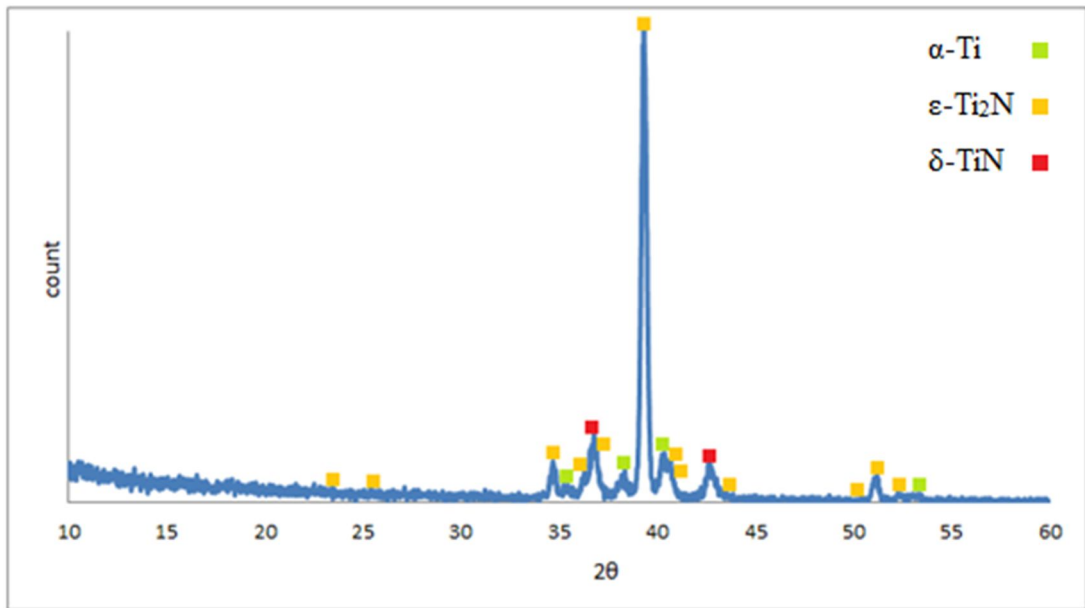
6.2 XRD Phase Identification

It was reported that the diffraction pattern for untreated Ti-6Al-4V consists of the hexagonal α -Ti and the cubic β -Ti phases. XRD diffractions of the plasma nitrided (at 650 °C, 700 °C and 750°C) and TiN deposited Ti-6Al-4V samples are illustrated in Figure 6.3.

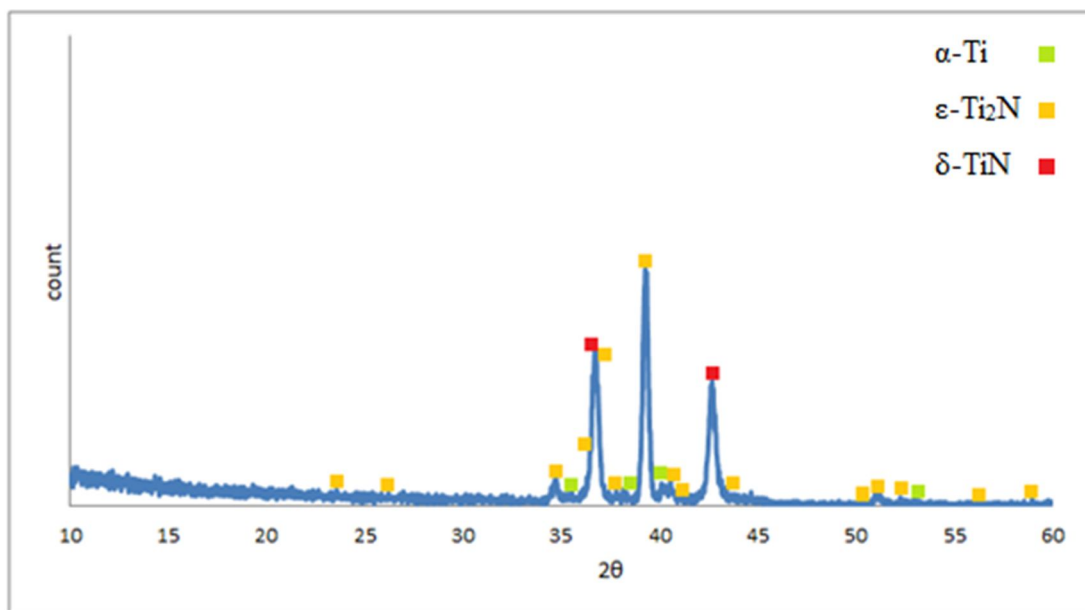


(a) Plasma nitrided at 650°C.

Figure 6.3: X-ray diffractions of Ti-6Al-4V alloy specimens plasma nitrided at (a) 650°C, (b) 700°C, (c) 750°C and (d) TiN deposited by PVD.

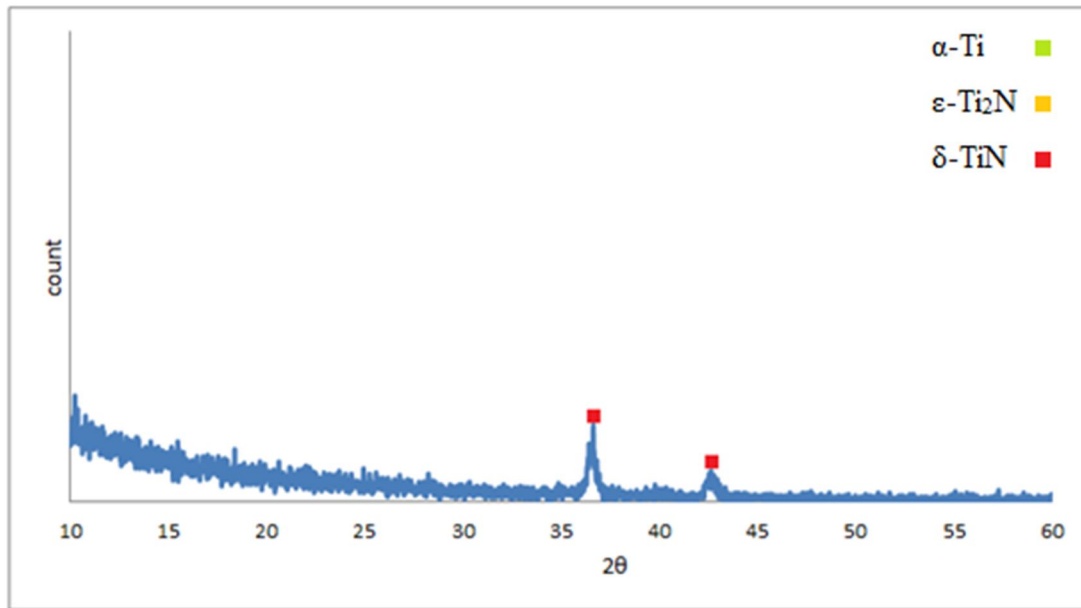


(b) Plasma nitrided at 700°C.



(c) Plasma nitrided at 750°C.

Figure 6.3: (continued) X-ray diffractions of Ti-6Al-4V alloy specimens plasma nitrided at (a)650°C, (b) 700°C, (c) 750°C and (d) TiN deposited by PVD.



(c) TiN deposited by PVD.

Figure 6.3: (continued) X-ray diffractions of Ti-6Al-4V alloy specimens plasma nitrided at (a) 650°C, (b) 700°C, (c) 750°C and (d) TiN deposited by PVD.

Cubic δ -TiN and tetragonal ϵ -Ti₂N phases have been found to grow after plasma nitriding and were both detected at the diffraction patterns of the samples nitrided at 650 °C, 700 °C and 750°C.

According to the XRD results the surface nitrided layer detected by SEM micrographs is composed of δ -TiN and ϵ -Ti₂N phases. Additionally, these two phases are expected to be the reason for the high values of microhardness of the nitrided Ti-6Al-4V alloy.

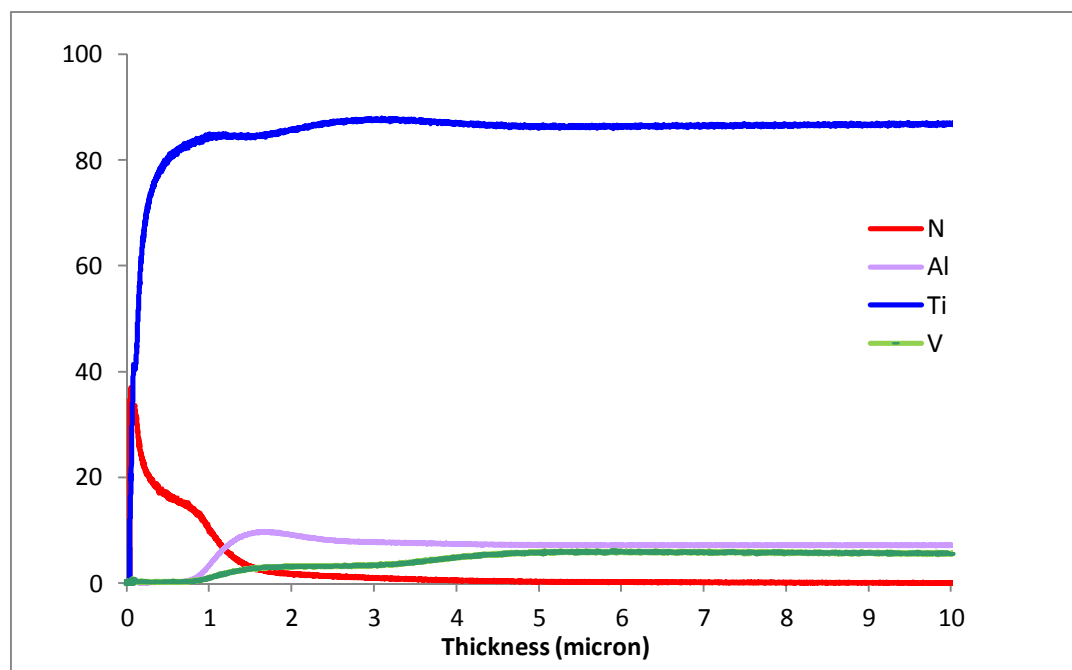
The weight fractions of these phases vary within the nitrided layer. For all nitriding treatment temperatures, the XRD pattern of the plasma nitrided sample is predominantly that of the Ti₂N phase, with only minor indication of TiN.

As the nitriding temperature increases, new peaks corresponding to the Ti₂N phase can be identified, and the intensity of peaks corresponding to the TiN phase increases. In other words, as the nitriding temperature increases, the amount of both TiN phase and Ti₂N phase seems to increase.

In case of PVD coated sample, the XRD pattern for the TiN thin film deposition treatment shows that TiN single phase grows on the substrate surface.

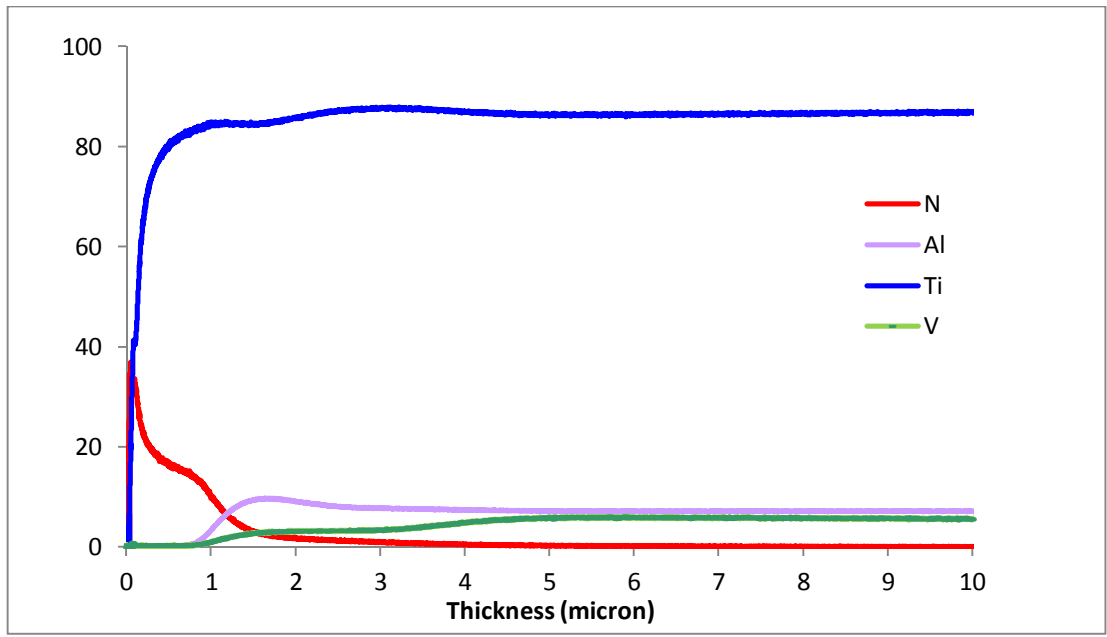
6.3 GDOES Analysis

GDOES analysis results of Ti-6Al-4V samples plasma nitrided at 650 °C, 700 °C and 750°C are shown in Figure 6.4. It can be clearly seen that nitrogen has penetrated into a certain depth value for each different plasma nitriding treatment temperature. This is also an evidence for the formation of nitrided layer on the surface. Penetration depth of nitrogen increases by increasing treatment temperature due to an accelerated rate of nitrogen diffusion at higher temperature. However, there is not a noticeable depth difference between the specimens nitrided at 700 °C and 750°C.

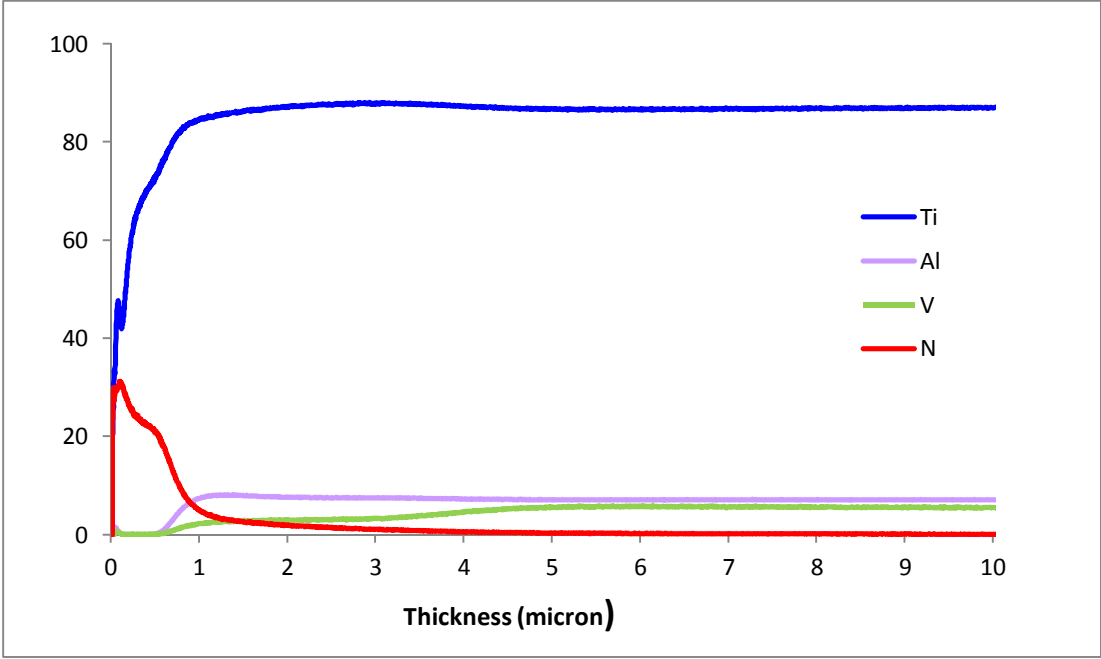


(a) 650°C

Figure 6.4: GDOES results of Ti-6Al-4V alloy specimens plasma nitrided at (a) 650°C, (b) 700 °C, and (c) 750°C.



(b) 700 °C



(c) 750 °C

Figure 6.4: (continued) GDOES results of Ti-6Al-4V alloy specimens plasma nitrided at (a) 650 °C, (b) 700 °C and (c) 750 °C.

6.4 Microhardness Profiles

Vickers microhardness profiles obtained for the untreated Ti-6Al-4V, different nitriding runs and PVD process on the Ti-6Al-4V substrate are shown in Fig.6.5.

Microhardness depth profiles presented in Figure 6.5 indicate that both surface modification processes improve the surface hardness of the Ti-6Al-4V sample. Additionally, the microhardness measurements show that TiN deposited samples have significantly high hardness values compared with the plasma nitrided ones. The result is expected, since TiN layer thickness of the PVD coated sample (about 6 μm) is significantly higher than the nitrided layer thickness of plasma nitrided samples (0,5-2 μm).

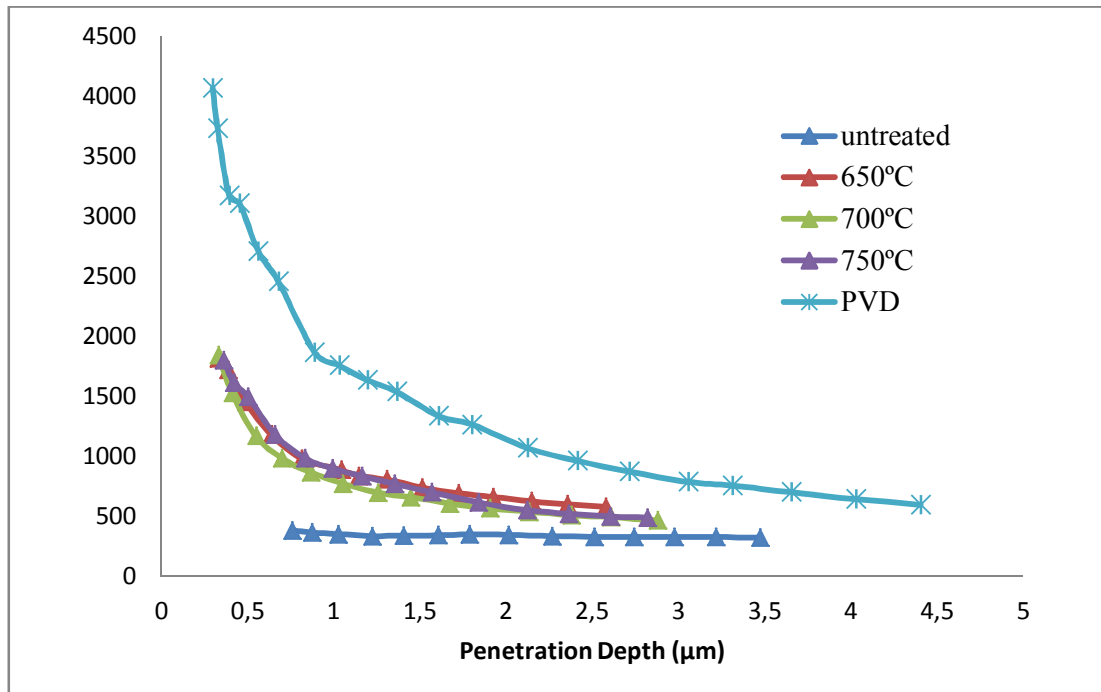


Figure 6.5: Microhardness depth profiles for untreated, plasma nitrided and PVD coated Ti-6Al-4V substrate.

The profiles of the nitrided samples obviously show that the microhardness values decrease gradually with the penetration depth (similar profile as nitride concentration) and the surface hardness values increase as the nitriding process temperature increases due to the diffusion effect. The diffusion of nitrogen into the bulk material produces a continuous hardness profile and provides an optimal support to the hard surface layer. Increase in hardness after plasma nitriding is caused by the formation of this hard surface layer which is composed of titanium nitride phases (faced central cubic δ -TiN and the tetragonal ϵ -Ti₂N) as confirmed in XRD analysis. In Figure 6.5, in case of the plasma nitrided sample at 650°C, a significant increase in surface hardness can be observed compared with untreated sample. At 700°C and 750°C, the nitride layer has significantly higher hardness than at 650°C due to deeper nitrogen penetration depth, since there has not been a significant difference between the surface hardness values of these two samples (700 °C and 750°C) as confirmed in GDOES results. In case of the deeper penetration depths, as process temperature increases, hardness values decrease due to the annealing effect.

6.5 Wear Tests

6.5.1 Results of dry sliding tests

Wear depth profiles and optic microscope images of wear track of the untreated sample and samples nitrided at 650°C, 700°C and 750°C and PVD coated sample after dry sliding tests are shown in Table 6.1.

By measuring the width and the depth of the wear tracks from the profiles which are illustrated in Table 6.1, average area of the wear tracks are found.

$$\text{average wear track area} = \frac{\text{width of the track} \times \text{depth of the track} \times \pi}{4} \quad (6.1)$$

Average wear track area (μm^2) values of the untreated sample, samples nitrided at 650°C, 700°C, 750°C, and PVD coated sample are calculated by the help of formula (6.1) and given in Table 6.2.

Table 6.1: Wear depth profiles and wear track optic images of the untreated, plasma nitrided and PVD coated Ti-6Al-4V samples after dry sliding tests.

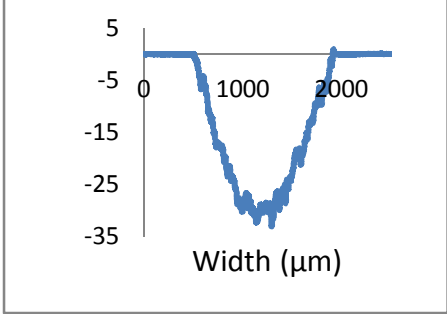
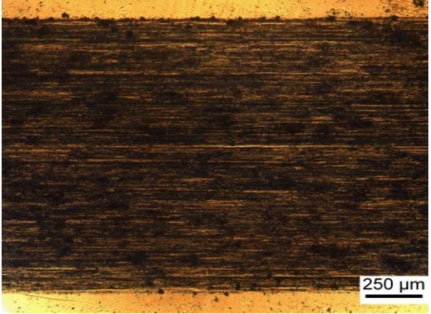
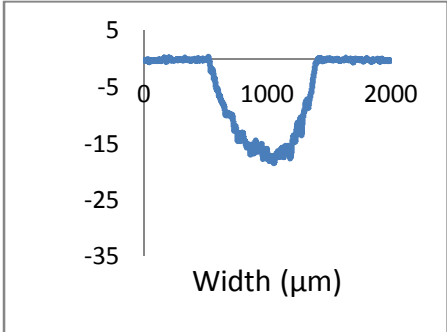

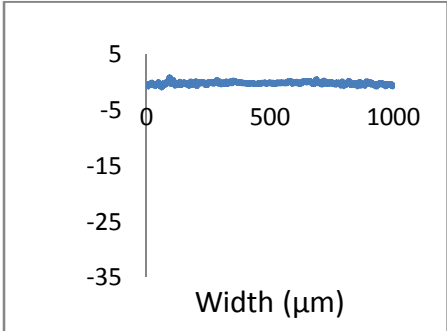
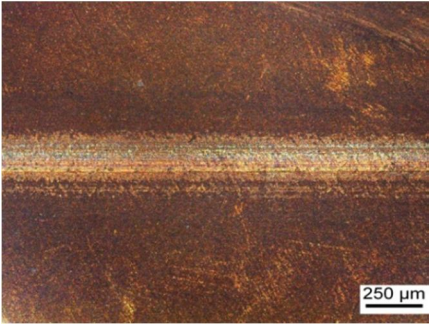
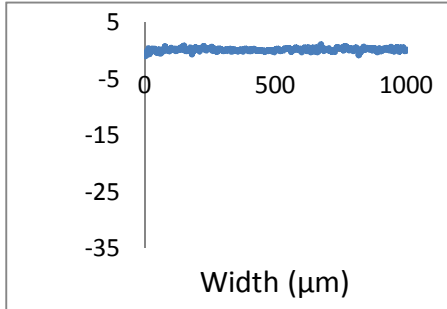
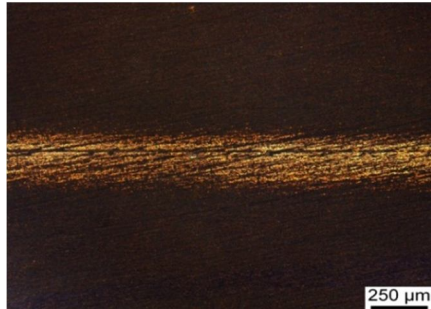
| Ti-6Al-4V Sample | Wear Depth Profile | Wear Track Morphology |
|--------------------------|---|--|
| Untreated |  |  |
| Plasma nitrided at 650°C |  |  |
| Plasma nitrided at 700°C |  |  |
| Plasma nitrided at 750°C |  |  |

Table 6.1: (continued) Wear depth profiles and wear track optic images of the untreated, plasma nitrided, and PVD coated Ti-6Al-4V samples after dry sliding tests.

| Ti-6Al-4V Sample | Wear Depth Profile | Wear Track Morphology |
|------------------|--------------------|-----------------------|
| PVD coated | | |

Table 6.2: Average wear track area values of the untreated and treated samples after dry sliding tests.

| Ti-6Al-4V sample | Average wear track area (μm^2) |
|--------------------------|---|
| Untreated | 32639,75 |
| Plasma nitrided at 650°C | 2955,07 |
| Plasma nitrided at 700°C | 870,22 |
| Plasma nitrided at 750°C | 298,45 |
| PVD coated | 992,59 |

In order to calculate the relative wear resistances of the samples, it is assumed that the wear resistance of the sample which has the highest wear track area value, is equal to 1. In present study the highest value belongs to the untreated sample so we accept its relative resistance as 1, and calculate the relative wear resistances of the treated samples according to this assumption by formula (6.2). The calculated relative wear resistance values are shown in Table 6.3.

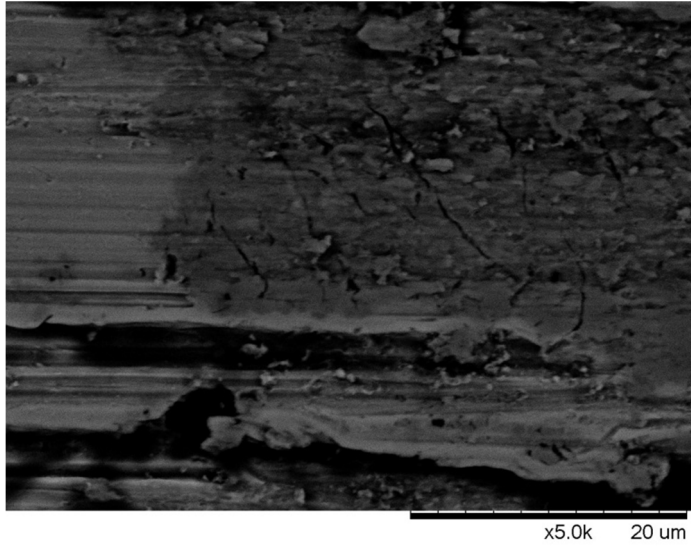
$$\text{relative wear resistance of the nitrided sample} = \frac{\text{wear track area of the untreated sample}}{\text{wear track area of the nitrided sample}} \quad (6.2)$$

Table 6.3: Relative wear resistance of the untreated and treated samples after dry sliding tests.

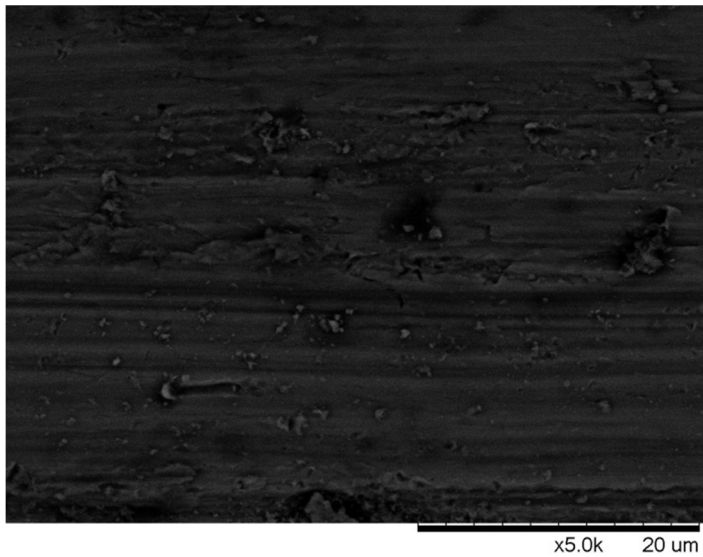
| Ti-6Al-4V sample | Relative wear resistance |
|--------------------------|--------------------------|
| Untreated | 1,0 |
| Plasma nitrided at 650°C | 11,0 |
| Plasma nitrided at 700°C | 37,5 |
| Plasma nitrided at 750°C | 109,4 |
| PVD coated | 32,9 |

It is clarified that both plasma nitriding and PVD processes reduce the wear area of Ti-6Al-4V alloy, increasing the wear resistance, being the highest wear resistance that of the sample nitrided at 750°C, followed by the sample nitrided at 700°C and then the PVD coated sample and finally the one nitrided at 650 °C. In case of the nitrided samples, wear resistance increases by increasing temperature. This result is consistent with the microhardness measurements of the nitrided samples, since the surface hardness values increases by increasing nitriding process temperature due to the diffusion effect.

The wear resistance of the PVD coated sample is less than the samples nitrided at 700°C and 750°C. This result is not consistent with the microhardness profiles which have shown that the highest surface hardness results belong to the PVD coated sample. This situation is attributed to the absence of the diffusion layer, and the distinct interface with the substrate surface in the case of PVD coating. In the plasma nitrided sample, nitrogen diffusion layer provides increased strength, probably as a result of solid solution and/or precipitation hardening. Thus, PVD TiN coating increases surface microhardness and consequently the sliding wear resistance, but provides limited load support. Wear track optic images of the untreated, nitrided, and PVD coated samples are shown in the Table 6.1. Additionally, SEM images at 5000x magnification of the wear tracks are shown in Figure 6.6.

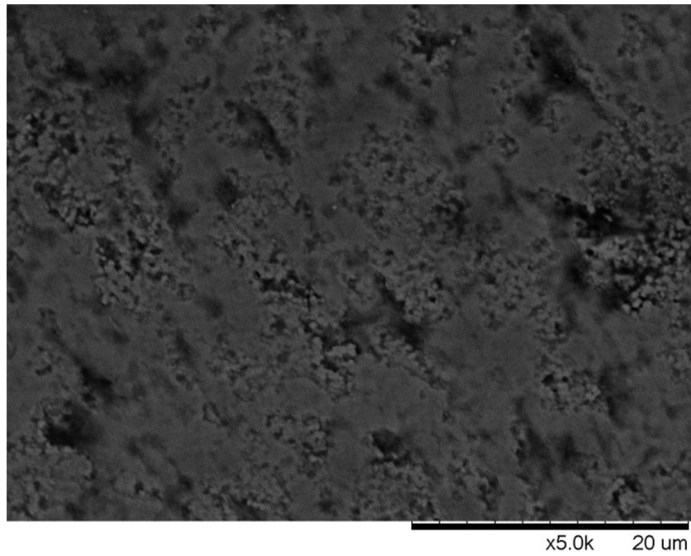


(a) Untreated.

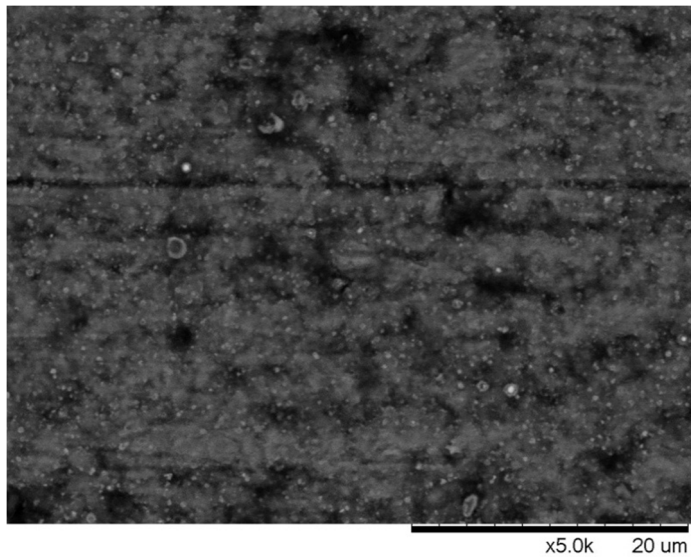


(b) Plasma nitrided at 650°C.

Figure 6.6: SEM images at 5000x of the wear tracks of the (a) untreated sample, (b) sample plasma nitrided at 650°C, (c) sample plasma nitrided at 700°C, (d) sample plasma nitrided at 750°C, and (e) PVD coated sample after dry sliding tests.

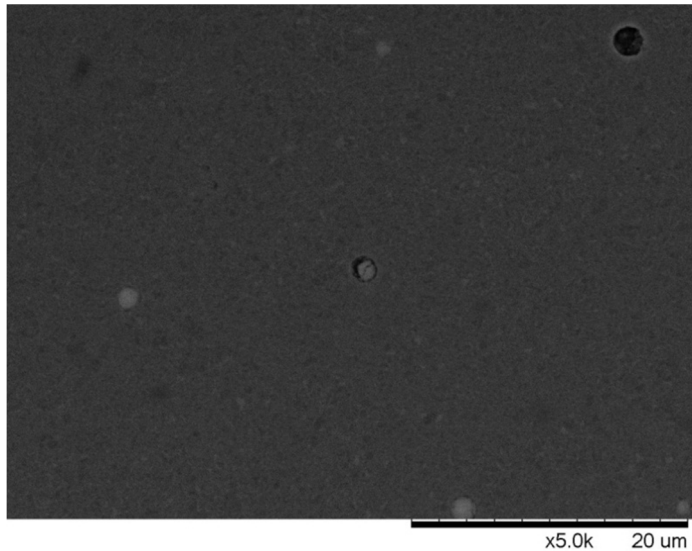


(c) Plasma nitrided at 700°C.



(d) Plasma nitrided at 750°C.

Figure 6.6: (continued) SEM images at 5000x of the wear tracks of the (a) untreated sample, (b) sample plasma nitrided at 650°C, (c) sample plasma nitrided at 700°C, (d) sample plasma nitrided at 750°C, and (e) PVD coated sample after dry sliding tests.



(e) PVD coated.

Figure 6.6: (continued) SEM images at 5000x of the wear tracks of the (a) untreated sample, (b) sample plasma nitrided at 650°C, (c) sample plasma nitrided at 700°C, (d) sample plasma nitrided at 750°C, and (e) PVD coated sample after dry sliding tests.

In the untreated sample, a wide, deep and rough wear track with large plastic deformation could be observed due to the very low hardness of the sample. It has shown adhesive wear and delamination. The sample nitrided at 650°C has shown the same wear mechanism and delamination but with a less effect. A considerable improvement in the wear property could be detected with a less wide wear track but not as significant as the other treated samples due to the low hardness of the nitrided layer confirmed by hardness test results. The samples nitrided at 700°C and 750°C demonstrated a narrow, shallow and less rough wear track compared to the unnitrided, low temperature nitrided and PVD coated samples. In both samples, there could not be observed any severe deformation on the wear track due to the hard nitrided layer while local detachments of the particles were characterised. However, less local detachments could be observed in the sample nitrided at 750 °C due to the harder nitrided layer. PVD coated sample exhibited wider and deeper wear track than the samples nitrided at 700°C and 750°C. Although TiN coating has the highest hardness, during the wear, TiN thin film was broken and wear mechanism was accelerated due to the absence of diffusion layer supporting the film. Smoothing of the coating by wear could be observed by SEM images.

6.5.2 Results of sliding tests in simulated body fluid

Wear depth profiles and optic microscope images of wear track of the untreated sample and samples nitrided at 650°C, 700°C and 750°C and PVD coated samples after sliding test in simulated body fluid are shown in Table 6.4.

The relative wear resistances of the samples after sliding tests in simulated body fluid are calculated by following the same way as calculating those of the samples after dry sliding tests. Again, depth and width of the wear tracks are determined by the wear depth profiles illustrated in Table 6.4 and formula (6.1) is used to calculate wear track areas of the samples which are shown in Table 6.5. Only difference is that, in the present study the highest wear track area value belongs to the sample nitrided at 650°C, so its relative resistance is taken as 1 and the relative wear resistances of the other samples are calculated by formula (6.2). The calculated relative wear resistance values are shown in Table 6.6.

Table 6.4: Wear depth profiles and wear track optic images of the untreated, plasma nitrided and PVD coated Ti-6Al-4V samples after sliding test in simulated body fluid.

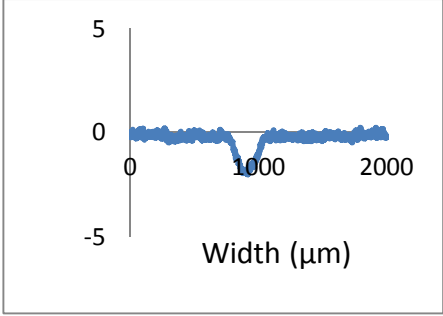

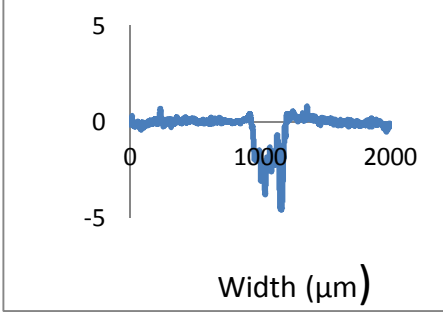

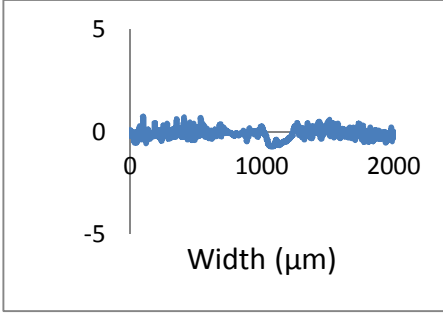
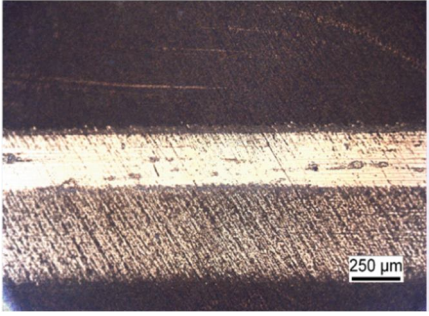
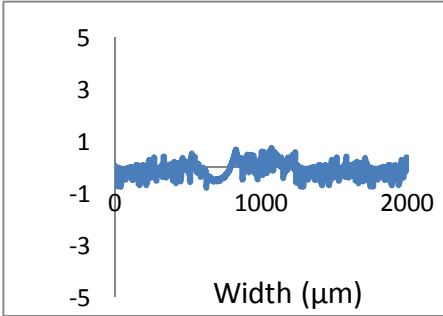
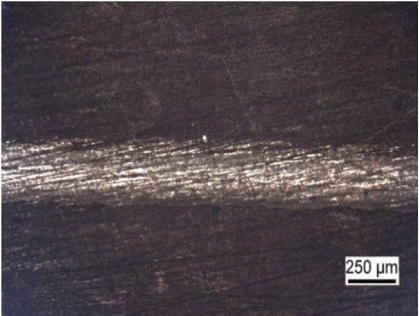
| Ti-6Al-4V Sample | Wear Depth Profile | Wear Track Morphology |
|--------------------------|---|--|
| Untreated |  |  |
| Plasma nitrided at 650°C |  |  |
| Plasma nitrided at 700°C |  |  |
| Plasma nitrided at 750°C |  |  |

Table 6.4: (continued) Wear depth profiles and wear track optic images of the plasma nitrided and PVD coated Ti-6Al-4V samples after sliding tests in simulated body fluid.

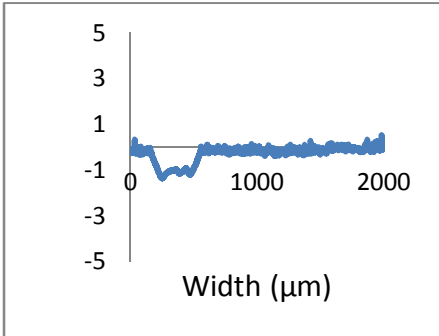
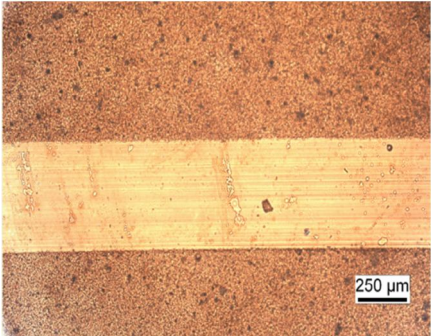
| Ti-6Al-4V Sample | Wear Depth Profile | Wear Track Morphology |
|------------------|---|--|
| PVD coated |  |  |

Table 6.5: Average wear track area values of the untreated and treated samples after sliding tests in simulated body fluid.

| Ti-6Al-4V sample | Average wear track area (μm^2) |
|--------------------------|---|
| Untreated | 302,63 |
| Plasma nitrided at 650°C | 984,89 |
| Plasma nitrided at 700°C | 125,19 |
| Plasma nitrided at 750°C | 82,18 |
| PVD coated | 358 |

Table 6.6: Relative wear resistance of the untreated and treated samples after sliding tests in simulated body fluid.

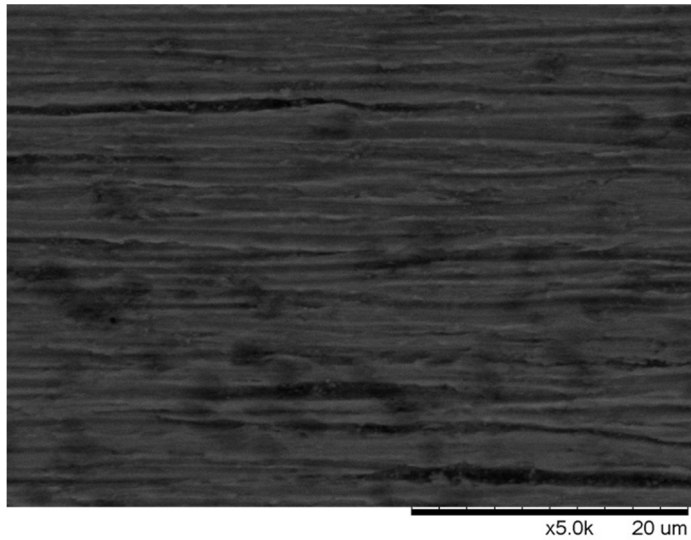
| Ti-6Al-4V sample | Relative wear resistance |
|--------------------------|--------------------------|
| Untreated | 3,3 |
| Plasma nitrided at 650°C | 1 |
| Plasma nitrided at 700°C | 7,9 |
| Plasma nitrided at 750°C | 12,0 |
| PVD coated | 2,8 |

It is clarified that wear resistance of both the sample plasma nitrided at 650°C and the PVD coated samples are less than the wear resistance of the untreated sample. On the other hand, nitriding processes at 700°C and at 750°C increase the wear resistance of the sample significantly. It is expected due to the hard and continuous nitrided layer which is supported by a diffusion layer that provides increased strength. This situation can also reduce the corrosion effect on wear. The wear resistance of the sample nitrided at 750°C is higher than that of the sample nitrided at 700°C due to the increased surface hardness values by increasing nitriding temperature.

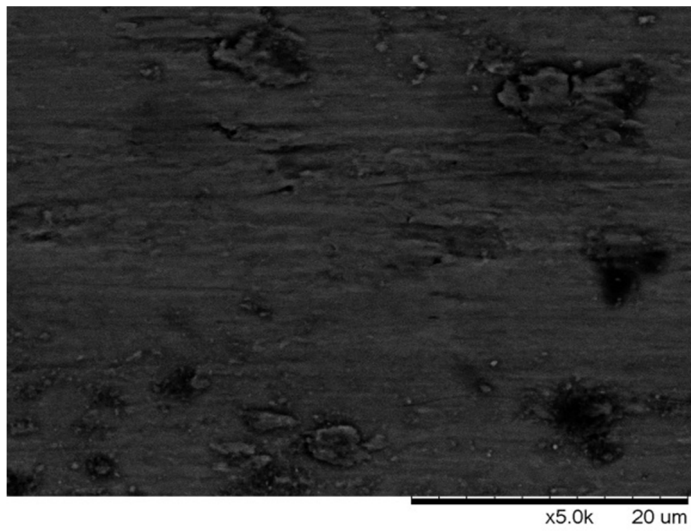
The result is not consistent with the microhardness profiles which have shown that the highest surface hardness results belong to the PVD coated sample. It is presumed that TiN coating is broken and TiN particles which have a hard nature, increase the wear rate and decrease the wear resistance. This situation is attributed to the combined effect of the absence of the diffusion layer, the distinct interface between the coating and the substrate surface, and the corrosion caused by the simulated body fluid.

Despite the hardness of the nitrided samples has shown considerable improvement at microhardness profiles, the sample plasma nitrided at 650°C has lower wear resistance than the untreated sample. This is assigned to the effect of broken, hard nitrided film particles which accelerate the wear rate due to the thinner and softer nitrided layer and thinner diffusion layer that supports the nitrided layer and corrosion effect by the simulated body fluid on the thin nitrided layer.

Wear track optic images of the untreated, nitrided, and PVD coated samples are shown in the Table 6.4. SEM images at 5000x magnification of the wear tracks are shown in the Figure 6.7.

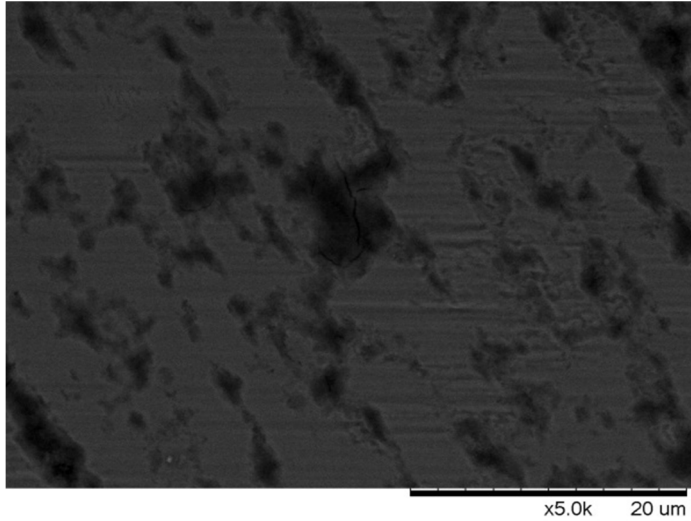


(a) Untreated.

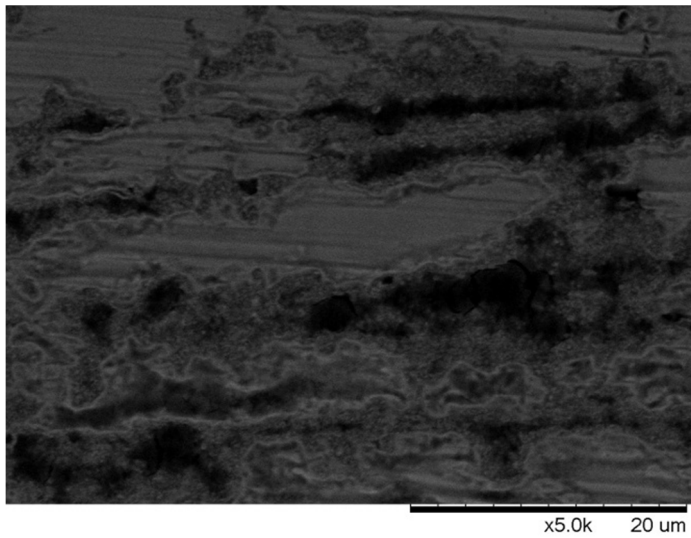


(b) Plasma nitrided at 650°C.

Figure 6.7: SEM images of the wear tracks of the (a) untreated sample, (b) sample plasma nitrided at 650°C, (c) sample plasma nitrided at 700°C, (d) sample plasma nitrided at 750°C, and (e) PVD coated sample after sliding tests in simulated body fluid.

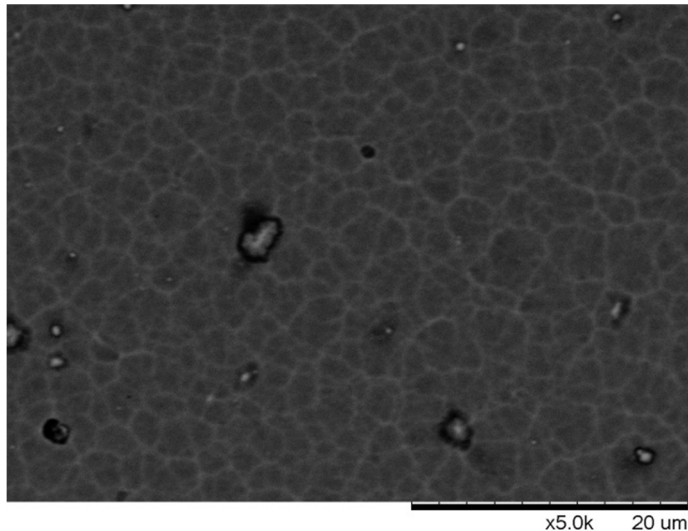


(c) Plasma nitrided at 700°C.



(d) Plasma nitrided at 750°C.

Figure 6.7: (continued) SEM images of the wear tracks of the (a) untreated sample, (b) sample plasma nitrided at 650°C, (c) sample plasma nitrided at 700°C, (d) sample plasma nitrided at 750°C, and (e) PVD coated sample after sliding tests in simulated body fluid.



(e) PVD coated.

Figure 6.7: (continued) SEM images of the wear tracks of the (a) untreated sample, (b) sample plasma nitrided at 650°C, (c) sample plasma nitrided at 700°C, (d) sample plasma nitrided at 750°C, and (e) PVD coated sample after sliding tests in simulated body fluid.

Simulated body fluid solution decreased the effect of wear on the samples. Moreover, in simulated body fluid, the same wear mechanisms as in the dry sliding have been detected for the untreated, low temperature nitrided and PVD coated samples. In the untreated sample, again, a wide, deep and rough wear track and delamination could be observed due to the very low hardness of the untreated sample. Not only the sample nitrided at 650°C, but also PVD coated sample has shown a worse performance than the untreated sample, wider and deeper wear track area could be seen due to the broken, and hard nitrided or coated film particles which accelerate the wear rate and decrease the wear resistance. The samples nitrided at 700°C and 750°C have shown narrow and shallow wear tracks exhibiting oxidative wear mechanism. And at 750°C, the sample exhibits the least wide and deep wear track in consistence with the wear depth profiles and wear resistance results.

7. CONCLUSION

In this study, plasma nitriding process for 3 different process temperatures and PVD coating has been applied on Ti-6Al-4V alloy in order to improve the surface characteristics. Then, several characterization procedures were carried out to understand the effect of plasma nitriding with different temperatures and PVD coating on surface properties. Following conclusions can be derived according to the results of the present study:

1. SEM micrographs has demonstrated that the cross-sectional surface microstructure of the nitrided samples clearly includes a well-defined, uniform and continuous nitrided layer, when nitriding is performed at 700 °C and 750 °C. There has not been observed a distinct difference between the thickness of the nitrided layers for the two samples. At 650°C, this nitrided layer is less pronounced, thinner, irregular and discontinuous. Underneath the nitrided layer, a diffusion layer can be assigned for all the nitriding process temperatures. The thickness of this layer increases by the increasing treatment temperature. The PVD coated sample has significantly thicker, very uniform, dense and continuous TiN layer with a very distinct and flat interface with the substrate, with the lack of the diffusion layer.
2. For the Ti-6Al-4V samples nitrided at 650°C, 700 °C and 750 °C, two phases (δ -TiN and ϵ -Ti₂N) have been found to grow after the process, with the major XRD pattern indication of Ti₂N. As the treatment temperature increases, the amount of TiN and Ti₂N phases increases. In case of the PVD coated sample, single TiN phase can be observed to grow after the coating process.
3. It is confirmed by GDOES analysis that nitrogen has penetrated into a certain depth value for each plasma nitriding temperature. Nitrogen concentration decreases with increasing distance from the surface. Nitrogen penetration depth increases as the treatment temperature increases due to the accelerated rate of nitrogen diffusion at higher temperature, however there couldn't be seen any significant depth difference between the samples nitrided at 700 and 750°C.

4. The microhardness depth profiles indicated that both of the surface modification techniques improve the surface hardness of the Ti-6Al-4V sample. TiN deposited sample has significantly higher hardness values than the plasma nitrided one due to the high difference of the nitrided layer thickness. The microhardness values of the nitrided samples decrease gradually with the penetration depth showing a similar profile to nitrogen concentration. The surface hardness values were found to increase as nitriding temperature increased, since the increase in surface hardness is caused by the formation of the hard surface layer (which is composed of titanium nitride phases as confirmed in XRD analysis) and the diffusion of the nitrogen into the sample which is highly affected by temperature, provides an optimal support to the hard surface layer. However, a significant difference was not observed between the improvement of the hardness of the samples nitrided at 700 °C and 750°C, as confirmed in GDOES results.

5. The plasma nitriding and PVD coating processes have a positive effect on the dry sliding behaviour of the Ti-6Al-4V alloy by improving the wear resistance considerably. In case of the nitrided samples, wear resistance increases as temperature does, in consistence with the microhardness measurements. Thus, the sample plasma nitrided at 750°C has the highest wear resistance. The wear resistance of the PVD coated sample was found to be less than that of the samples nitrided at 700 °C and 750°C. However, the surface hardness of the PVD coated sample was found to be the higher than these samples. This result is attributed to the break down of the PVD coating due to the absence of the diffusion layer and distinct interface with substrate surface of the PVD coated sample.

The sample nitrided at 650°C has shown the same wear mechanism (adhesive wear) and delamination with the untreated sample but with a less effect. The samples nitrided at 700°C and 750°C demonstrated a narrow, shallow and less rough wear track than the other samples, while local detachments of the particles were characterised. However, less local detachments could be observed in the sample nitrided at 750 °C due to the harder nitrided layer. TiN PVD coated sample exhibited wider and deeper wear track than that of the samples nitrided at 700°C and 750 °. Smoothing of the coating by wear could also be observed by SEM images.

6. The plasma nitriding and PVD coating processes have a considerable effect on the sliding behaviour of the Ti-6Al-4V alloy in simulated body fluid. Additionally, simulated body fluid solution decreased the effect of wear on the samples.

It is clarified that wear resistance of both the sample plasma nitrided at 650°C and the PVD coated sample are less than the untreated sample while nitriding processes at 700°C and at 750°C increase the wear resistance of the sample significantly. The result is not consistent with the microhardness profiles which have shown that the highest surface hardness results belong to the PVD coated sample. It is presumed that TiN coating is broken and TiN particles which have a hard nature, increase the wear rate and decrease the wear resistance. This situation is attributed to the combined effect of the absence of the diffusion layer, the distinct interface with the substrate surface in the case of PVD coating and the corrosion caused by the simulated body fluid.

Despite the hardness of the nitrided samples has shown considerable improvement at microhardness profiles, the sample plasma nitrided at 650°C has lower wear resistance than the untreated sample. This is assigned to the effect of broken, hard nitrided film particles which accelerate the wear rate due to the thinner nitrided layer and thinner diffusion layer. The corrosion effect by the simulated body fluid on the thin nitrided layer can be considered for this result.

Moreover, in simulated body fluid, the same wear mechanisms as in the dry sliding have been detected for the untreated, low temperature nitrided and PVD coated samples. The samples nitrided at 700°C and 750°C have exhibited oxidative wear mechanism. At 750°C, again, the sample exhibits the least wide and deep wear track in consistence with the wear depth profiles and wear resistance results.

As a general result, the optimal surface properties has been obtained by the sample that was plasma nitrided at 750°C.

REFERENCES

- [1] **Oshida, Y.**,2006. *Bioscience and Bioengineering of Titanium Materials*. Pergamon, Oxford, United Kingdom. 3-4, 13-7, 26, 37, 110-119, 217, 349.
- [2] **Brunette, D.M., Tengvall, P., Textor, M., Thomsen, P.**, 2001. *Titanium in Medicine: Material Science, Surface Science, Engineering, Biological Responses and Medical Applications*. Springer, Germany. 26, 37, 111, 119, 217.
- [3] **Rahman, M., Reid, I., Duggan, P., Dowling, D.P., Hughes, G., Hashmi, M.S.J.**, 2007. Structural and tribological properties of the plasma nitrided Ti-alloy biomaterials: Influence of the treatment temperature, *Surface and Coating Technology*, **201**, Elsevier. 4865-4872.
- [4] **Lütjering, G., Williams, J.C.**, 2007. *Titanium*, second edition. Springer, Germany. 15.
- [5] **Johns, S.M., Bell, T., Samandi, M., Collins, G.A.**, 1996. Wear resistance of plasma immersion ion implanted Ti6Al4V, *Surface and Coatings Technology*, **85**, Elsevier. 7-14.
- [6] **Fouquet, V., Pichon, L., Straboni, A., Drouet, M.**, 2004. Nitridation of Ti6Al4V by PBII: study of the nitrogen diffusion and of the nitride growth mechanism, *Surface and Coatings Technology*, **186**, Elsevier. 34-39.
- [7] **Yildiz, F., Yetim, A.F., Alsaran, A., Çelik, A.**, 2008. Plasma nitriding behaviour of Ti-6Al-4V orthopedic alloy, *Surface and Coatings Technology*,**202**, Elsevier. 2471-2476.
- [8] **Destefani, J., Lampman, S., Eylon, D. Newman, J.R., Thorne, J.K.**,1991. Introduction to Titanium Alloys, Wrought Titanium and Titanium Alloys , Titanium and Titanium Alloy Castings, *ASM Handbook Vol 2: Properties and Selection: Nonferrous Alloys & Special Purpose Materials, tenth edition*. ASM International. 1770-1791, 1808-1818, 1892-1896.
- [9] **Geetha, M., Singh, A.K., Asokamani, R., Gogia, A.K.**, 2009. Ti based biomaterials, the ultimate choice for orthopedic implants – A review, *Progress in Materials Science*,**54**, Elsevier. 397-425.
- [10] **Rack, H.J., Qazi, J.I.**, 2006. Titanium alloys for biomedical applications, *Materials Science and Engineering*,**C26**,Elsevier. 1269-1277.
- [11] **Luckey, H.A., Kubli, F.Jr.**, 1983. *Titanium Alloys in Surgical Implants*. ASTM, Baltimore, USA. 1-9, 35, 106, 123.

- [12] **Harper, C.A.**, 2001. *Handbook of Materials for Product Design*. McGraw-Hill Professional. 302.
- [13] **Fleck, C., Eifler, D.**, 2009. Corrosion, fatigue and corrosion fatigue behaviour of metal implant materials, especially titanium alloys, *International Journal of Fatigue*,**32**, Elsevier. 929-935.
- [14] **Niomi, M.**,2007. Fatigue characteristics of metallic biomaterials, *International Journal of Fatigue*,**29**, Elsevier. 992-1000.
- [15]**Hoeppner, D.W., Chandrasekaran, V.**, 1996. Characterizing the fretting fatigue behaviour of Ti-6Al-4V in modular joints, *Medical Applications of Titanium and its Alloys: The Material and Biological Issues*. ASTM STP **1272**.
- [16] **Niinomi, M.**, 2008. Mechanical biocompatibilities of titanium alloys for biomedical applications, *Journal of the Mechanical Behaviour of Biomedical Materials I*, Elsevier. 30-42.
- [17] **McKellop, H.A., Rostlund, T., Ebramzadeh, E., Sarmiento, A.**, 1996. Wear of titanium 6-4 alloy in laboratory tests and in retrieved human joint replacements, *Medical Applications of Titanium and its Alloys: The Material and Biological Issues*. ASTM STP **1272**.
- [18] **Freudenberger, J., Göllner, J., Heilmaier, M., Mook, G., Saage, H., Srivastava, V., Wendt, U.**, 2009. Materials Science and Engineering, *Springer Handbook of Mechanical Engineering*. Springer, Germany. 191-194.
- [19] **Dobbs, H.S., Scales, J.T.**, 1983. Behaviour of commercially pure titanium and Ti-318 (Ti-6Al-4V) in orthopedic implants, *Titanium Alloys and Surgical Implants*. ASTM STP **796**. 173-186.
- [20] **Pye, D.**, 2006. Nitriding Techniques, Ferritic Nitrocarburizing, and Austenitic Nitrocarburizing Techniques and Methods, *Steel heat treatment: Metallurgy and Technologies, Second Edition*. Taylor & Frances Group, Portland, Oregon, USA. 477-510.
- [21] **Knerr, C.H., Rose, T.C., Filkowski, J.H., O'Brien, J.M., Goodman, D.**, 1991. Gas nitriding of Steels, Liquid Nitriding of Steels, Plasma (Ion) Nitriding of Steels, *ASM Handbook Vol 4: Heat Treating, tenth edition*. ASM International. 903-923, 953, 2149.
- [22] **Schwartz, M.**, 2010. New Innovative Heat Treating Processes, *Innovations in materials manufacturing, Fabrication, and Environmental Safety*. CRC Press, Florida, USA. 495-499.
- [23] **Korwin, M.J., Morawski, C.D., Tymowski, G.J., Liliental, W.K.**, 2004. Design of Nitrided and Nitrocarburized Materials, *Handbook of Metallurgical Process Design*. Marcel Dekker, New York, USA. 548-578.
- [24] **Beer, O.**,2006. Plasma Assisted Heat Treating Processes of Bearing Components, *Journal of ASTM International*, Vol. **3**,no. 3. ASTM International.

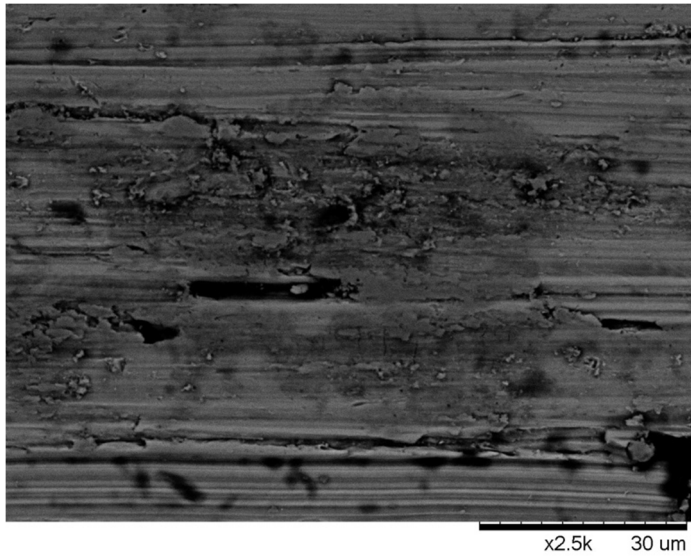
- [25] **Bloyce, A., Morton, P.H., Bell, T.**, 1994. Surface Engineering of Titanium and Titanium Alloys, *ASM Handbook Vol 5: Surface engineering, tenth edition*. ASM International. 2253.
- [26] **Leclair, P.R.**, 1998. Titanium Nitride Thin Films by the Electron Shower, *Partial Fulfillment of the Requirements for the Degree of Bachelor Of Science in Materials Science and Engineering at the Massachusetts Institute of Technology, May*. Massachusetts Institute of Technology.
- [27] **Molinari, A., Straffelini, G., Tesi, B., Bacci, T., Pradelli, G.**, 1997. Effects of load and sliding speed on the tribological behaviour of Ti-6Al-4V plasma nitrided at different temperatures. *Wear*,**203**, Elsevier. 447-454.
- [28] **Yilbaş, B.S., Şahin, A.Z., Al-Garni, A.Z., Said, S.A.M., Ahmed, Z., Abdulaleem, B.J., Sami, M.**, 1996. Plasma nitriding of Ti-Al-4V alloy to improve some tribological properties. *Surface and Coatings Technology*,**80**, Elsevier. 287-292.
- [29] **Chen, K.C., Jaung, G.J.**, 1997. D.c. diode ion nitriding behaviour of titanium and Ti-6Al-4V, *Thin Solid Films*,**303**, Elsevier. 226-231.
- [30] **Ali, M.M., Raman, S.G.S., Pathak, S.D., Gnanamoorthy, R.**, 2010. Influence of plasma nitriding on fretting wear behaviour of Ti-6Al-4V. *Tribology International*,**43**, Elsevier. 152-160.
- [31] **Zhecheva, A., Sha, W., Malinov, S., Long, A.**, 2005. Enhancing the microstructure and properties of titanium alloys through nitriding and other surface engineering methods, *Surface and Coatings Technology*,**200**, Elsevier. 2192-2207.
- [32] **Avelar-Batista, J.C., Spain, E., Housden, J., Matthews, A., Fuentes, G.G.**, 2005. Plasma nitriding of Ti-6Al-4V alloy and AISI M2 steel substrates using D.C. glow discharges under a triode configurations, *Surface and Coatings Technology*,**200**, Elsevier. 1954-1961.
- [33] **Nolan, D., Huang, S.W., Leskovsek, V., Braun, S.**, 2006. Sliding wear of titanium nitride thin films deposited on Ti-6Al-4V alloy by PVD and plasma nitriding processes, *Surface and Coatings Technology*,**200**, Elsevier. 5698-5705.
- [34] **Mattox, D.M.**,1998. *Handbook of Physical Vapor Deposition Processing*, William Andrew Publishing. 406-413
- [35] **Korhonen, A.S., Harju, E.**, 2000. Surface engineering with light alloys, hard coatings, thin films and plasma nitriding, *Journal of Materials Engineering and Performance*, ASM International. 302-305.
- [36] **Long, M., Rack, H.J.**, 1998. Titanium alloys in total joint replacement – a materials science perspective, *Biomaterials*,**19**, Elsevier. 1621-1639.
- [37] **Bhushan, B.**,1987. Overview of Coating Materials, Sniface Treatments, and Screening Techniques for Tribological Applications - Part 1: Coating Materials and Surface Treatments, *Testing of Metallic and Inorganic Coatings*. ASTM, Philadelphia, USA. 289-309.

APPENDICES

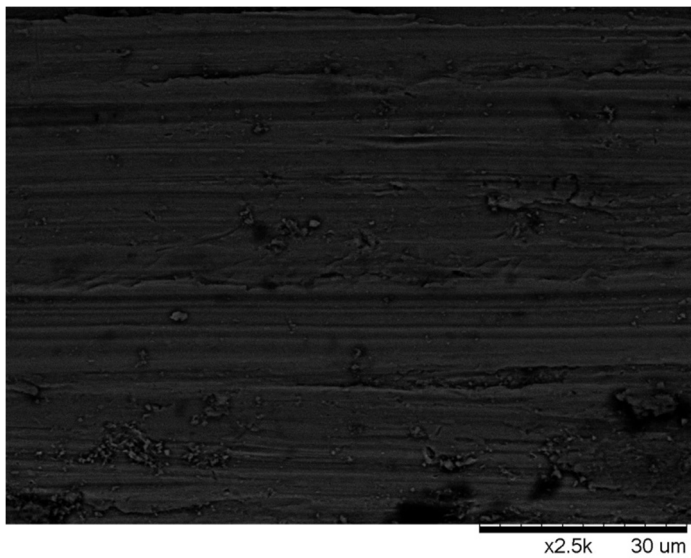
APPENDIX A.1 : SEM images at 2500x magnification of the wear tracks of (a) untreated sample, (b) sample plasma nitrided at 650°C, (c) sample plasma nitride at 700°C, (d) sample plasma at 750°C, and (e) PVD coated sample after dry sliding tests.

APPENDIX A.2 : SEM images at 2500x magnification of the wear tracks of (a) untreated sample, (b) sample plasma nitrided at 650°C, (c) sample plasma nitride at 700°C, (d) sample plasma at 750°C, and (e) PVD coated sample after sliding tests in simulated body fluid.

APPENDIX A.1

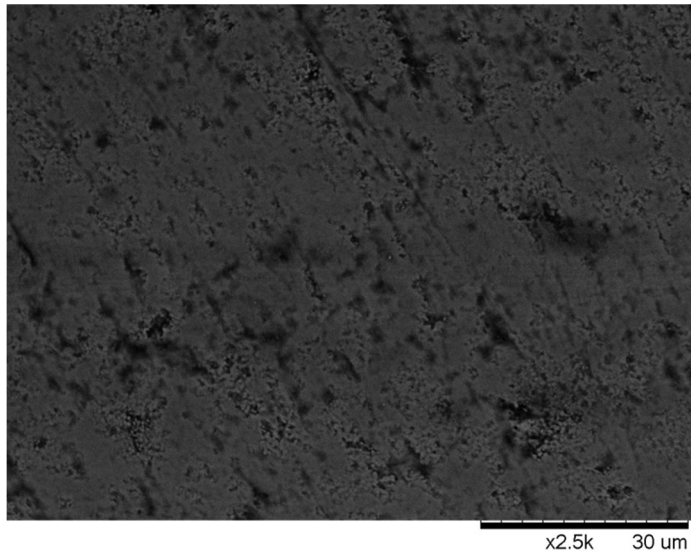


(a) Untreated.

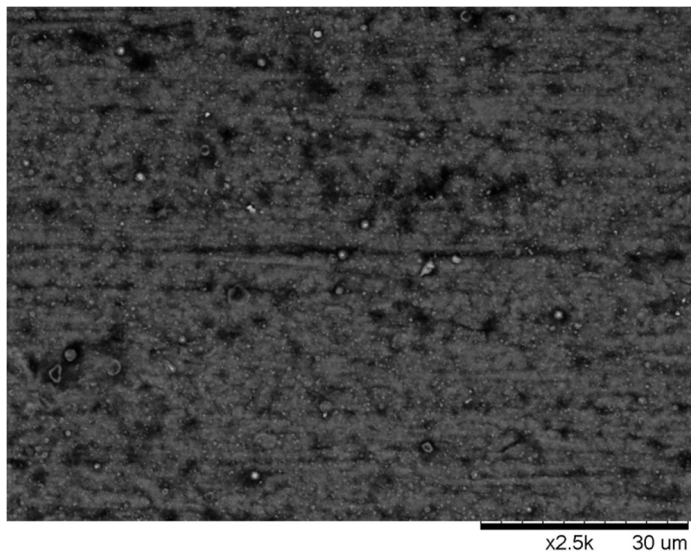


(b) Plasma nitrided at 650°C.

Figure A.1 : SEM images at 2500x magnification of the wear tracks of (a) untreated sample, (b) sample plasma nitrided at 650°C, (c) sample plasma nitride at 700°C, (d) sample plasma at 750°C, and (e) PVD coated sample after dry sliding tests.

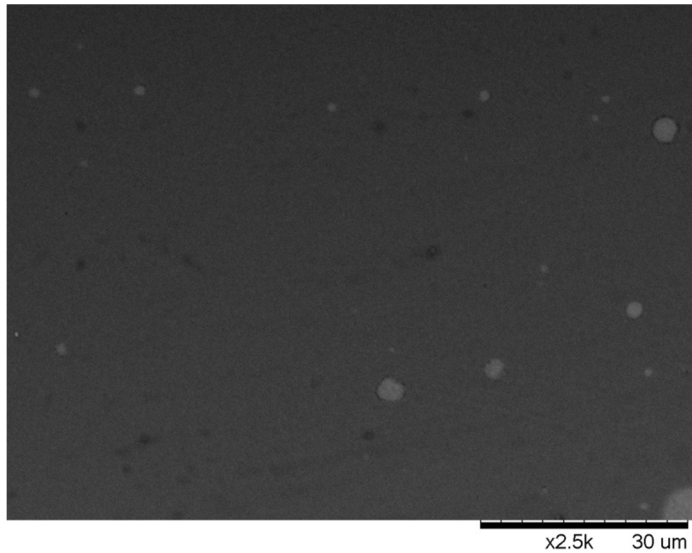


(c) Plasma nitrided at 700°C.



(d) Plasma nitrided at 750°C.

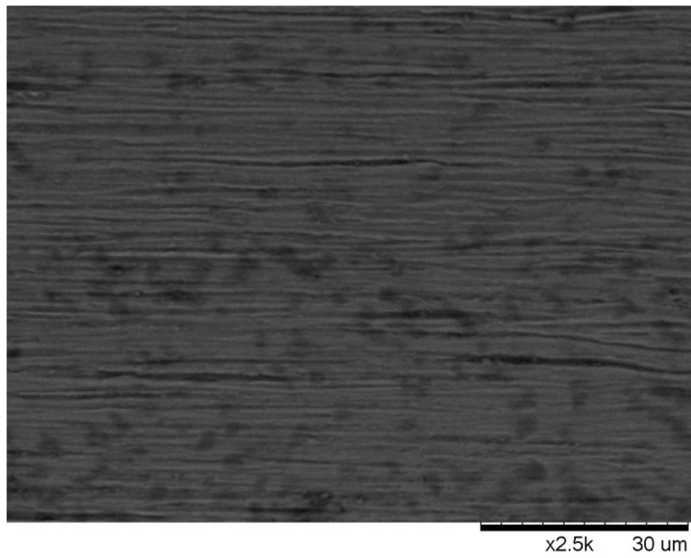
Figure A.1 : (continued) SEM images at 2500x magnification of the wear tracks of (a) untreated sample, (b) sample plasma nitrided at 650°C, (c) sample plasma nitride at 700°C, (d) sample plasma at 750°C, and (e) PVD coated sample after dry sliding tests.



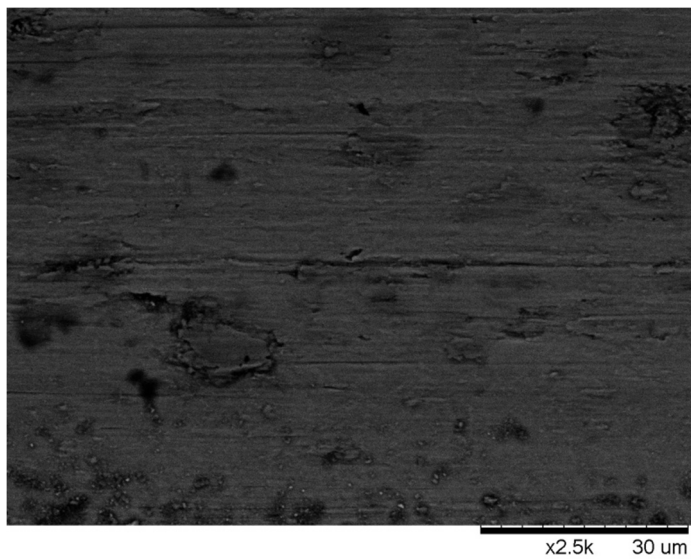
(e) PVD coated.

Figure A.1 : (continued) SEM images at 2500x magnification of the wear tracks of (a) untreated sample, (b) sample plasma nitrided at 650°C, (c) sample plasma nitride at 700°C, (d) sample plasma at 750°C, and (e) PVD coated sample after dry sliding tests.

APPENDIX A.2

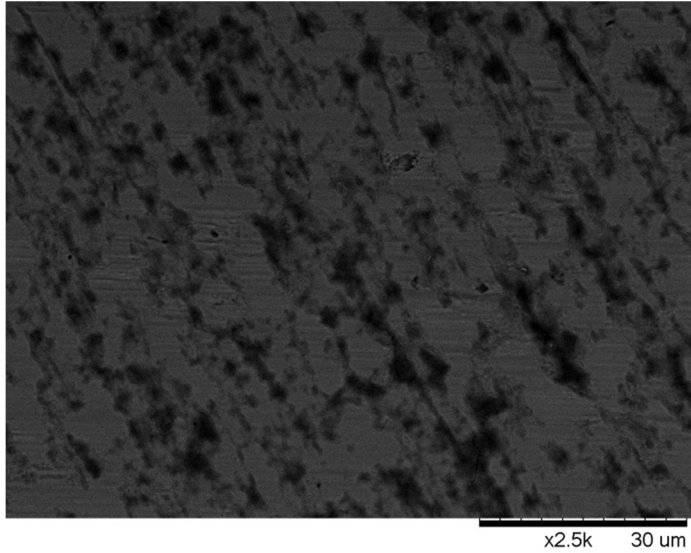


(a) Untreated.

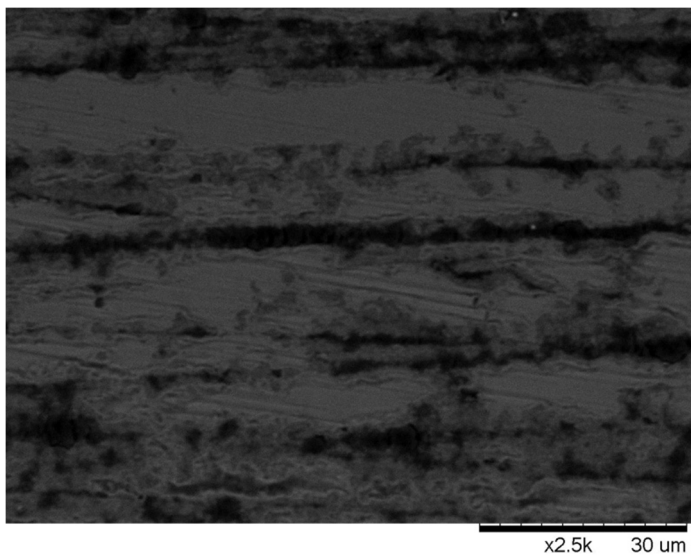


(b) Plasma nitrided at 650°C.

Figure A.2: SEM images at 2500x magnification of the wear tracks of (a) untreated sample, (b) sample plasma nitrided at 650°C, (c) sample plasma nitride at 700°C, (d) sample plasma at 750°C, and (e) PVD coated sample after sliding tests in simulated body fluid.

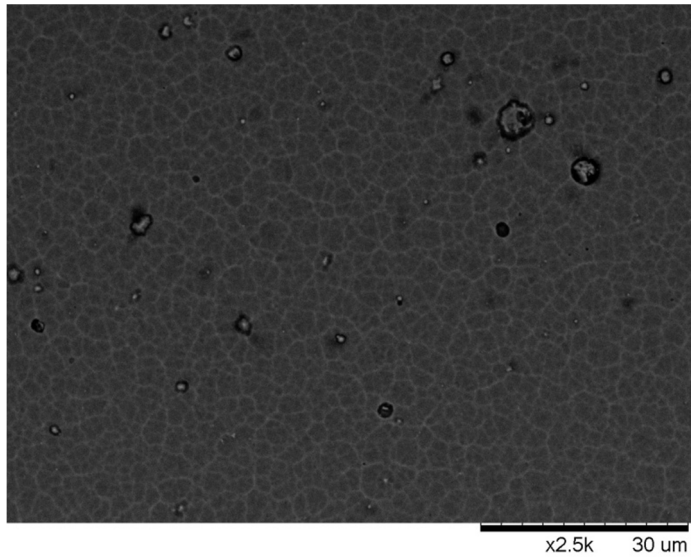


(c) Plasma nitrided at 700°C.



(d) Plasma nitrided at 750°C.

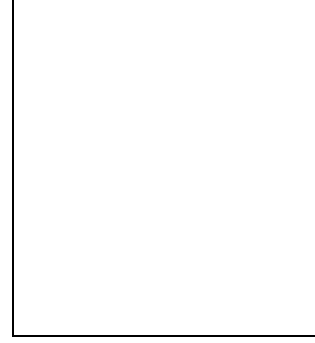
Figure A.2: (continued) SEM images at 2500x magnification of the wear tracks of (a) untreated sample, (b) sample plasma nitrided at 650°C, (c) sample plasma nitride at 700°C, (d) sample plasma at 750°C, and (e) PVD coated sample after sliding tests in simulated body fluid.



(e) PVD Coated.

Figure A.2: (continued) SEM images at 2500x magnification of the wear tracks of (a) untreated sample, (b) sample plasma nitrided at 650°C, (c) sample plasma nitride at 700°C, (d) sample plasma at 750°C, and (e) PVD coated sample after sliding tests in simulated body fluid.

CURRICULUM VITAE



Candidate's full name: Tuğçe Akyazı

Place and date of birth: Ankara, 09 January 1986

Permanent Address: Çankaya, Ankara

Universities and

Colleges attended: Istanbul Technical University, Politecnico di Milano

Publications: